Università degli Studi di Salerno

Dipartimento di Ingegneria dell'Informazione ed Elettrica e Matematica Applicata

Dottorato di Ricerca in Ingegneria dell'Informazione
XIV Ciclo – Nuova Serie

TESI DI DOTTORATO

Ancillary services in Smart Grids to support distribution networks in the integration of renewable energy resources

CANDIDATO: **FRANCESCO LAMBERTI**

TUTORS: **PROF. VINCENZO GALDI**
PROF. GEORGE GROSS

VALUTATORI: **PROF. LUIS FERNANDO OCHOA**
PROF. FABRIZIO PILO

COORDINATORE: **PROF. MAURIZIO LONGO**

Anno Accademico 2014 – 2015

I have been impressed with the urgency of doing.

Knowing is not enough; we must apply.

Being willing is not enough; we must do.

LEONARDO DA VINCI

Acknowledgements

I would like to thank and dedicate this Thesis to my family for their unconditional support and love throughout my life and my studies

I would like to express my sincere gratitude to my advisor Prof. Vincenzo Galdi for his continuous support and his motivation during my PhD course; your advice on both research as well as my career have been priceless.

I would like also to thank Prof. George Gross and Prof. Nando Ochoa for encouraging my research and for allowing me to grow as a research scientist.

A very special acknowledgment to Vito Calderaro who supported me in each step of my research activities and in the realization of this PhD thesis.

Special thanks go also to Prof. Antonio Piccolo and the guys of S.I.S.T.E.M.I. lab for their astounding support during these years.

My deepest thanks to the colleagues and friends of the University of Salerno, the University of Manchester and the University of Illinois at Urbana-Champaign for helping me to improve my work and for sharing some amazing moments in this period of my life.

It would have been impossible to achieve this without my dearest friends to which I will be forever grateful. I will never be able to thank enough Pasquale, Gianluca, Mariagrazia, Guido and Alessandro for having constantly supported and encouraged me along the journey of my PhD.

Finally, I want to thank my girlfriend Valentina who patiently revised this Thesis and supported me during the final months of my dissertation.

Fisciano, 20/04/2017

Table of contents

Acronyms

AC	Alternative Current
APCM	Active Power Control Method
AS	Ancillary Services
BESS	Battery Energy Storage System
CCD	Charging/Discharging Control
CCM	Coordinated Control Method
CEER	Council of European Energy Regulators
CLC	Coordinated Local Control
CVR	Conservation Voltage Reduction
DC	Direct Current
DCM	Decentralized Control Method
DG	Distributed Generation
DN	Distribution Network
DNO	Distribution Network Operator
DSO	Distribution System Operator
ESR	Energy Storage Resource
ESS	Energy Storage System
EU	European Union
FACTS	Flexible Alternating Current Transmission System
GDP	Gross Domestic Product
GHG	Greenhouse Gas
HV	High Voltage
ICT	Information and Communication Technologies
IEA	International Energy Agency
IEC	Internation Electrotechnical Commission
IGO	Independent Grid Operator
IPP	Independent Power Producer
LCOE	Levelised Cost Of Energy
LV	Low Voltage
MV	Medium Voltage
OECD	Organisation for Economic Co-operation and Development

OLTC	On Load Tap Changer
ORC	Optimal Reactive Control
P	Active Power
PCC	Point of Common Coupling
PV	Photovoltaic
Q	Reactive Power
RES	Renewable Energy Sources
SoC	State of Charge
STATCOM	Static Synchronous Compensator
THD	Total Harmonic Distortion
TSO	Transmission System Operator
UCD	Uncoordinated Charging/Discharging
V	Voltage

Abstract of the dissertation

In recent years, progresses have been made in developing cleaner and more efficient technologies to produce, transmit and distribute energy. Pledges made in the recent summit in Paris (21°conference of the parties - COP21, Paris 2015) and Marrakech (COP22, Marrakech 2016) on climate changes promise to give new impetus to the move towards a lower-carbon and more efficient energy system. Nowadays, mandatory energy efficiency plans are expanding worldwide to cover over a quarter of the total global consumption. Furthermore, renewables represent almost half of the world's new power generation capacity.

The deepening penetration of renewable energy resources (RESs) has forced grid operators to deal with both technical and economic challenges to harness as much green energy as possible from them. Renewable plants, solar photovoltaic (PV) based and wind farms, are often small-medium scale generation plants connected at the distribution network level. The conventional distribution networks were designed to be operated as passive networks but with the continuing integration of RESs must accommodate bi-directional flows. Indeed, the implementation of the *Smart Grid* into distribution grids will bring about the effective deployment of advances in information and communication technologies (ICT) to improvements in the reliability, resiliency, flexibility and efficiency of such grids. Under the resulting new paradigm, it is possible to identify new roles that the distribution network operator (DNO) can play as well as additional activities and services that the DNO can provide to bring out marked improvements in the distribution grid management arena. The rapid changes in the distribution grid need to be accompanied by associated changes in their operations and provide the flexibility for the operators to evolve from the conventional DNO who manages passive networks to that of the distribution system operator (DSO) to run the new bi-directional flow distribution grid.

This thesis is presented within the context of the newly evolving distribution grids managed by their DSOs. The aim of the work is to

investigate the feasibility and implementation of the provision of ancillary services able to support current and future DSOs to facilitate improvements in the harnessing of the energy produced by deeper penetrations of RESs into the distribution grids. To this end, specific services must be provided by resources in the distribution network (DN) to provide congestion relief, as well as various ancillary services (AS), such as frequency control, voltage regulation, spinning and non-spinning reserves and in some cases energy services from distributed energy resources or DERs. A key contribution of the thesis is to address the potential of three DER types – distributed generations (DGs), demand response and energy storage resources – to provide such services in DNs. Proposed strategies and approaches are tested and validated on real-world DN test systems.

In detail, the thesis discusses two proposed decentralised approaches to provide voltage support from DG resources. These approaches' objective is to avoid active power curtailments or the disconnection of RESs due to rises in voltage that usually occur in periods of high generation and low demand. The inverter that usually interfaces a DG to the DN into which it is integrated is used to implement a practical control strategy to provide reactive power support, be it either via injection or absorption of vars. Capability curves define the actual operational area that defines the amount of reactive power that is possible to absorb or inject into the grid, making curtailments/disconnections the least frequent solution performed by DSO when contingencies occur. To extend the approach of this control technique, it is possible to coordinate reactive power flows coming from different DG units of an independent power producer (IPP). The idea is to maximise active power production (and, then, reduce curtailments/disconnections) of PV and wind generators by optimising reactive power injections/absorption of DG units connected to different point of the DNs. The first decentralised but coordinated approach calculates the set points of each DG units by using the coefficients of the mixed sensitivity matrix of the network. This method results to be very fast to perform but it requires the calculation of the mixed sensitivity matrix; moreover, in some conditions, it could not give the best solution in terms of reactive power. The second method is based on the solution of a non-linear optimisation problem in order to calculate the active power-reactive power set points. By solving a

global problem, the method points out an optimal solution even if the number DG units involved in the control is nontrivial; anyway, a communication framework must be developed for the exchange of information between DSO and IPP. Each scheme with applications to an actual Italian distribution network is illustrated and a comparative analysis of their performance is provided.

To provide ancillary services by demand response resources in the DN, it is necessary to develop new load models. Two alternative formulations of the well-known ZIP model to explicitly represent the dependence of the demand on voltage changes under steady state conditions are presented. These model representations are able to provide acceptable estimates of the impacts of schemes, such as conservation voltage reduction (CVR), on the energy consumption by these loads. More in detail, the study wants to estimate how much demand it is possible to unlock by changing voltage values along the lines. To this end, an experimental study on a next-generation home appliance (a washing machine with digital control and motor drive fed by inverter) is conducted. The time-varying behaviour of domestic appliances is represented by using a *discrete-time ZIP model* to describe each phase of the appliance operations. The proposed model is capable of modelling the active power absorption of thermostatic loads, which exhibit periodic behaviour that depends on the applied voltage as well as equipment settings and the surrounding environment. To reduce the number of loads to be modelled during a time-series simulation, a time-varying formulation of the ZIP model is presented. It allows the aggregation of ZIP parameters at a given instant in time by using a polynomial structure. This model is tested on a real UK distribution network in order to estimate the amount of demand subject to change when the voltage at the primary substation is modified via an on load tap changer (OLTC).

The deployment of energy storage resources (ESRs) for the provision of certain ancillary services is investigated. The focus of the work is specifically on battery energy storage system integrated into PV systems. Two specific situations, under which the battery energy storage system (BESS) provides voltage support at the DN level, are proposed. The BESS is integrated into a PV solar farm. In detail, two controls, in which BESSs are co-located with PV units in order to provide voltage support in DNs, are presented. The former is a

sensitivity-based decentralized control approach described above reduces the reactive power needed to maintain the voltage within a specified interval when compared to the case of the same solar PV unit farm without the integrated BESS. The latter ancillary service envisages the possibility to coordinate charging/discharging periods of BESSs co-located with PV units with DSO needs. Assuming that the DSO is able to estimate generation and demand peaks during the day (when the possibility of having voltage rises and voltage drops increases), then it is possible to identify the periods of the day in which the possibility that voltage issues occur is higher. Thus, DSO can require BESSs to provide voltage support in these periods by charging/discharging according to the possibility of having voltage rises/drops. The proposed method is compared with the case in which PV/BESS are operated without supporting network operation. Energy self-consumption resulted to be comparable; moreover, the opportunity cost is estimated to associate a cost to the proposed ancillary service.

The initial design of an analytic framework to assess the deployment of ESRs within a market environment and their performance in terms of reliability, environmental and economic impacts is presented. The rather comprehensive framework provides the capability to represent all the interactions among the embedding environment of the deployed ESR with all other players/stakeholders in the grid and in the markets. The framework has the flexibility to incorporate relevant and appropriate policy issues and policy alternatives as well as to represent new market products to effectively harness ESR capabilities. The framework is able to represent the physical grid, the ESR embedding environment, if any; all resources and loads; the communication of control signals; the broadcast of market information/forecasts/data; submission of ESR offers for provision of various services; the evaluation of all reliability, environmental and economic/financial metrics of interest; attributes and sensor measurements; the physical/financial/information flows between physical resources, market players, asset owners and resource and grid operators. The design of the framework provides an interconnected four-layer framework structure consisting of a separate layer for the physical, information, market and environmental flows with the various interactions among the layers. The four- layer structure

can accommodate the consideration of all issues in the operations of ESR deployment.

Despite the number of studies available in the literature, there is limited activity in the provision of services in DNs by RESs. Technical issues as well as economic considerations has been addressed in the Thesis, giving a contribution in the field of voltage regulation by using dispersed resources for reducing the risk of curtailments and maximizing the hosting capacity. This work also contributed to the understanding that decentralised approaches can, in certain case, have similar performance of centralised ones. In addition, the role of load as an active resource in the grid has been investigated. Load models that correlate consumption and voltage have been improved and reformulated. Finally, the role of BESSs in providing ASs in DNs has been demonstrated and a preliminary framework for the assessment of their economics has been presented.

Chapter 1

The key role of DG in decarbonising the electricity sector

The world is at a critical point and needs concrete action to assess climate change. Energy is critical to global prosperity, as it underpins economic growth, social development and poverty reduction.

The current energy scenario shows that 80% of global energy sourced from fossil fuels, growing energy demand has led to increasing greenhouse gas emissions, as shown in Figure 1 [1].

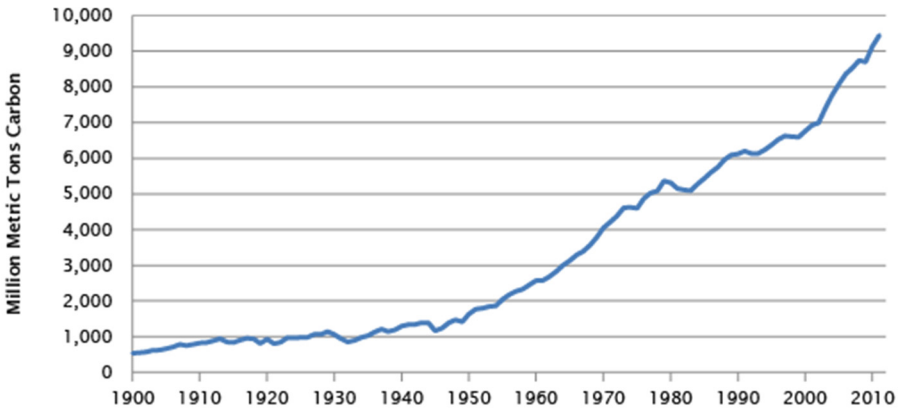

Figure 1. Global carbon emissions from fossil fuels

The energy sector generates approximately two-third of global greenhouse emissions and over 80% of total CO_2. It produced 32.1 Gt of CO_2 in 2015 [2], the largest share of which came from power generation (Figure 2).

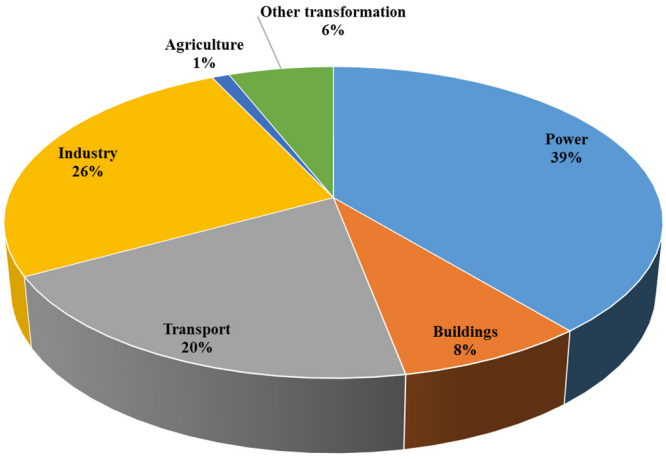

Figure 2. Global greenhouse gas emissions by economic sector

Today's challenge is to decouple economic growth and social development from increasing emissions. Energy is the key of international policy discussions, with the G7 focusing on the decarbonisation of the energy sector [3] and the G20 delivering plans on energy efficiency and energy access [4]. The Conference of Parties (COP21), held in Paris in December 2015, has established a global agreement on the reduction of climate change by setting a limit to global warming to less than 2°C compared to pre-industrial levels and to pursue efforts to limit the temperature increase to 1.5°C above pre-industrial levels [5]. To reduce global emissions, IEA identifies five key actions [6]:

- increasing energy efficiency in the industry, buildings and transport sectors;
- progressively reducing the use of the least-efficient coal-fired power plants and banning their construction;
- increasing investment in renewable energy technologies in the power sector to reach $400 billion in 2030;
- gradually phasing out fossil-fuel subsidies to end-users by 2030;

- reducing the methane emissions arising from oil and gas production.

This requires action by central and local governments, publicly and privately owned businesses, communities and individuals to support specific strategies such as energy efficiency and investments in renewables. To this end, a brief but exhaustive analysis of the key roles that distributed generations (DGs) and renewable energy sources (RESs) have in the electricity sector is presented later.

1.1 Global trends

Worldwide, the need for energy continues to increase although rate of growth in primary energy demand slows over time: from 2.5% in 2000-2010, it falls to 1.4% in the current decade and it is expected to decrease to 1% in the next and below 1% in the 2030s, as depicted in Figure 3 [7].

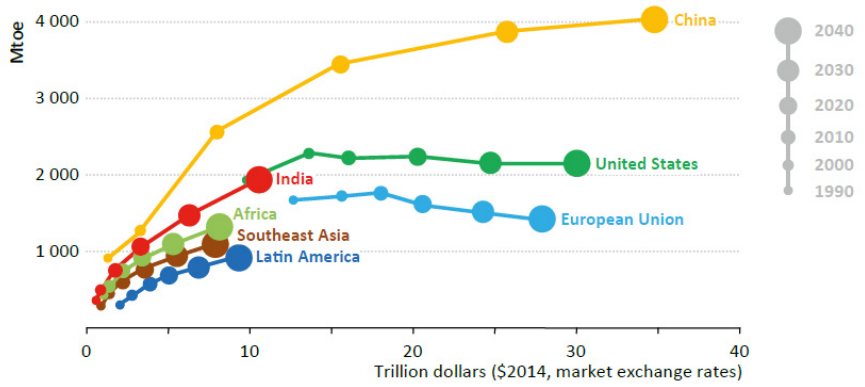

Figure 3. Primary energy demand and GDP by selected region [7]

Deceleration of global economic and population growth, coupled with robust energy efficiency policies in developed country and the slowing economic expansion of countries such as China, play a major role in the forecasted trend of future energy demand. United States and the European Union have instead already experienced a significant

de-industrialisation process with energy efficiency policies being implemented across all sectors. While in China energy consumption has grown at a pace close to the economic growth in recent decades, in Europe energy demand falls while the economy continues to expand. Countries must identify the energy resource mix capable of satisfying the growth of future demand and of reducing pollution rather than increasing greenhouse gas emissions. As depicted in Figure 4, renewable energy production should cover around 34% of the demand growth in 2040. Natural gas accounts for other 31%, nuclear for 13%, oil for 12% and coal for only 10%. Unfortunately, global oil demand is forecasted to increase around 15% in 2040 in transport and petrochemicals sectors. Asia is projected to account for four out of every five tonnes of coal consumed globally. India's industrial sector sees coal demand more than tripled by 2040, reflecting the massive industrial growth of recent and future year.

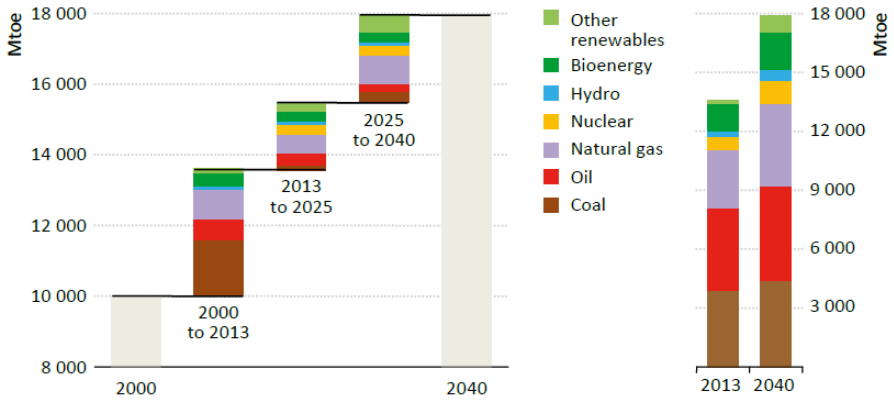

Figure 4. Primary energy demand by fuel in 2013 and 2040 [7]

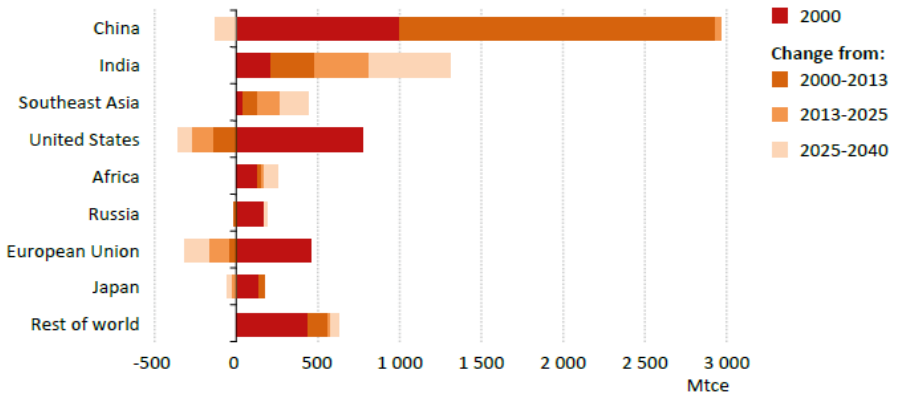

Figure 5. Coal demand changes by region [7]

By contrast, coal demand declines in almost all the developed countries. The reduction of coal demand is driven by a combination of low natural gas prices, which encourages coal-to-gas switching, increased installation of RES and policies aimed at reducing emissions in the power sector. The bar graph in Figure 5 illustrates the forecasted coal demand changes up to 2040.

1.1.1 Electricity demand

Electricity demand in a country is historically correlated to its GDP. Nowadays, growth in electricity demand and GDP gradually begin to decouple because of energy efficiency policies and the decline of energy-intensive industries in developed regions, such as Europe and the United States. Thus, electricity intensity, defined as electricity use per unit of GDP, is going to decrease in the future (Figure 6). Different rates of economic growth across regions contribute to variations in electricity demand trends. Non-OECD[1] countries, such as India and China, drive the growth in global electricity demand because of their rapid economic and population growth.

[1] The Organisation for Economic Co-operation and Development is an intergovernmental economic organization with 35 member countries. Most OECD members are high-income economies and are regarded as developed countries.

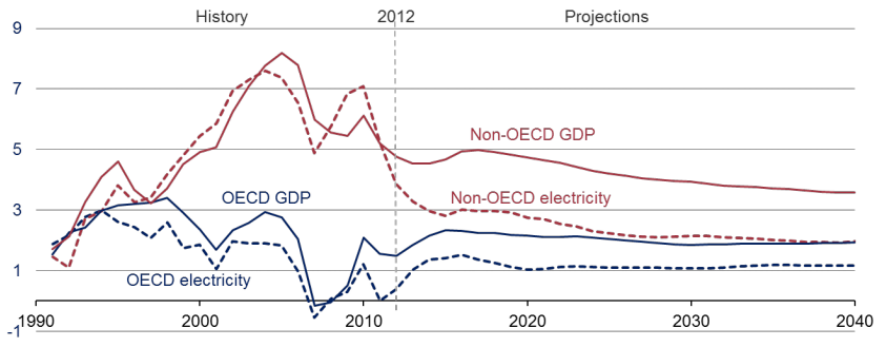

Figure 6. GDP and electricity percent growth

The International Energy Agency[2] estimates an average of 2.9% per year of electricity demand expansion for these areas with an average GDP growth rate of 4.5% and population growth of 1.0% [7]. Contrariwise, OECD electricity demand is forecasted to growth with an average of 0.7% per year. Concerning to the individual countries, as depicted in Figure 7, the increase in electricity demand in China between 2000 and 2040 is almost equivalent to the total electricity demand growth of all OECD countries between 2000 and 2013, even if its contribution in the future is set to slow over time.

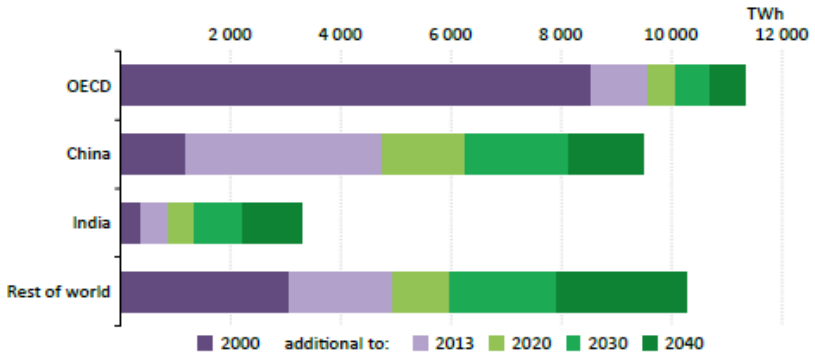

Figure 7. Electricity demand by region [7]

[2] https://www.**iea**.org/

By contrast, the projection estimates that in India the rate of growth will increase over time up to 2040. Indeed, while many regions of the OECD, such as the European Union or the United States, see a modest growth of electricity demand compared to total energy consumption, developing countries, as India, see a particularly strong increase.

1.1.2 Electricity supply

Nowadays, about two-thirds of global power generation comes from fossil fuels. Decarbonisation of the electricity sector and, in wider terms, of the energy sector is possible by investing in low carbon technologies for power production. However, this shift is highly influenced by the nature of policies that different regions pursue in addition to economic factors, such as the capital cost of power generation technologies and fuel prices.

As seen earlier, energy and also electricity demand is increasing. Considered that some generation units will be retired in the future, capacity addition in power generation is needed. Actually, OECD countries are more involved in replacing existing capacity than in adding new generation capacity, in contrast with non-OCED regions where new capacity is needed to meet the increasing electricity demand.

The choice of the technology identified to meet these different requirements will determine not only the future generation mix but also the trajectory of global greenhouse gas (GHG) emissions. In [7] the installed capacity is expected to expand by about 4400 GW. Considering that 2300 GW of generators will be retired, total capacity addition up to 2040 should be around 6700 GW (Figure 8). Of this, wind power is expected to cover around 1450 GW, while solar installation should be just below 1150 GW. Global capacity additions of renewables total just over 3600 GW, which is more than 50% of the new capacity addition.

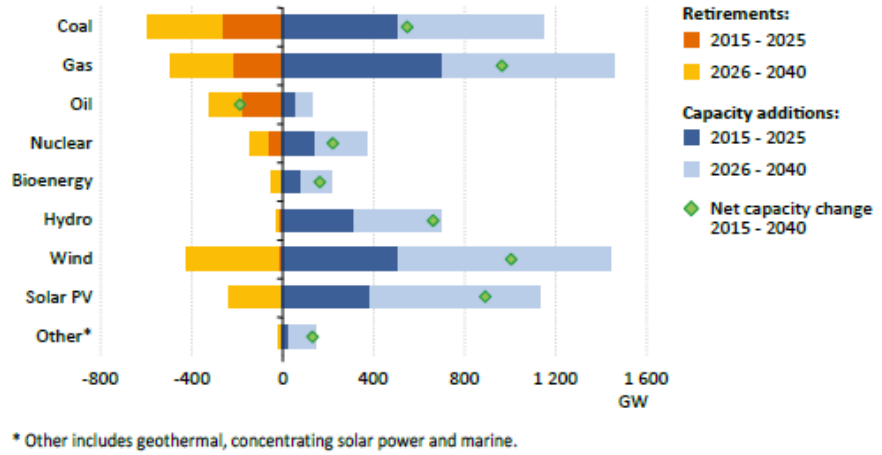

Figure 8. Global generation capacity retirements and additions [7]

The capacity of coal-fired unit is expected to increase due mostly to non-OECD countries, even if oil-fired capacity additions will not cover retirements for both OECD and non-OECD countries. Indeed, over half of the existing fleet of coal-fired plants will be retired by 2040. The change is driven by different factors, such as the availability of abundant natural gas in the United States [8] and the implementation of policies to reduce pollution in the energy sector [5]. Like the United States, the European Union retires more coal-fired units than it builds. Furthermore, the majority of capacity additions comes from renewables (about 575 GW against 135 GW of gas-fired capacity additions).

In Europe, this trend is mostly due to the low electricity demand growth up to 2040, the ageing existing fleet of power plants and a stringent commitment to decarbonise the power sector. The effort that the European Union is doing in shifting energy production in favour of low-carbon technologies is evident in Figure 9: in the European Union (EU), reliance on coal is projected to decline and by 2040 coal retains just a 6% share of electricity generation (a decline of 22%).

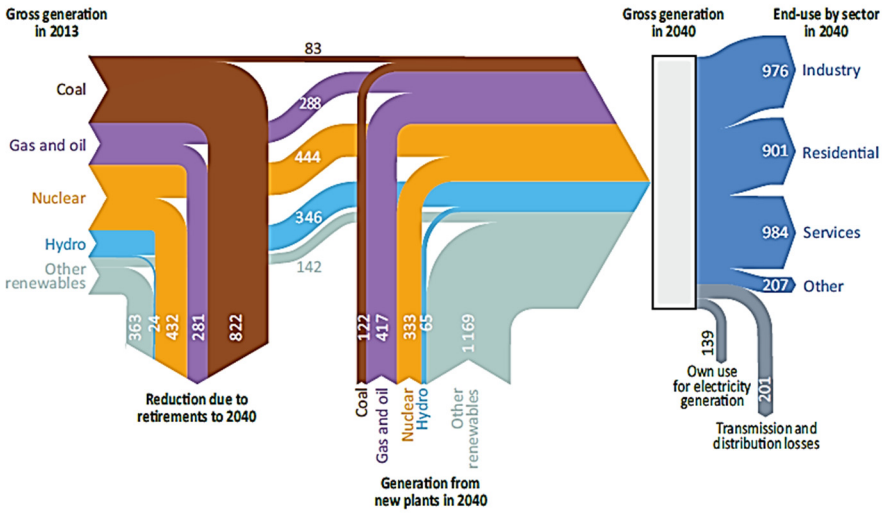

Figure 9. Power generation by fuel and demand by sector in the EU [7]

By contrast, natural gas will play a key role in the future due to its flexibility and reliability compared to renewables such as wind and solar. The increasing penetration of renewables to tackle climate change together with retirements of coal units have increased the need for a flexible generation to complement uncertainty and variability of RESs.

1.2 Technical and economic benefits of DG

Climate change can be mitigated and global temperature can be stabilized only if the total amount of CO_2 emitted is limited and emissions eventually approach zero [9]. Electrification of the energy system has been a key driver of the historical energy transformation from an originally biomass-dominated energy system in the 19th century to a modern system with high reliance on coal and gas. Electricity and heat are the largest sectors emitting fossil fuel CO_2 as shown also in Figure 10. Reducing GHG emissions from the electric power sector requires infrastructure investments and changes in the operations of power systems.

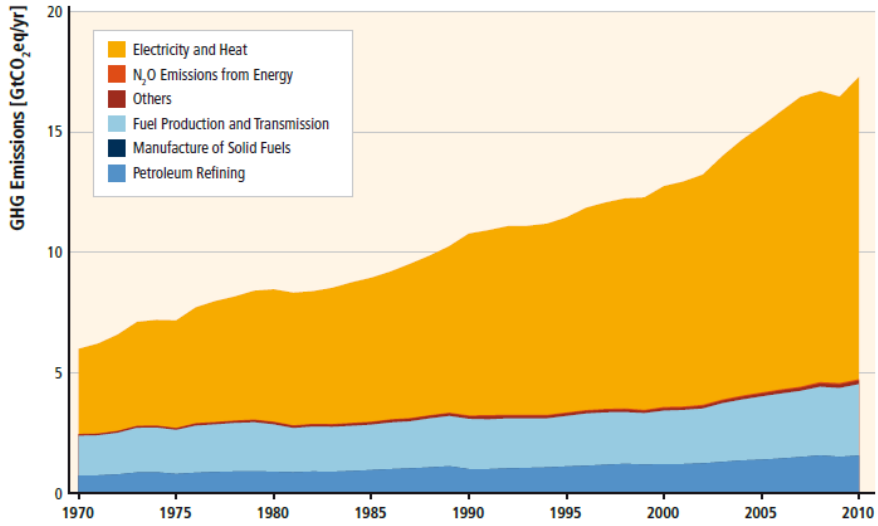

Figure 10. Energy supply sector GHG emissions by sectors [10]

Options to replace fossil fuel usage are adopting technologies for power production without direct GHG emissions, such as renewables and nuclear energy sources as well as increasing energy efficiency in transmission, distribution and at customer-side. Renewables are a major, if not the main, option to reduce GHG emissions in the electricity sector. Renewable energy is a fundamental and growing part of the ongoing energy transformation: more than 170 countries have established renewable energy targets around the world, and nearly 150 have enacted policies to catalyse investments in renewable energy technologies [11].

For instance, Europe is moving beyond the objectives of the well-known *EU Climate and Energy Package*, which aims at reducing GHG emissions of 20%, cut energy consumption of 20% and increase use of renewable of 20% by 2020 [12]. New targets intent to reduce GHG emissions to 40%, increase energy efficiency up to 40%, and increase generation from renewables to 27% by 2030 [13]. These are just part of a roadmap that wants to reduce GHG emissions by 80% by 2050 in the European Union [14].

Anyway, renewables are rapidly spreading worldwide. Wind and solar power command about 90% of 2015 investments in renewable

power because they have become competitive with conventional generators, as their costs have plunged in recent years. Unfortunately, wind and solar are variable and distributed resources that present opportunities but also challenges. To capitalise on the opportunities, adjustments are required in power market design and system regulations. On the other hand, challenges come from the integration of high penetration of RESs in distribution networks (DNs), particularly solar and wind that are intrinsically time-variable and unpredictable and can cause higher system balancing costs. Higher RES penetrations require additional flexibility in the power system. The use of RESs to limit GHG emission has been exhaustively described so far. However, from an environmental perspective, DGs allow also the reduction of the construction of new transmission lines and large power plants. Technical benefits come from the installation of RESs in power system such as the improvement of system reliability [15]. A consequence of bringing generation closer to the load is to reduce the amount of electrical losses in the system. Distribution line losses can be reduced by decreasing the current flowing in distribution feeders. To this end, if DG units are strategically located into the DN, the amount of losses can be reduced of a certain percentage.

From an economic point of view, the reduction of power system losses results in lower energy costs to final customers. Moreover, this may contribute to defer network upgrading [16]. DG units can also improve voltage stability margin and voltage profiles by supplying locally the demand [17]. This reduces the amount of current on the feeders and boosts the voltage supply at the load points. These goals can be achieved by determining a correct location, penetration level and size of RES units compared to the electricity demand of the specific DN.

1.2.1 Energy market considerations

The cost of renewable generator units is extremely different from conventional thermal power plants. It has a very low or zero marginal cost because no fuel is needed to produce energy. Anyway, the fixed costs make the levelised cost of energy (LCOE) of wind and solar comparable and sometimes higher than those of some conventional plants, as reported by Lazard in [18] (Figure 11). Since energy market

operations are based on the principle that, in normal condition, the least marginal cost energy should be used before more expensive energy, renewables usually displace generation with higher marginal costs in some periods of the day. The shift of more expensive power plants usually lowers the market clearing price (price per MWh) in wholesale markets. This behaviour has an impact on the planning program of some power plants that because of renewables may become uneconomical. By contrast, renewable energy sources are often variable and unpredictable, increasing therefore the need of flexible system resources in the grid. If flexibility is provided entirely by existing generating assets that now must recover their fixed cost by selling fewer units of energy in specific periods of the day, the market clearing price may increase. Thus, it becomes challenging to forecast the long-term impact on the average price of RESs. For sure, RESs increase competition in energy markets with an impact on electricity prices. As a consequence of increasing DG penetration, competition grows in electricity markets increasing the risk of all the players of the electricity sector.

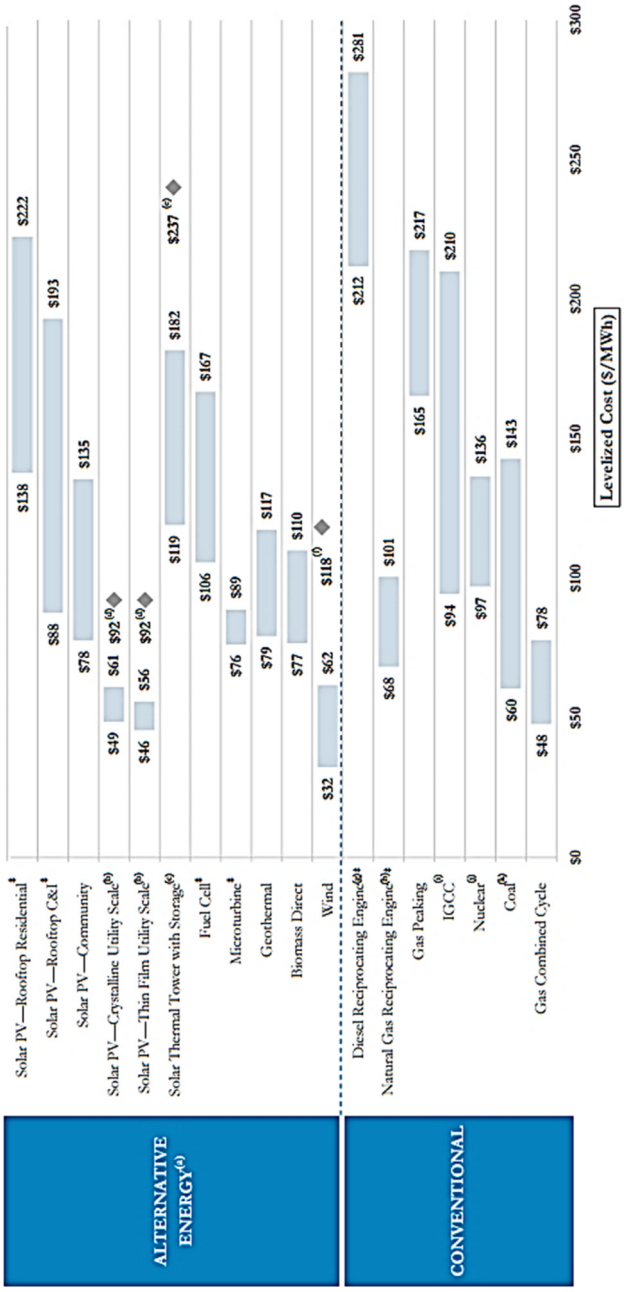

Figure 11. Unsubsidized levelised cost of energy comparison

1.3 Challenges to increase DG penetration

Distribution systems were designed to accommodate power coming from the substation and to distribute it to customers. As a consequence, power flows were always from higher to lower voltage levels. Nowadays, the significant penetration of distributed generation may reverse power flows making the distribution network an active system with power flows and voltages determined by the generators as well as the loads. This behaviour has important technical and economic implications for the operation of power systems.

1.3.1 Technical issues

Technical issues often limit the installation of RESs into the DN. Large scale integration of DG units in DNs not only affects grid planning but also has an impact on the grid operation. Several technical issues may arise with high penetration level of RESs, some of these are [19]:

- voltage control;
- power quality;
- protection system;
- fault level;
- grid losses.

The effect of RESs on grid operations strongly depends on the type of DG unit and on the type of the network. The aim of the distribution network operator (DNO) is to ensure that DGs will not reduce the quality of supply offered to the customers [19].

1.3.1.1 Voltage control

Increasing the penetration level of DGs into DNs can change voltage values along distribution lines, failing the obligation to supply customers within specified voltage limits. For instance, in Italy, the

national standard CEI EN50160 [20] limits voltage values under normal operating conditions to:

- U_n ± 10% for 95% of the 10 min mean r.m.s. during each period of one week;
- U_n + 10% / - 15% for all 10 min mean r.m.s.

where U_n is the nominal voltage of the distribution network. DGs may alter power flows and hence change the voltage dropped along the lines. Depending on the impedance of the lines, the local demand and the amount of power injected into the grid, this change in the voltage can be conspicuous and raise the voltage above the allowable values. Voltage profiles are not significantly influenced when the power injected into the grid by DG units do not overcome the load of the feeders. Indeed, the energy supplied by the grid as well as the current are decreasing, resulting in a voltage drop on the feeder. However, when the power generated by DG units exceeds the load of the feeder, voltage rises may occur. This behaviour may limit the capacity of the DN to accommodate high penetration level of DGs. Thus, the connection of DGs along the feeder may affect the proper voltage control of the distribution grid.

Keeping voltage values within mandatory limits can be achieved in several ways. An option is to reduce the voltage on the primary substation in case the transformer is equipped with an on load tap changer (OLTC). This solution works well in case all feeders have a certain amount of DGs connected, otherwise voltage may be too low on some of them. Ignoring the possibility to enforce the lines by increasing the conductor diameter, another solution is to control the reactive power and in this way to reduce the value of the voltage. This solution can be applied in several ways by using FACTS, STATCOM, synchronous machines or the DG power electronic interface [21]. However, controlling voltage profiles by controlling the reactive power flow works for distribution feeders with a sufficient X/R ratio.

1.3.1.2 Power quality

Power quality can also be affected by the DG integration in DN. The effects usually concerns three main factors:

- transient and steady-state voltage variations;
- voltage flicker;
- harmonic distortion.

Besides the steady-state effect on voltage profiles previously described, DG can also have a transient effect on voltage level. Voltage variations are usually caused by relatively large current changes during connection and disconnection of DG units or by quickly variations of their output. For instance, a rapid change in the output of a wind turbine, due to the wind that starts to blow, may cause a voltage transient. A sudden change can also occur when the wind exceeds the cut-off limit of the turbine. At that point, the wind turbine is disconnected from the grid to be protected against overload and strong mechanical forces. This disconnection can cause an increase in the feeder current and, hence, a dip in the supply voltage. Voltage flickers occur when there is a rapid and regular variation of the current. An example is the well-known effect of the tower of a wind turbine: this effect is due to the wind shielding effect of each blade of a three-blade turbine as it passes the tower. When each single blade passes the tower, the injected current is reduced, having an effect on the voltage at the point of common coupling (PCC), which results in a power oscillation with a frequency that is three times the blade turning speed [22].

Lastly, harmonic distortions are caused by power electronic interfaces that connect DG units such as wind and solar generators to the DN. The injection of harmonic currents can lead to unacceptable network voltage distortions (CEI EN50160 limits the voltage THD factor to 8% or less): a possibility to reduce it is to filter the output current.

1.3.1.3 Protection system

A number of different problems affects protection systems [23]. The majority of protection systems in DNs operates based on unidirectional power flows from the upstream network down through the lower voltage network. Due to the installation of RES units, reverse power flows may occur causing false tripping of protection systems. Moreover, the connection of the DG to the distribution grid leads to

multiple sources of the fault current, which can affect the correct detection of disturbances. Potential problems are presented in the literature, such as [19], [24], [25]:

- prohibition of automatic reclosing;
- unsynchronized reclosing;
- fuse-recloser coordination;
- islanding problems;
- blinding of protection;
- false tripping.

1.3.2 Economic and regulatory challenges

Technical issues due to DGs on DNs are usually well known. In some cases, solution and control techniques to solve them are well established. By contrast, economic and market challenges are sometimes still open questions. Liberalisation of electricity markets has enhanced competition among power producers. At the same time, promoting renewable energy has been a key in worldwide energy policies seeking to decarbonise the energy sector. Incentives/credits have been fundamental to unlock the RES market and make a project economically viable [26]. In most cases, these incentives are exclusively for renewable energy technologies, such as in Italy where the photovoltaic (PV) installations have been supported with five feed-in schemes.

Anyway, there are numerous economic variables to consider when evaluating the economics of DG units. The structure of deregulated electricity has been designed with large power producers in mind. Consequently, it is more challenging for DG units to participate in these markets than bulk power producers. For example, there are few market mechanisms able to hedge the risk coming from the variability and uncertainty of DG production. In case of any failure, they should follow balance and spot markets prices and purchase backup power at high prices to meet the offer submitted in the day-ahead market. Public policies in form of feed-in tariff programs or market mechanisms must be able to recognize positive external effects such as the reduction of

GHG emissions. This is necessary because, although costs for renewable technologies are falling, installed and established capacity such as coal-fired plants still benefits from relatively low investments and operations and maintenance costs.

Chapter 2

The transition from DNO to DSO

The deepening penetration of DERs requires technical and economic changes in order to operate efficiently these resources in current and future DNs. Smart Grid paradigm and new technologies allow the improvement of network control systems in the presence of DERs thanks also to the integration of information and communication technologies (ICT) into power systems.

From a technical perspective, DNO needs to evolve from a passive to an active role. Furthermore, the cost of renewable resources can be reduced as well as network reinforcements can be avoided or shifted over time, improving network reliability and flexibility [27].

By contrast, from an economic point of view, business models must evolve and expand beyond the current only-connection and use-of-system charges. In an environment with high DERs penetration, distribution system operator (DSO) should be allowed to expand its revenues sources beyond the provision of connections and energy transport charges only. The increasing installation over time of DGs closer to demand will reduce the volume of energy transmitted in the grid and, consequently, shrinks the revenue base of network companies [28]. New DSO business models should include interactions of utilities with different players such as transmission system operator (TSO), DER operators and customers. DSO can offer certain services to increase its revenue as well as receive certain services from different players, which will constitute part of its costs. These services, often knows as *ancillary*, will bring new stream of revenue for DSOs as well as will allow the improvement of DER management, making the most of their characteristics. The shift from the current to the described new models will see the traditional DNO evolve into an active, flexible and engaged DSO, as summarised in Figure 12.

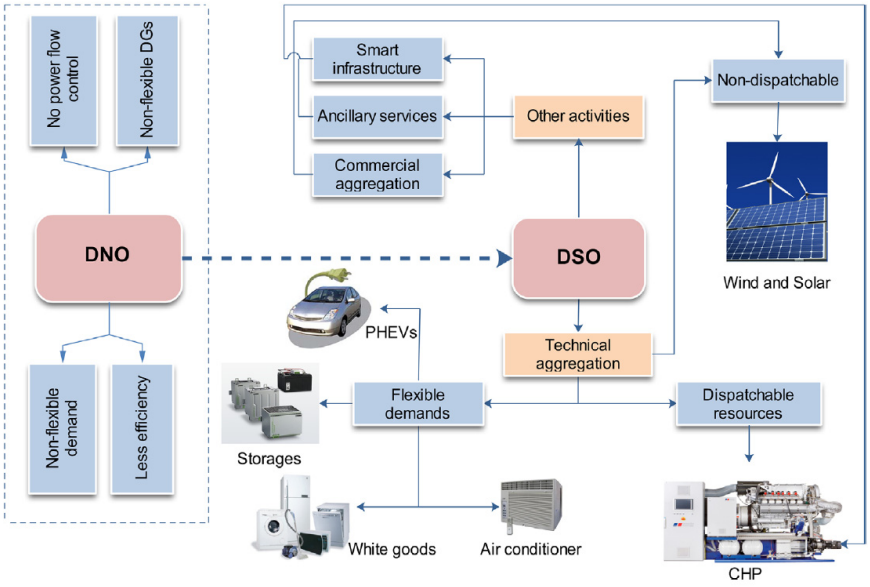

Figure 12. DNO to DSO framework transition [28]

A key point in this scenario becomes the concept of flexibility. Flexibility of operation is the ability of a system to deploy its resources to meet changes in net load, where net load is defined as the remaining system load not served by variable generation [29]. System flexibility is determined not only by the resources available, their magnitude, frequency and duration of changes in the net load, but also by scheduling decisions [30]. Source of flexibility may be found at the supply and demand sides across the power system. From a market perspective, flexibility can be used for portfolio optimisation, balancing and constraints management in transmission and distribution networks. To this end, DSO needs to improve its roles and implement new ones in order to provide new services and enhance the management of distribution network from an operational and economic point of view. Nowadays, distribution operators are in the middle of this transition that will allow to manage efficiently future distribution network. To avoid any confusion, in the following of the discussion the distribution operator will be identified as DSO.

2.1 DSO roles in an evolving environment

Up until recently, the role of distribution operators was to distribute energy to customers and design the grids based on a top-down approach. Under the paradigm *networks follow demand*, the primary role of a DSO was to deliver energy flowing in one direction, from the transmission system down to end users. This approach does not require sophisticated monitoring or control system and had perfectly worked for distribution networks with predictable flows. To this end, current DSO are in charges of the following responsibilities [31]:

- distribution planning, system development, connection & provision of network capacity;
- distribution network operation/management and support in system operation;
- ensuring high reliability and quality in their networks (power flow management);
- voltage quality.

Anyway, the paradigm is changing: networks should follow the net demand and then DSO must take into account the stochasticity due to RESs, such as wind and solar. DSO needs to evolve in the future. According to members of Council of European Energy Regulators (CEER), there are four principles that future DSOs should be taken into account [32]:

- DSOs must run their businesses in the reasonable expectations of network users and other stakeholders, including new entrants and new business models;
- DSOs must act as neutral market facilitators in undertaking core functions;
- DSOs must act in the public interest, taking into account costs and benefits of different activities;
- consumers own their data that should be safeguarded by DSOs when handling them.

However, also considering these four principles, it is not easy to clarify what are the specific actions that a DSO should undertake or not. Legislation and regulatory decisions must change to accomplish the evolving role of future DSOs. To this end, CEER has developed a conceptual framework for regulators and policy makers to identify the tasks that a DSO should accomplish in the future. The conceptual framework, depicted in Figure 13, allows the classification of DSO activities in three main categories:

1. core activity;
2. allowed activity (under specific conditions and justification);
3. not allowed, competitive non-DSO activity.

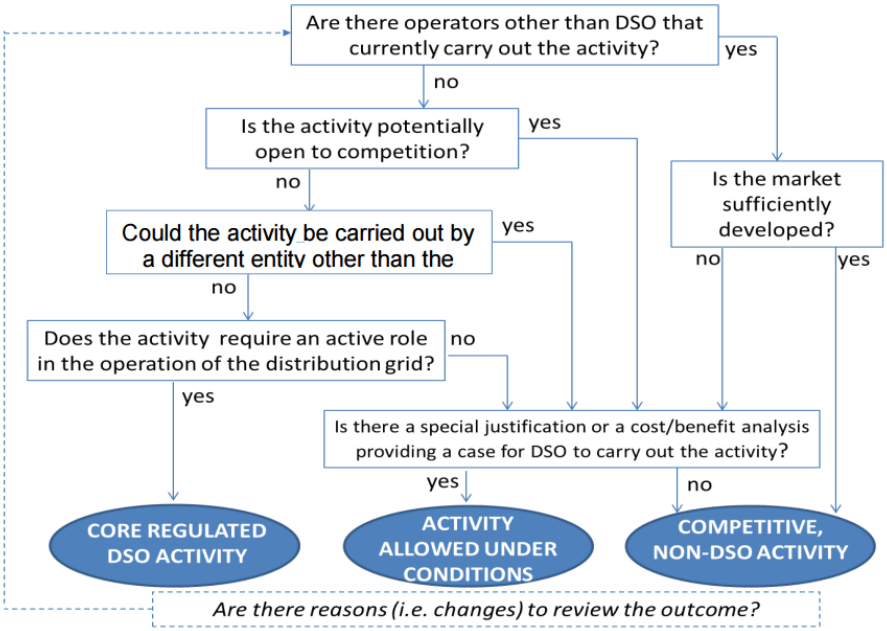

Figure 13. CEER's conceptual framework

The CEER's framework should help understanding what activities a DSO should undertake or not; anyway, for certain activities the answer is not direct and depends upon specific conditions within the considered country. Activities that fall in this grey area, where the

conceptual framework can be used, include energy efficiency or market signal advice, the extent of involvement in flexibility and storage and engagement with end customers. More DSOs are involved in non-core activities, greater is the need for regulatory control or unbundling. Furthermore, the more the energy market is developed, the less DSOs is directly involved in carrying new activities.

Nowadays, DSOs are searching for ways to enhance their observability and controllability of DNs and to cooperate with different actors such as TSOs. This requires not only to consolidate current roles of network operators but also to create new ones: an optimal use of flexibility in the network is required and must support this transition. A set of potential future DSO roles of paramount importance for the implementation of an active distribution system are identified in the *evolvDSO* project [33]. Some of these roles are completely new, others represent just an evolution of existing ones, and still others are just part of the current roles and existing responsibilities of the network operator. To tackle the challenges concerning DERs but also to exploit the opportunity that these resources can create, DSOs are interested in developing new activities in the following sectors [33]:

- planning and network development;
- forecasting, operational scheduling and grid optimization;
- real-time operation.

The aim of planning and network development is to improve network configuration of future DNs through investments able to support grid operators on the distribution of electricity. For instance, it is possible to optimise network expansion via locational signals with a clear indication of preferred location of DERs into the grid. These signals are static: they just provide an incentive at the time of the connection of the distributed resource in order to push their installation in a place where the network management is optimised.

Another crucial point is the investment on smart metering infrastructure that are massive in this area and are taking place in several countries, although at difference paces. As a matter of fact, smart meters are the first step to move toward smart grids. Investing in ICT solutions is the key to handle DERs in DNs. DSOs can harness relevant and accurate information from the grid that can be used to

enhance network observability and controllability. For instance, in Italy 95% of customers already have smart meters, as showed in Figure 14. Italian DSOs use the collected data to plans purposes and to check reverse power flows.

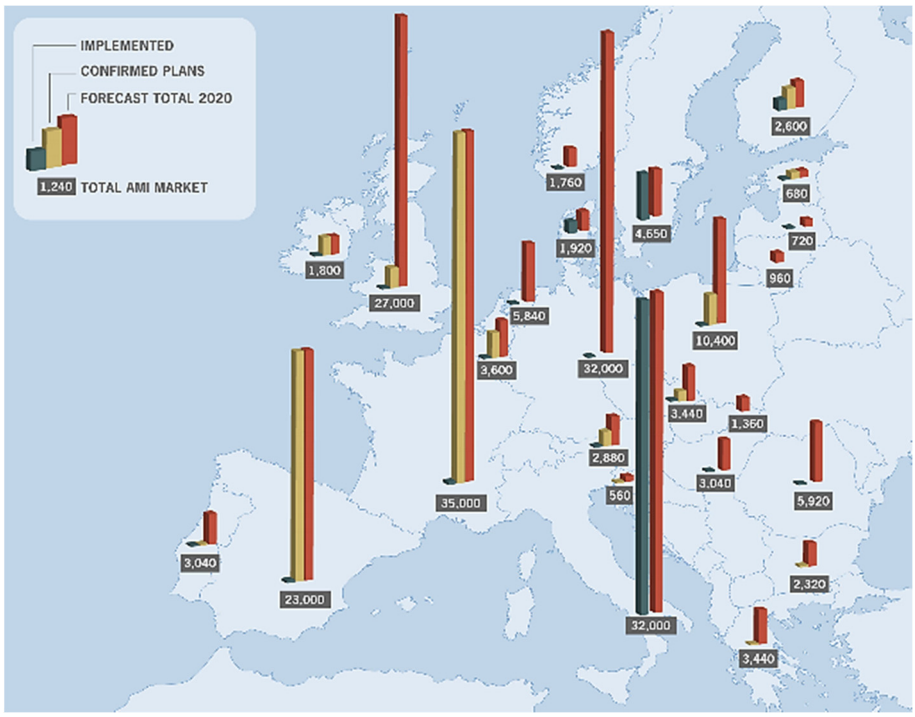

Figure 14. Smart metering status in Europe by 2016

The second area regards the forecasting, operational scheduling and grid optimization. The aim is to provide network operators with possible scenarios that might arise during real-time operation. Improving forecasting tools for DGs can anticipate possible issues such as voltage problems and grid congestions, but also reduce possible penalties due to the stochasticity of some renewable plants. Moreover, network operators are responsible for the loss of energy in the grid when serving end customers as well as for grid losses refers to the obligation of DSOs to compensate for incurred losses. They can follow an efficiency indicator, which considers a threshold for energy losses set by the regulator, or a market price mechanism. Improving grid

management can cut energy losses and therefore reduce costs that a DSO must bear to compensate. A correct application of these practices into a DN with high penetration of DERs needs a strong cooperation between DSO and TSO. Challenges imposed by DERs require an exchange of information in an effective and timely manner between both operators. By exchanging scheduling information of generation units it is possible to optimise the management of distribution grids. For instance, TSO can activate reserves from the generation located at distribution system level, when it is needed, increasing the flexibility of the entire system. Improving this cooperation is particularly relevant for the dealing with congestions and RES connections at distribution level. As previously discussed, the deepening penetration of RES may also increase situations in which congestions appear. DSO try to avoid DG disconnections or curtailments but, as more congestions appear, it will have to become familiar with those practices since TSO is not allowed to act on DNs. To this end, an intensified and standardized TSO-DSO interaction can enhance not only the operation management of the entire system, but is highly relevant for defining services to handle current and future DERs capacity as well as demand flexibility and the efficient operation of energy storage resources (ESSs).

Lastly, DSO should be able to operate in real-time for an efficient distribution of the energy. The ability to control a generation resource may provide the DSO with the possibility to alleviate congestions, to defer network reinforcements and to increase network usage. In some countries, DSO may curtail generation from RESs if the system stability is in jeopardy. Anyway, this is just a temporal measure under emergency situations that is not able to improve network operations, to increase the hosting capacity of current DNs or to increment green energy harvest from renewables. Therefore, practices that provide a direct and/or indirect control of DERs capacity, such as net metering or time-variable pricing schemes, would help DSOs to reduce RES curtailments. In that case, the overall benefits that these technologies provide would offset its integration costs.

2.1.1 Need for flexibility in distribution networks

As mentioned in Chapter 1, over a certain DG penetration level, technical issues and economic challenges arise in current DNs. Building

new networks could be a trivial but expensive solution, taking into account that in many areas the network would be constrained only for few hours per year. To this end, future DSO should be able to contract and activate flexibility resources in order to:

- enhance the hosting capacity of the distribution grid (increasing RES penetration);
- solve congestions to maintain normal operation while respecting security boundaries;
- optimize network planning;
- keep voltage levels within mandatory limits.

Flexibility can be procured directly from the resources or by means of an aggregator. Anyway, DSO must be able to contract flexibility resources based on the needs of the system. The possibility to procure flexibility in a cost-efficient way (i.e. flexibility actions would be evaluated against their opportunity costs) brings benefits not only to the entire power system, but also to stakeholders and end-users. These benefits range from the addition of capability to support the integration of RESs, to the increment of the usage of the grid and the possibility to defer or reduce investments for expanding and reinforcing distribution networks. Thus, DSO must be able to manage the increasing operational complexity of DNs. The installation of advanced monitoring systems. as well as the control of technologies together with ICT infrastructure allows the implementation of flexibility-based services to optimise network planning and operation. The integration of ICT technologies gives DSO the possibility to apply different architectural control approaches such as centralised, hierarchical, fully distributed and hybrid. Thus, DSO is capable of implementing most efficient methods and processes for operation and planning of DNs. Consequently, it becomes more proactive, able to adapt to different scenarios and to develop cost-efficient approach to manage future distribution grids. An active approach would allow an interaction between planning, operational timeframes, access and connection. Different levels of connection firmness and real-time flexibility can reduce investment needs.

On the other hand, integration of advanced monitoring and controlling systems will increase the amount of data and information available. A big amount of data must be managed in a cost-effective manner taking into account privacy and security regulations. Data collected and managed can be used to optimise the operation of the different resources in the DN and to support market players in their actions. For instance, DSO-TSO collaboration and information exchange must be empowered in the future to provide local solutions to system-wide problems such as security and reliability. Furthermore, DSOs must collaborate with market players DERs for their optimal participation in the electricity market. For instance, generation installed in DNs in the last and in the coming years can participate to different markets and providing different services. Depending by the size of the considered resources, generators can participate directly in the energy market or by means of aggregation; anyway, DSO have to collaborate to take into account distribution networks constraints and to assess the grid status in concert with potential market actions. A framework able to exchange information at different stages of the market, from resource characterisation over bidding to settlement, must be implemented. Lastly, developments in communication systems allow a higher data resolution: DSO can provide advanced services to end-customers such as flexibility services or time-of-use tariffs.

2.1.2 Potential DSO services

In order to increase flexibility and adopt the new roles previously discussed, DSO must identify and provide new services to stakeholders, such as [33]:

- optimising the development of the network by using available assets in DNs;
- elaborating distribution network multiannual master plan considering contracted flexibility;
- contracting flexibility resources to solve distribution network issues;
- optimising network operations in medium and short-term;

- optimising installation, maintenance and repair of network assets;
- delivering data to eligible actors;
- managing TSO requests.

For instance, DSO can activate services to optimise the usage of the available assets in order to prevent network constraints, to increase hosting capacity and improve the usage of the lines. Based on measurements, network data and weather forecasting DSO can optimise, for example, the number of tap change of MV/LV transformers as well as improving decisions of single-phase connection in LV networks. Although these services use only flexibility related to assets managed by DSO, it is possible to envisage the possibility to contract additional long-term flexibility connected to the distribution network via a call for tender. In a short-term period, DSO can imagine to manage, in a flexible way, grid connection and access contracts with grid users. With the final aim to prevent network constraints, DSO can stipulate new contracts as a temporal alternative to network reinforcement. Customers should benefit from fast distribution grid connection and access as well as lower connection costs. Furthermore, DSO must be able to develop services to optimise grid operation in medium-term and short-term. These services should prevent and anticipate contingency conditions based on local load and generation forecasts. In this way, these services validate flexibility activations from a technical perspective. Lastly, DSO can manage and transmit relevant data in respond to the demand of external but eligible actors by means of the implementation of a proper service. This service can enforce also the interaction and the information exchange with the TSO at different timeframes: planning, operation, real-time and ex-post.

The thesis focuses the attention on the management of the different assets in the DN to provide specific auxiliary services. To this end, DERs connected at distribution level are able to provide ancillary services in order to optimise network operations and solve technical issues in case these are located in an active distribution network.

2.2 Ancillary services in distribution networks

Ancillary services are typically defined to be used by TSOs. Anyway, the increasing penetration of RESs requires a more active management of the system in order to utilise efficiently both the network and the DERs. This scenario makes ancillary services essential at distribution level to support the DSO in operating the system. There are several definitions of AS: according to IEC "*ancillary services are services necessary for the operation of an electric power system provided by the system operator and/or by power system users*" [34]. Ancillary services can be procured by TSO or DSO and delivered by DERs at transmission or distribution level. Not all the ancillary services (AS) available at transmission level are currently in use or relevant at distribution level. Furthermore, the possibility to provide AS to the TSO by the DSO is not a common and standardised practice.

In transmission systems, ancillary services are mainly provided by large power plants to the TSO. Nowadays, ancillary services can be provided also by controllable distributed energy units to DSOs in ADNs. DERs can provide multiple ancillary services. *REserviceS* project try to grouped AS into three main categories: frequency support, voltage support and restoration services [35]. However, these are just a part of the possible ancillary services that can be provided. Some of these are:

- frequency control;
- voltage control;
- load following;
- spinning and non-spinning reserve;
- peak shaving;
- congestion management;
- reduction of power losses;
- islanded operations;
- black start.

For instance, it is possible also to improve the power quality acting on the current, the voltage or the frequency at a given point in the system. Another interesting service deals with the mitigation of voltage unbalance on the lines, in particular in LV networks. Lastly, DSO can use DGs as well as demand resources and storage systems in certain periods of the day to balance efficiently the system.

Another distinction is in terms of the willingness to provide these services. Indeed, some AS are mandatory (can be paid or not) and some are subject to payments. AS providers need to be motivated to modify their business model or their behaviour in order to support the network. The increasing penetration of DERs makes possible to operate DNs more reliably and cost-efficiently by making use of AS. DERs such as DG, demand resources and energy storage systems will be the main players in providing these services.

To incentivise their participation, markets for ancillary services are being developed: this is the case of CAISO in California or PJM in the northeast of the United States. Anyway, it is non-trivial to define products for some services (i.e. voltage control) in these new markets. The price paid for the service should cover not only the cost related to the ability of providing the service, but also the opportunity cost related to the energy not sold to energy markets, a component related to the operation and in general any extra cost incurred by the resource.

2.2.1 Ancillary services control capabilities

Some basic control capabilities for the provision of AS are active power control, reactive power control, (direct) voltage control and (direct) frequency control [36]. Active and reactive power control take advantage from the relationship that exists between active power and reactive power and voltage and frequency in the network.

In a transmission network, the flows of active and reactive power are independent. Active power control is closely related to frequency control, while reactive power control is closely related to voltage control [37]. This is due to the high X/R ratio of HV networks. Overhead lines in HV have a ratio of $R/X << 1$ and can therefore be considered as inductive. The clear functional dependency P/f and Q/V is applicable in transmission networks resulting in simple control functions for frequency and voltage. At LV level, for example, the cross

section of cables is often below 150 mm² resulting in R/X > 1 and at MV the cross section is normally around 150 mm² resulting in R/X ≈ 1. For these reasons, in DNs there are no clear dependences that can be verified and the voltage is usually function of the reactive power and the active power. These interdependencies result sometimes in more complex approaches in distribution networks for frequency and voltage control. Lastly, direct voltage and frequency control refer to control capable of defining frequency and voltage set points.

Table 1. AS basic control capabilities

Ancillary Services	Active Power Control	Reactive Power Control	Direct Voltage Control	Direct Frequency Control
Frequency Control	✓			
Voltage Control	✓	✓		
Load following	✓			
Spinning and non-spinning reserve	✓			
Peak Shaving	✓			
Congestion Management	✓	✓		
Reduction of Power Losses	✓	✓		
Islanded operations	✓	✓	✓	✓
Black Start	✓	✓	✓	✓

Active power control is necessary to control the frequency while the regulation of the voltage is the second-best option because of the higher economic value of the active power compared to reactive power. Congestion management and reduction of losses along the lines can be handled both on active and reactive power control. Active and reactive power controls are also necessary for islanded operation and black start. In addition, it is necessary for these two services to define directly the frequency and the voltage set points, as showed in Table 7.

Chapter 3

The capability of DG to provide ancillary services

There are numerous benefits but also implementation challenges in integrating DG into power systems [38], [39], [40], [41]. Power and voltage quality could worsen because of high RES penetration, which could cause unexpected voltage rises in distribution networks [42], [43].

In the literature, reactive power regulation has been proposed for voltage control at the connection bus by using decentralised approaches, often without any coordination between DG units [44], [45], [46], [47]. Lately, however, thanks to advances in Information and Communication Technologies (ICTs), which addresses power systems toward smart grids, centralised approaches are becoming of interest, although both techniques can be applied to yield good performances. Nonetheless, it is reasonable to assume that centralised controls are typically more robust and overall give better results. Refs. [48], [49], [50], [51], [52] have dealt with the voltage control problem considering a centralised approach. In particular, in [48] an optimal control voltage method with coordination of distributed installations, such as OLTC, step voltage regulator, shunt capacitor, shunt reactor and static var compensator, has been proposed. Casavola *et al*. presented a control strategy based on a predictive control idea for on-line reconfiguration of OLTC voltage set-point in MV power grids with DG [50], while in [51] a centralised approach to reduce voltage rises in distribution grid in presence of high DG penetration has been discussed. The same approach was used in [52] to provide ancillary services in distribution systems: a centralised control system in real time produces the reference signals to all converters of the DG units in order to control the reactive power injections. Furthermore, it partially compensates or eliminates

distortions and voltage unbalances either at all system buses or in areas with more sensitive loads. Interesting works on the development of ancillary services to support voltage profiles in distribution networks are described in [53], [54], [55], [56]. In particular, Authors in [53] and [54] deal with new procedures for reactive/voltage ancillary services market: the former proposes a minimization of reactive power payments by DSO to independent power producers (IPPs), power losses and voltage profile index; the latter addresses voltage control in multi-microgrid systems. The minimization of losses is also the goal of [55], where an optimal management of the reactive power, supplied by photovoltaic unit inverters, has been proposed, while a steady-state voltage control by using reactive power ancillary service provided by synchronous generators is described in [56]. Many of these approaches allow DSO to take advantage of DGs without considering potential benefits to IPPs.

To this end, two ancillary services that offer the mandatory voltage control to the DN are developed. Controls are based on a coordinated strategy able to increase active power production of RES units owned by a single IPP. Moreover, DG units disconnections or power curtailments due to the voltage issues are reduced. Control strategies operate controlling DGs' reactive/active power exchange with the distribution network by means of the power electronic converter used to interface DGs to the DN [41], [57]. Inverters can provide reactive power support within physical and technical limits. Capability curves limit the amount of reactive power that the DG unit can inject/absorb at fixed active power while international standards give a range of admissible power factor variation.

3.1 DG power electronic interface

Smart Grid paradigm, based on active/autonomous distribution networks, allows many technologies and control strategies, such as smart inverters and intelligent distribution transformers, to provide ancillary services for voltage control on distribution networks [58]. DG units can be either directly connected to the DN, such as synchronous

or asynchronous generators, or via a power electronic converter. Power electronic converters are currently used to interface renewable energy resources, such as wind and solar generators, and energy storage devices with distribution networks. Inverters have the ability to synthesise a waveform from a DC source. Figure 15 shows a typical connection of a RES unit by means of an electronic converter.

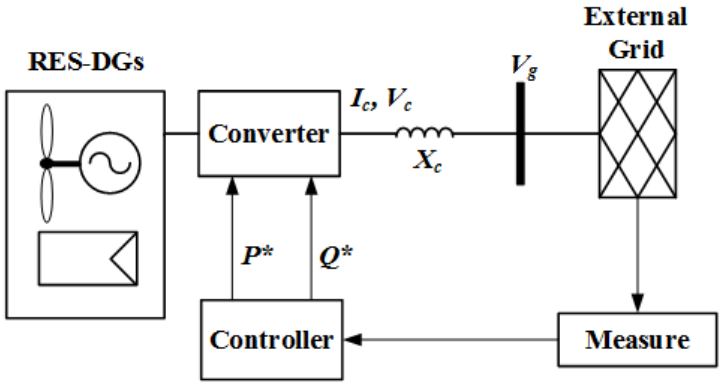

Figure 15. Voltage source converter topology

The energy resources supply power to the DC bus, which ideally is held at a constant voltage. The inverter then converts the voltage from DC to AC, injecting a current into the network across the reactor X_c, which considers both the grid filters and the transformer used for the connection of DGs into the network; finally, V_g is the voltage connection bus value. It is possible to take advantage of this electronic interface to control the voltage at the PCC by varying the P/Q ratio output of the inverter. If the DC bus voltage is fixed, the inverter may control both the phase and the magnitude of the output waveform for controlling independently real and reactive power flows [41].

3.1.1 Model of the inverter capability curve

Figure 15 depicts also the structure of the proposed control system that includes a generic electronic interface, where V_{act}, P_{DG}, and Q_{DG} are the voltage, the active power and the reactive power measured at

grid connection point, respectively (they are used in order to calculate the reference signals P^* and Q^* that drive the converter); I_c and V_c are the current output and the voltage output of the inverter, respectively; X_c represents the total reactance of the DG transformer, which adapts the DG's output voltage to the grid voltage (V_g), and the reactance of the grid filters.

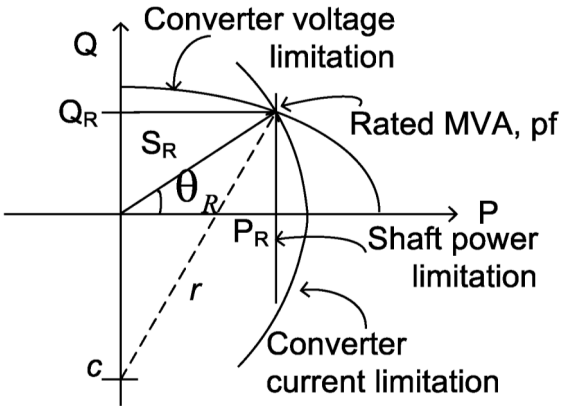

Figure 16. Capability curve [59]

The converter output power (active and reactive) is limited by the capability curves, shown in Figure 16, of the grid-side inverter connection, indicated as the converter in Figure 15. Here, without loss of generality, RES units based on Distributed Wind Turbines (DWTs) with synchronous generators and Photovoltaic (PV) systems are considered. Set the maximum available active power, the capability curves can be calculated as described in [59]. Thus, the grid-side inverter has a maximum current capacity that limits the *P*- and *Q*-capability of the RES unit. In the *PQ* plane, it traces a circle as the armature current limit for a synchronous generator (Figure 16). The relationship between active and reactive power is:

$$P_{DG}^2 + Q_{DG}^2 = (V_g I_c)^2 \quad (1)$$

where I_c is the converter current. The limit imposed by the converter voltage V_g. is similar to the field current limit of a synchronous

generator, as shown in Figure 16. Based on these analogies, the study in [59] proposes the following formulation:

$$P_{DG}^2 + \left(Q_{DG} + \frac{V_g^2}{X_c} \right)^2 = \left(\frac{V_g V_c}{X_c} \right)^2 . \quad (2)$$

The converter current can be obtained by (1) and expressed as:

$$I_c = \frac{\sqrt{P_{DG}^2 + Q_{DG}^2}}{V_g} \quad (3)$$

The converter maximum current is obtained when the active (P_R) and reactive (Q_R) power of the DG are at rated value and the grid voltage is at the minimum value $V_{g_{\min}}$ and can be formulated as:

$$I_{c_{\max}} = \frac{\sqrt{P_R^2 + Q_R^2}}{V_{g_{\min}}} = \frac{\sqrt{P_R^2 + \left(P_R \tan \vartheta_R\right)^2}}{V_{g_{\min}}} \quad (4)$$

where ϑ_R is the rated power factor of the DG unit. Considering P_R the mega volt-ampere base of the system, then $I_{c_{\max}}$ in p.u. reduces to:

$$I_{c_{\max}} = \frac{\sqrt{1 + \tan^2 \vartheta_R}}{V_{g_{\min}}} . \quad (5)$$

The converter voltage V_c can be found from the relation:

$$\left(\frac{V_g V_c}{X_c} \right) = P_{DG}^2 + \left(P_{DG} \tan \vartheta + \frac{V_g^2}{X_c} \right)^2 \quad (6)$$

$$V_c = \frac{X_c}{V_g}\sqrt{P_{DG}^2 + \left(P_{DG}\tan\vartheta + \frac{V_g^2}{X_c} \right)^2} \quad . \qquad (7)$$

The maximum value of the converter voltage is when the grid voltage and the system frequency are at maximum, and the active and reactive power at rated values. The maximum line to line converter voltage (*rms*) in p.u. is:

$$V_{c_{\max}} = \frac{f_{\max} X_c}{V_{g_{\max}}}\sqrt{1 + \left(\tan\vartheta_R + \frac{V_{g_{\max}}^2}{f_{\max} X_c} \right)^2} \quad . \qquad (8)$$

Assuming a non-sinusoidal pulse width modulation technique, the maximum dc-link voltage is:

$$V_{DC_{\max}} = \sqrt{2} V_{c_{\max}} \quad . \qquad (9)$$

The maximum available reactive power of the DG unit is:

$$Q = \min\left\{ Q_{DG}^c, Q_{DG}^v \right\} \qquad (10)$$

where Q_{DG}^c and Q_{DG}^v are:

$$\begin{cases} Q_{DG}^c = \sqrt{(V_g I_{c_{\max}})^2 - P_{DG}^2} \\ Q_{DG}^v = \sqrt{\left(\frac{V_g V_{c_{\max}}}{X_c} \right)^2 - P_{DG}^2} - \frac{V_g^2}{X_c} \end{cases} \qquad (11)$$

Furthermore, the constraints imposed by Grid Code on the power factor are taken into account in this study to better simulate reality conditions. Lastly, PF_{min} indicates the minimum value of power factor (leading and lagging) at the PCC.

3.2 Proposed voltage control strategies

Voltage regulation is normally carried out by using Automatic Voltage controller applied on On-Load Tap Changer on HV/MV transformer, off-line setting MV/LV tap position and/or by capacitor banks. As the connection of RES modifies voltage levels at customer's end and introduces different degrees of complexity, new control strategies are expected to be developed [46]. In order to offer a sustainable penetration of RESs, it is necessary to guarantee benefits for both the IPP and system operators: for the former, the network should be able to ensure the dispatching of the maximum produced power; instead, for the system operators RESs could offer ancillary services to improve the resources utilisation on the distribution systems. Among the ancillary services, the reactive power support for voltage regulation appears very promising [51].

Two coordinated control methods are proposed in the following both based on reactive power modulation injected by RES units connected to DN by means of electronic power converters. Inverter capability curves are used to define the reactive power reserve for the regulation. At the end, a comparison between the two decentralised approaches is proposed [60]. Both strategies keep voltage levels within mandatory limits and maximizing active power injection in the grid at the PCC of wind turbines and PV systems. The two coordinated approaches suppose that the considered wind turbines and PV systems belong to a single IPP able to control each RES unit. In particular, the first strategy considers a coordinated local control (CLC) approach based on a mixed DN sensitivity analysis [61]; while the second one, named as ORC [62], is based on cooperation and data transfer between DSO and IPP. Data are obtained by solving an optimisation problem with the aim of providing active and reactive power set point of the DG units to the IPP.

3.2.1 Coordinated local control

The Coordinated Local Control is based on the calculation of a mixed sensitivity matrix that allows the coordination of reactive/active

power injections/absorption of a group of DG units in order to regulate voltage along the lines. The proposed methodology assures low computational effort in order to guarantee an effective *on-line* solution to the voltage regulation problem. To set the reference values to the electronic converter, a mixed sensitivity method is introduced to regulate and coordinate active and reactive power injections at RES connection bus. In fact, the sensitivity analysis allows the evaluation of the relationship among power injections and voltage changes: in particular, sensitivity coefficients give information concerning the qualitative as well as the quantitative effect, produced by a variation of reactive power injection/absorption at RES connection bus.

3.2.1.1 Sensitivity analysis

The sensitivity analysis consists in calculating the sensitivity coefficients (ρ_Q^{xy} and ρ_P^{xy}) by varying P_{DG} and Q_{DG} injections at a generic bus x at each time step and evaluating voltage variations at generic bus y. Analytically, ρ_Q^{xy} and ρ_P^{xy} can be calculated as follows:

$$\begin{cases} \rho_Q^{xy} = \dfrac{\Delta V_{DG_Q}^x(k)}{\Delta Q_{DG}^y(k)} \\ \rho_P^{xy} = \dfrac{\Delta V_{DG_P}^x(k)}{\Delta P_{DG}^y(k)} \end{cases} \quad \textbf{(12)}$$

where $\Delta V_{DG_Q}^x(k)$ and $\Delta V_{DG_P}^x(k)$ represent voltage variations at bus x due to reactive power $\Delta Q_{DG}^y(k)$ and active power $\Delta P_{DG}^y(k)$ variations at bus y. The sensitivity matrices $\underline{\underline{\Lambda}}_Q$ and $\underline{\underline{\Lambda}}_P$ can be calculated by evaluating off-line the sensitivity coefficients ρ_Q^{xy} and ρ_P^{xy} . They can be estimated by fixing all network parameters, including load and the active power generation profiles, and by varying only the reactive/active power at each bus:

$$\underline{\Delta V}_{DG_Q} = \begin{pmatrix} \rho_Q^{11} & \rho_Q^{12} & \cdots & \rho_Q^{1n} \\ \rho_Q^{21} & \rho_Q^{22} & \cdots & \rho_Q^{2n} \\ \cdots & \cdots & \cdots & \cdots \\ \rho_Q^{n1} & \rho_Q^{n2} & \cdots & \rho_Q^{nn} \end{pmatrix} \underline{\Delta Q}_{DG_Q} = \underline{\underline{\Lambda}}_Q \underline{\Delta Q}_{DG_Q} \qquad (13)$$

$$\underline{\Delta V}_{DG_P} = \begin{pmatrix} \rho_P^{11} & \rho_P^{12} & \cdots & \rho_P^{1n} \\ \rho_P^{21} & \rho_P^{22} & \cdots & \rho_P^{2n} \\ \cdots & \cdots & \cdots & \cdots \\ \rho_P^{n1} & \rho_P^{n2} & \cdots & \rho_P^{nn} \end{pmatrix} \underline{\Delta Q}_{DG_P} = \underline{\underline{\Lambda}}_P \underline{\Delta Q}_{DGP} \qquad (14)$$

where n is the number of RES units, the elements out of diagonal are the mixed sensitivity coefficients and the diagonal elements are the sensitivity of the bus used in decentralised approach [61], [60].

3.2.1.2 Control method

The proposed control method is able to control the voltage by injecting/absorbing reactive power and, only if necessary, reducing active power. It can be explained by means of a voltage plane in which four threshold levels are defined around the rate value (V_{opt} = 1 p.u.). Considering the allowable voltage range $[V_{\min}, V_{\max}]$, it is possible to define an *operative voltage range* and a *control voltage range* by using two threshold levels $(\varepsilon_u, \varepsilon_d)$, as depicted in Figure 17.

If the measured voltage at the PCC is within the operative voltage range, no control actions are carried out; otherwise, if the value is within the control voltage range and the voltage variation is greater than zero, a certain amount of reactive/active power is injected or absorbed proportionally to the voltage variation. The amount of reactive/active power is calculated by using the sensitivity coefficients. The flow chart in Figure 18 describes duly each step of the proposed control strategy.

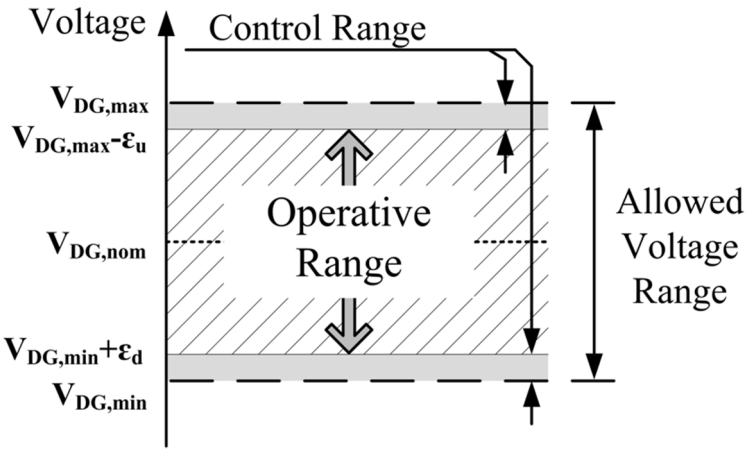

Figure 17. Allowed, Operative and Control Ranges used in the proposed control method.

The procedure begins by evaluating the difference at the PCC at bus x (ΔV_{DG}^{x}) between the voltage measured at the generic instant k and the previous one $(k-1)$:

$$\Delta V_{DG}^{x}(k) = V_{DG}^{x}(k) - V_{DG}^{x}(k-1) \quad (15)$$

If (15) is positive and the voltage is greater than $(V_{\max} - \varepsilon_u)$, the control computes the maximum value of the sensitivity vector:

$$\underline{\rho}_{Q}^{xy} = \left[\rho_{Q}^{x1}, \rho_{Q}^{x2}, ..., \rho_{Q}^{xn}\right] \quad (16)$$

where n is the number of the generator with a sensitivity different from zero at the bus x. The value of reactive absorption/injection is:

$$Q_{DG}^{xy}(k) = Q_{DG}^{xy}(k-1) - \frac{\Delta V_{DG}^{x}(k)}{\rho_{Q}^{xy}} \quad (17)$$

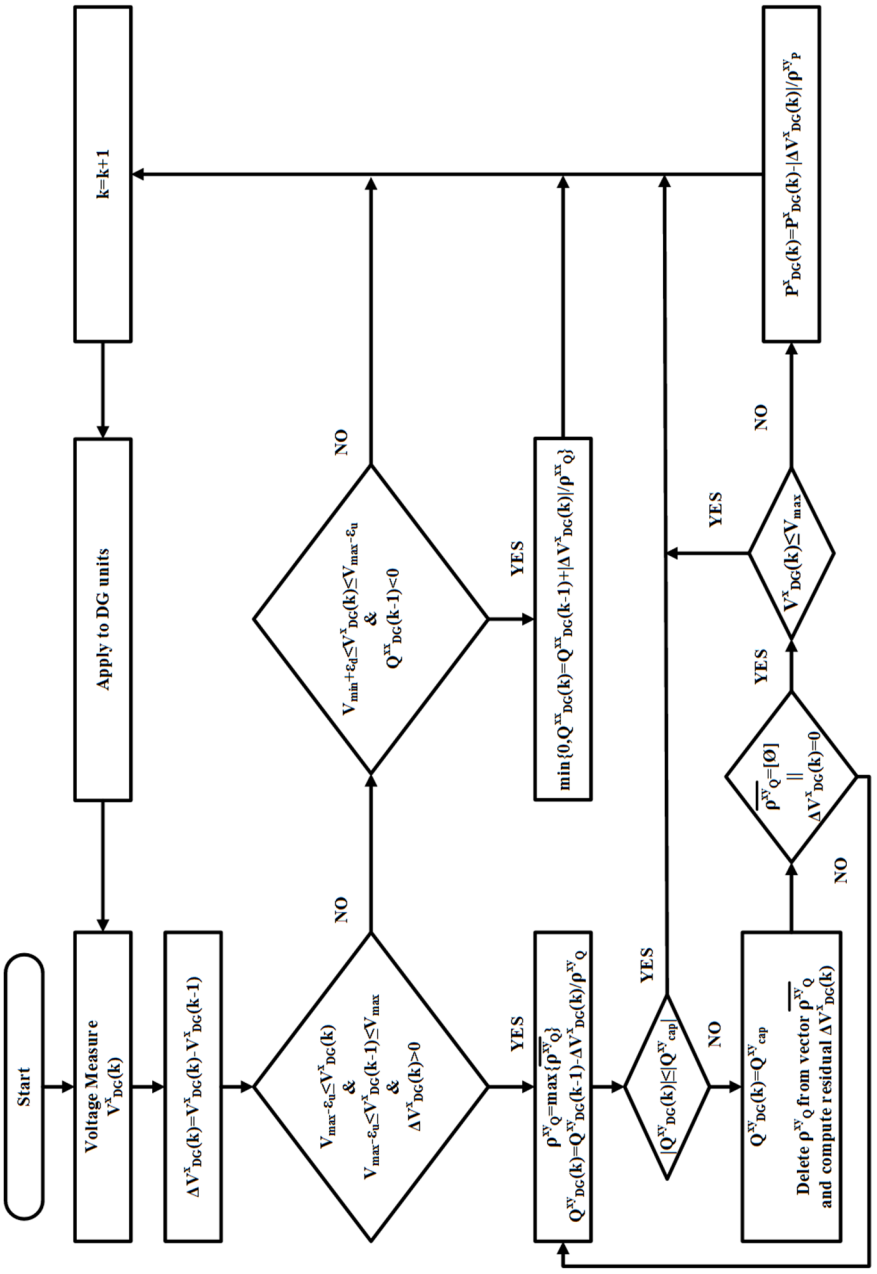

Figure 18. Control Algorithm for CLC Method

If the amount of reactive power is within the capability curve of the inverter, then the algorithm ends; otherwise, if $Q_{DG}^{xy}(k)$ is set at the value Q_{cap}^{xy}, then the maximum sensitivity value found (ρ_Q^{xy}) is eliminated from the vector $\underline{\rho}_Q^{xy}$ and the residual of $\Delta V_{DG}^{x}(k)$ is recalculated.

The cycle goes on trying to compensate the variation of voltage on the bus *x* by absorbing/injecting reactive power from the PCC of the DG within the limits imposed by capability curve until either the residual of $\Delta V_{DG}^{x}(k)$ is zero or the vector $\underline{\rho}_Q^{xy}$ is empty. At the end of this cycle the algorithm checks if the value of $V_{DG}^{x}(k)$ is smaller than the maximum allowed voltage ($V_{\max}$); otherwise, it reduces the amount of the active power at bus *x* according to:

$$P_{DG}^{xy}(k) = P_{DG_{av}}^{xy}(k) - \frac{\Delta\ (k)}{\rho_P^{xy}} \qquad \textbf{(18)}$$

where $P_{DG_{av}}^{xy}(k)$ is the power available at bus *x* at instant k.

3.2.2 Optimal reactive control

The ORC is based on a local regulation performed by an IPP, owner of some DG units connected to different PCC of the DN. In particular, the control is implemented through two different steps:

- IPP regulates the voltage profiles by means of reactive power using the sensitivity coefficients evaluated for each RES unit connected to PCC as shown in [42], [47] [51];
- IPP performs a coordinated regulation of the reactive powers among the DG units.

The previously cited references present control methods based on an *a priori* sensitivity analysis of the DN buses in order to calculate the sensitivity coefficients of the DG units that allow the variation of

voltage values on the PCC by means of reactive (or active) power. This result is achieved by applying a decentralised voltage control strategy that exploits the ability of the inverter of injecting/absorbing a certain amount of reactive power within the limits of its the capability curves. In case it is impossible to achieve a correct regulation by using only the reactive power, a variation (reduction) of the active power occurs as an ultimate solution; specifically, in case of voltage rises the control reduces the amount of active power injected into the grid. Contrariwise, in the proposed control, if the local reactive power compensation based on the sensitivity analysis fails (the reactive power reaches the capability limits), the IPP performs a coordinated regulation of the reactive powers among the DG units. The aim is to avoid possible curtailments or their disconnections due to the violation of the voltage limits. It is worth noting that only in this second case the proposed coordinated approach involves also the DSO during the control, which provides the power system state in order to develop ORC.

In detail, from an operational point of view, the *coordinated regulation of the reactive power* can be divided into three steps:

1) DSO sends data of DN state to IPP;
2) IPP control centre processes data estimating the power set points (active and reactive power) of each DG unit to control voltage profiles within technical and physical limits;
3) each generator changes the actual power set point with the new one received by IPP control centre.

Therefore, the core of the control described so far is carried out by IPPCC that solves a constrained optimisation problem to calculate the new set points.

The coordinated voltage control action takes place only if the first regulation strategy, based on the sensitivity analysis analytically described in [47], [60], fails.

3.2.2.1 Optimization problem formulation

The solution of an optimisation problem with nonlinear constraints gives as solution the set points that the IPP must use to regulate voltage

profiles. The objective function $f(\mathbf{Q_{DG}})$ to minimize is the sum of the DG Q_{DG_i} reactive powers owned by each single IPP:

$$\min_{\mathbf{Q_{DG}}}\{f(\mathbf{Q_{DG}})\} = \min_{\mathbf{Q_{DG}}}\left\{\sum_{i=1}^{N_{DG}} Q_{DG_i}\right\} \quad (19)$$

subject to the following constraints:

$$\begin{cases} V_{\min} \le V_{DG_i} \le V_{\max} \\ PF_{\min} \le PF_{DG_i} \le PF_{\max} \\ Q_{\min} \le Q_{DG_i} \le Q_{\max} \end{cases} \quad (20)$$

where N_{DG} is the number of DG units, $\mathbf{Q_{DG}}$ is the vector of the reactive powers injected/absorbed by DG units, V_{min} and V_{max} are, respectively, the minimum and maximum values of the voltage imposed by the standard [21], PF_{min} and PF_{max} are the power factor constraints (usually imposed by a national standard), Q_{min} and Q_{max} are the limits imposed by the physical capability of the converter, as described in the §3.1.1., V_{DG_i}, PF_{DG_i} and Q_{DG_i} are the voltage, power factor and reactive power values of the *i*-th DG. Furthermore, the power flow equations are considered as equality constraints of the optimisation problem.

The non-linear relationships between the constraints in (12) and the control variable Q_{DG_i} for the bus *i* are:

$$\begin{cases} Q_{DG_i} = V_i \sum_{h \in Ni} V_h \left[G_{ih} \sin(\vartheta_i - \vartheta_h) - B_{ih} \cos(\vartheta_i - \vartheta_h)\right] \\ PF_i = \cos\left(\tan^{-1}\left(\dfrac{Q_{DG_i}}{P_{DG_i}}\right)\right) \\ Q_{cap_i} = \min\left(Q^c_{DG_i}, Q^v_{DG_i}\right) \end{cases} \quad (21)$$

where V_i and V_h are the voltage values at bus *i* and *h*; G_{ih} and B_{ih} are the real and the imaginary part, respectively, of the element in the bus admittance matrix corresponding to the *i-th* row and the *h-th* column;

ϑ_i and ϑ_h are the voltage angles at the *i-th* and *h-th* bus; N_i is the number of buses directly connected to the *i-th* bus and P_{DG_i} is the total active power of the DG units connected to the *i-th* bus. $Q^c_{DG_i}$ and $Q^v_{DG_i}$ are the boundaries of the converter capability curves limited by current and voltage constraints, respectively. It is worth noting that the minimisation of the global reactive power needed to control voltage allows the reduction of conductor losses, inverter losses, transformer losses and opportunity costs.

3.2.2.2 Control method

The proposed control method realises a voltage regulation absorbing/injecting reactive power and, only if necessary, cutting active power taking into account the capability curves limits. The range delimited by standard limits [$V_{DG,min}$, $V_{DG,max}$] is defined as *Allowed Voltage Range,* as depicted in Figure 17. It is divided into three zones where the proposed control algorithm operates applying the following rules: no control actions are carried out within the *Operative Range*; an amount of reactive (active) power is absorbed/injected into the grid to satisfy the voltage constraints if the voltage variation is positive/negative within the *Control Ranges*, delimited by two threshold levels (ε_u, ε_d). In Figure 19 the flow chart of the control algorithm applied to a single DG unit is shown in the case of a voltage rise violation.

The IPPCC, after solving a power flow, calculates the existing difference between the actual (at step *k*) and the previous (at step *k*-1) voltage value at the PCC. If the voltage value $V_{DG}(k)$ exceeds [V_{max} - ε_u] and the voltage variation $\Delta V_{DG}(k)$ is positive, then the reactive power on the controlled bus is reduced according to:

$$Q_{DG}(k) = Q_{DG}(k-1) - \frac{\Delta V_{DG}(k)}{\rho_Q} \quad (22)$$

where ρ_Q is the reactive power sensitivity coefficient calculated as described in [13].

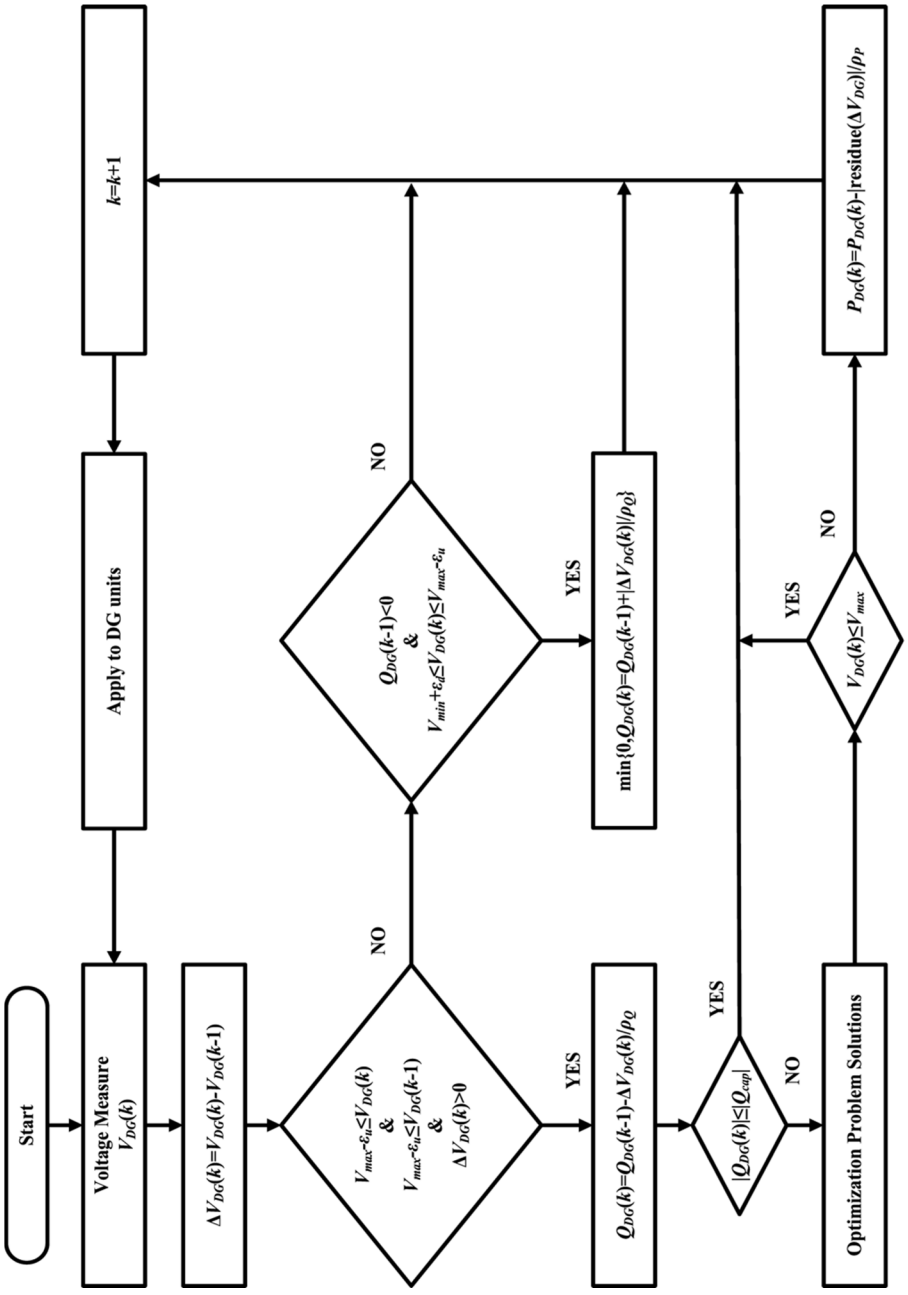

Figure 19. Control Algorithm for CLC Method

If the amount of reactive power is within the capability curves, the cycle ends; otherwise, the optimisation problem, illustrated in the previous paragraph, is solved. At the end, another voltage check on the controlled bus is carried out, and, if it fails, the active power is reduced proportionally to the residue voltage. In this case, it is possible to calculate the active power needed to satisfy voltage constraints by means of the DG unit sensitivity coefficient, ρ_P. On the other hand, if the voltage is within the *Operative Range* and the reactive power is different from zero, the algorithm reduces the reactive power absorption proportionally to the voltage variation. It is important to remark that the proposed procedure allows also the maximisation of the overall active power production because the active power curtailment is only a backup solution that occurs when it is impossible to control the voltage profiles within the mandatory limits by means of the coordination of the DG units owned by the same IPP.

3.2.2.3 Application of the SQP method

The optimisation problem is solved by means of an SQP method considering a quadratic approximation of the *Lagrangian function* as follows:

$$L(x,\lambda,\mu) = f(x) + \sum_{j=1}^{n} \mu_j h_j(x) + \sum_{i=1}^{m} \lambda_i g_i(x) \qquad \textbf{(23)}$$

where $f(x)$ is the objective function described in (19), $h_j(x)$ are the equality constraints of the power flow equations and $g_i(x)$ are the inequality constraints as in (20); n and m are the number of equality and inequality constraints included in the optimisation problem, respectively. Finally, μ and λ are the Lagrangian multipliers. Starting from the solution x_r defined in the previous iteration (r-1), at each new step the SQP algorithm provides an appropriate search direction d_r towards the solution of the following quadratic programming subproblem:

$$\begin{cases} \min\limits_{d} f(x_r) + \nabla f(x_r)^T d + \dfrac{1}{2} d^T \nabla^2_{rr} L(x_r, \lambda_r, \mu_r) d \\ \nabla h_j(x_r)^T d + h_j(x_r) = 0, \qquad j = 1, \ldots, n \\ \nabla g_i(x_r)^T d + g_i(x_r) = 0, \qquad i = 1, \ldots, m \end{cases} \quad (24)$$

The contribute d_k is used to create a starting solution for the next iteration as follows:

$$x_{r+1} = x_r + \alpha_r d_r \quad (25)$$

where α_r is the step length parameter determined by using an appropriated line search procedure, so that a sufficient decrease in a merit function is obtained [63]. The notable point of SQP is that it is a classical robust solution method in optimisation theory that can deal effectively with inequality constraints. It has good performances in solving nonlinear constrained problems, which makes it a quite effective approach among the normal line search methods and widely considered as one of the most prominent algorithms in nonlinear programming. Furthermore, SQP allows obtaining a global optimisation if a merit function is properly chosen extending the part convergence to global convergence [64].

3.3 Case studies

The two proposed voltage control methods are tested on a real Italian MV distribution network located in Sicily, south of Italy. The diagram of the network is depicted in Figure 20. It is a 20 kV distribution system with 4 feeders fed by a 132 kV, 50 Hz sub-transmission system through a 150/20 kV Δ/Y_g transformer with rated power of 25 MVA. The tap is set to 1.006 p.u., according to one of two classical Italian control strategies for distribution systems [46].

The network consists of 54 buses. Two wind farms (WFs) with a rated power of 5 MVA are connected at bus 46 and bus 54. Two PV

units with the same rated power are connected to bus 31 and bus 53. The four feeders have different load concentration levels (high concentration of *feeder A*, medium on *feeder B* and low on *feeder C*). Data of interest referred to the MV distribution network are reported in Table 2 [65].

The normalized time-series profiles used to simulate residential, commercial and industrial load profiles are depicted in Figure 21. The generation profiles of PV units and WFs are showed in Figure 22. The resolution of the daily time-series profiles is 10 minutes. The normalized profiles are multiplied for the rated power of each load/generator to have the daily absorption/generation on each bus of the distribution network. The rated powers of the loads are reported in Table 3, together with network data showed in Table 4.

Table 2. Network characteristics

Feeder	Total Length (km)	Cable Lines (km)	Uninsulated Overhead Lines (km)	Feeder Section Variation (mm^2)
A	17.23	7.63	9.60	3x(1x50) ÷ 3x(1x120)
B	4.30	4.30	---	3x(1x95) ÷ 3x(1x185)
C	20.37	---	20.37	3x(1x35) ÷ 3x(1x150)

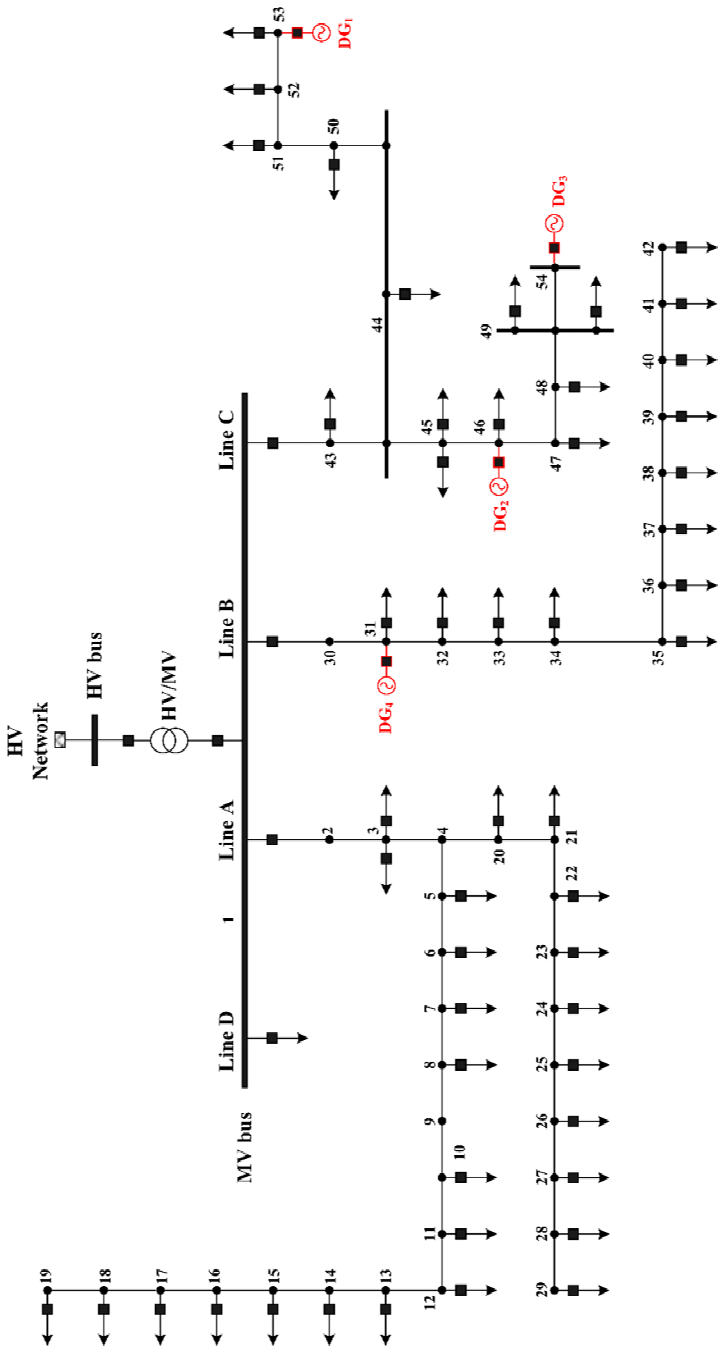

Figure 20. Distribution network diagram

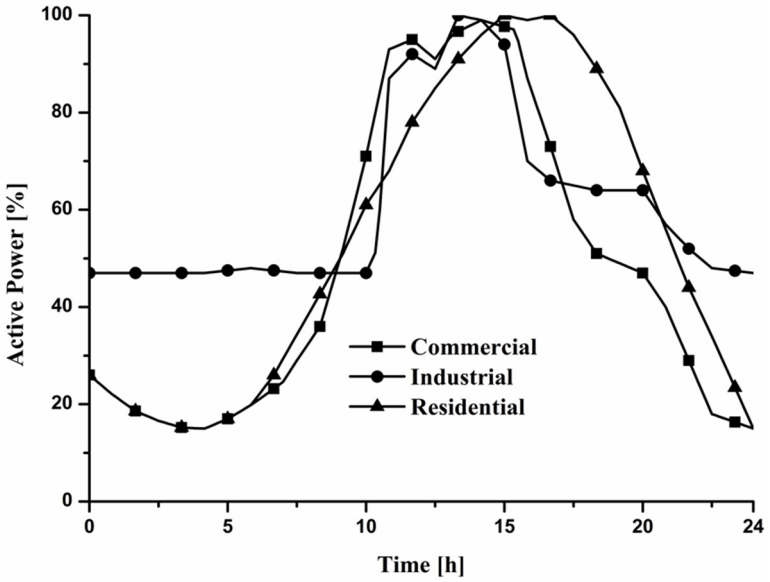

Figure 21. Normalised load profiles

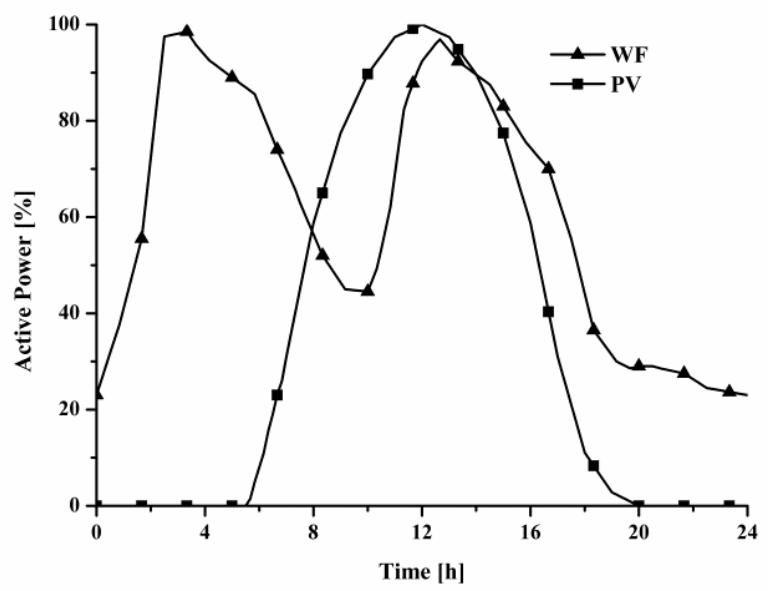

Figure 22. Normalised photovoltaic and wind generation profiles

Table 3. Line Parameters

N° of bus		Length	r	x
from	**to**	**[km]**	**[Ω/km]**	**[Ω/km]**
1	2	5.000	0.253	0.359
2	3	1.600	0.206	0.344
3	4	3.000	0.206	0.344
4	5	0.900	0.320	0.126
5	6	0.190	0.320	0.126
6	7	0.200	0.320	0.126
7	8	0.700	0.443	0.132
8	9	0.700	0.443	0.132
9	10	0.001	0.387	0.138
10	11	0.300	0.443	0.132
11	12	0.600	0.320	0.126
12	13	0.505	0.641	0.138
13	14	0.250	0.443	0.132
14	15	0.370	0.320	0.126
15	16	0.750	0.320	0.126
16	17	0.300	0.387	0.138
17	18	0.320	0.387	0.138
18	19	0.320	0.387	0.138
4	20	0.932	0.320	0.126
20	21	0.747	0.320	0.126
21	22	1.250	0.320	0.126
22	23	0.390	0.320	0.126
23	24	0.400	0.320	0.126
24	25	0.550	0.320	0.126
25	26	0.350	0.320	0.126
26	27	1.550	0.320	0.126
27	28	0.890	0.320	0.126
28	29	0.750	0.320	0.126
1	30	0.200	0.320	0.126
30	31	0.143	0.164	0.113
31	32	0.410	0.320	0.126
32	33	0.568	0.320	0.126
33	34	0.520	0.320	0.126
34	35	0.390	0.320	0.126
35	36	0.278	0.320	0.126
36	37	0.251	0.320	0.126
37	38	0.343	0.320	0.126
38	39	0.200	0.320	0.126
39	40	0.639	0.320	0.126
40	41	0.010	0.320	0.126
41	42	0.350	0.320	0.126
1	43	5.343	0.206	0.344
50	51	0.060	0.524	0.390
51	52	0.876	0.524	0.390
52	53	0.400	0.524	0.390
43	44	2.564	0.206	0.344
44	45	3.000	0.206	0.344
45	46	4.480	0.206	0.344
46	47	1.400	0.524	0.390
47	48	2.580	0.524	0.390
48	49	0.500	0.524	0.390
49	54	0.750	0.524	0.390
44	50	1.370	0.524	0.390

Table 4. Load Characteristics

Bus	Active Power* [MW]	Reactive Power*[Mvar]	Profile**
1	4.752	2.301	I
2	0.000	0.000	0
3	2.698	1.307	I
4	0.000	0.000	0
5	0.124	0.060	R
6	0.025	0.012	C
7	0.124	0.060	R
8	0.124	0.060	R
9	0.000	0.000	0
10	0.174	0.084	I
11	0.198	0.096	I
12	0.124	0.060	R
13	0.124	0.060	R
14	0.124	0.060	R
15	0.124	0.060	R
16	0.124	0.060	R
17	0.124	0.060	R
18	0.198	0.096	I
19	0.050	0.024	R
20	0.124	0.060	C
21	0.124	0.060	C
22	0.124	0.060	R
23	0.124	0.060	R
24	0.124	0.060	R
25	0.124	0.060	R
26	0.124	0.060	R
27	0.124	0.060	R
28	0.124	0.060	R
29	0.124	0.060	R
30	0.000	0.000	0
31	0.158	0.076	C
32	0.038	0.018	C
33	0.158	0.076	R
34	0.252	0.122	I
35	0.158	0.076	R
36	0.252	0.122	I
37	0.158	0.076	R
38	0.104	0.050	C
39	0.252	0.122	I
40	0.158	0.076	R
41	0.268	0.130	I
42	0.158	0.076	R
43	0.270	0.131	R
44	0.383	0.185	R
45	0.324	0.157	R
46	0.090	0.044	R
47	0.054	0.026	R
48	0.036	0.017	C
49	0.216	0.105	R
50	0.036	0.017	R
51	0.774	0.375	R
52	0.036	0.017	R
53	0.144	0.070	R
54	0.000	0.000	0

*The values of active and reactive power of the tables are multiplied for the normalised profiles shown in Fig. 5a

**R: Residential, I: Industrial, C: Commercial, 0: No Load

The workstation is an Intel Xeon E3-1230 V2 (3.30 GHz, 64 bit) processor, 16 GB of RAM. Power flows are solved by means of MATPOWER 6.0 [66] installed on MATLAB™ R2013a.

Time series simulations are carried out with a resolution of 10 minutes. The voltage limits are fixed to ±5% of the rated voltage, according to the IEEE Std. 1547. Power factor is limited between 0.95 lagging and 0.95 leading. Different countries have a standard in order to limit the power factor of DG connected at the distribution level. Without loss of generality, in Italy the standard CEI 0-16 limits the power factor at 0.95 (lagging and leading) for the WFs on MV networks. The threshold values are set to $\varepsilon_u = \varepsilon_d = 0.015$.

Voltage rises occur at the PCC of bus 54 and bus 46 during periods of high generation, as visible in Figure 23. The dashed lines of Figure 23 specify the band of the Control Range, where the greater one also indicates the maximum limit allowable for the voltage (1.05 p.u.). The DSO could send a request to reduce the active power injected into the grid or to disconnect the generator to solve voltage issues along the lines.

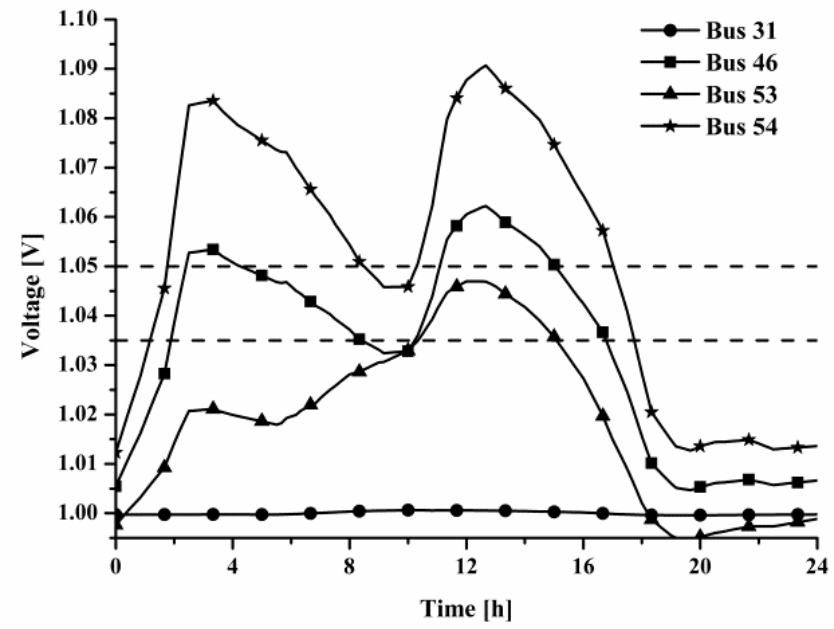

Figure 23. Daily voltage profiles at the PCC of DGs

3.3.1 CLC simulations and results

The sensitivity matrix is calculated by using the procedure described in the §3.2.1. The sensitivity coefficients relating to the generator connected to the bus 54 are represented by the average of the angular coefficients of the curves depicted in Figure 24.

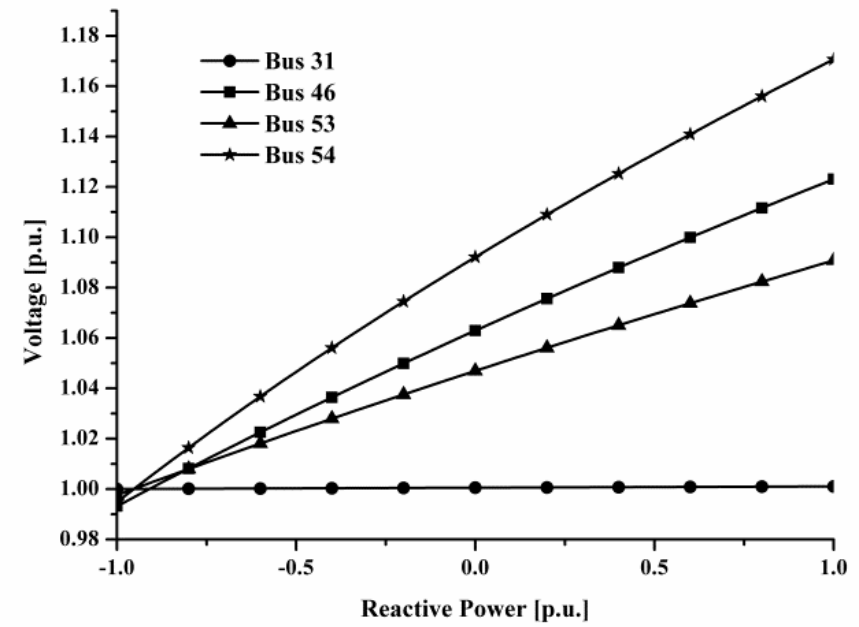

Figure 24. Reactive power sensitivity curves calculated at bus 54

The sensitivity is not zero for the bus on the same feeder of the DG connected at bus 54. It is worth to note that when the reactive power reaches the limit of the capability curves, the CLC takes advantage of reactive power availability provided by other RES units in order to achieve the voltage control. The CLC method exploits this intrinsic characteristic of the network by controlling the voltage at the bus 54 by using the reactive power of the DG-54 up to the limits of the capability (or the limits imposed by the standard) and then the reactive power of DG-46. Indeed, bus 46 is the second with the higher sensitivity coefficient at the bus 54. Thus, DG-46 is the one with the highest ability to modify the voltage at bus 54 after DG-54. Only if voltage issues

persist on the feeder, an active power curtailment is required. The results achieved by using the proposed CLC strategy are depicted in Figure 25.

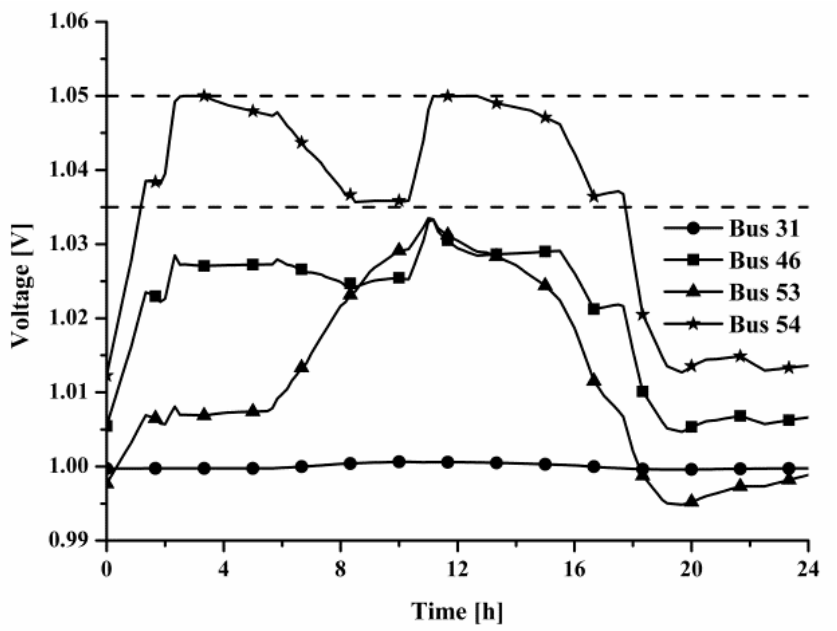

Figure 25. Daily voltage profiles at the PCC of DGs by using CLC

The method keeps voltage profiles within the limits imposed by the standard (±5% of the rated voltage) during the whole day. The reactive power absorption needed to achieve a correct voltage control is depicted in Figure 26. It is worth noting that DG-46 absorbs reactive power also if the voltage at its PCC is within the limits (below 1.05). The reason is that DG-54 cannot absorb more reactive power because in that period of the day its power factor is equal to 0.95. Therefore, DG-46 start to absorb reactive power trying to reduce the voltage values on the bus 54 avoiding a reduction of active power injection.

The capability curves, the standard limits (identified as power factor curve) and the operating points of DG-54 are depicted in Figure 27, where is possible to note that operating points do not violate any limits throughout the day: at the end, a correct voltage regulation is achieved.

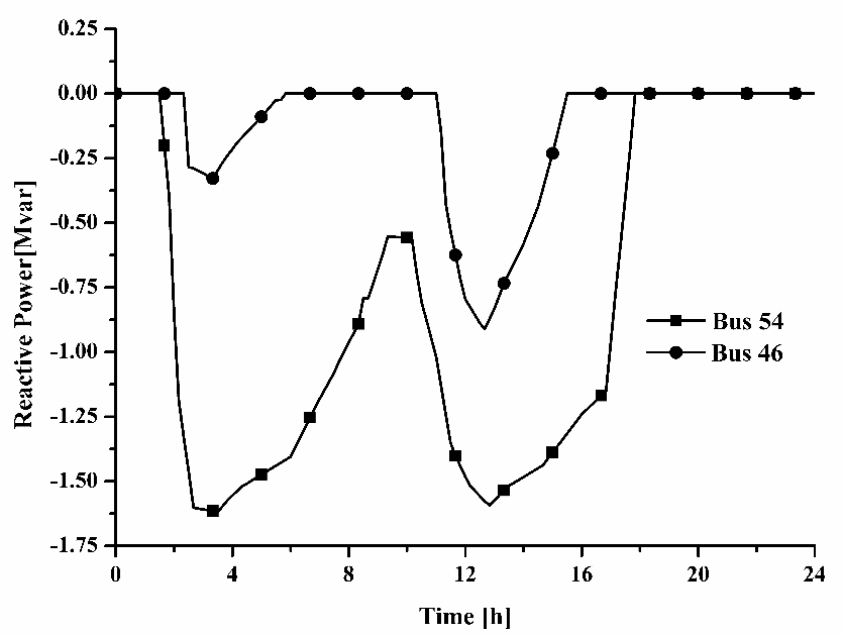

Figure 26. Daily reactive power profiles at PCC by using CLC

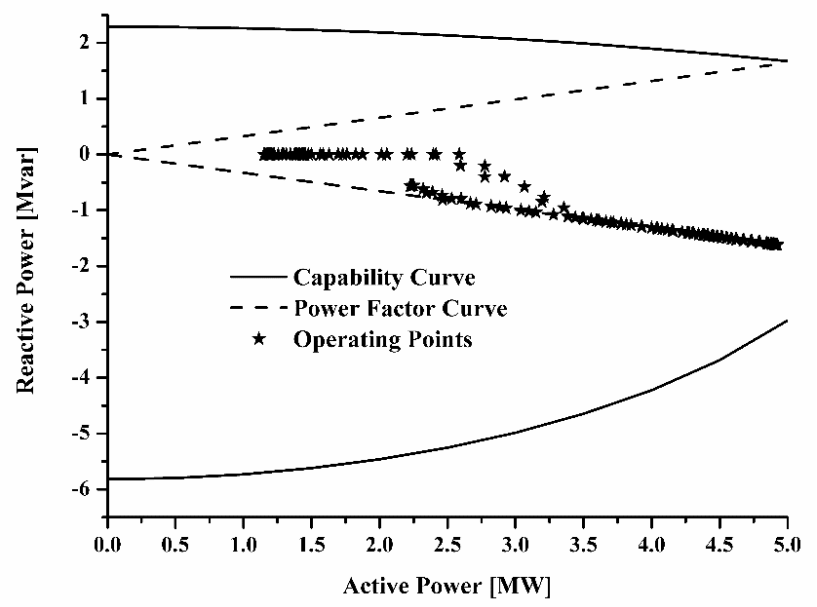

Figure 27. Capability curves of DG-54 by using CLC

3.3.2 ORC simulations and results

The aim is to illustrate the potential benefits introduced by the proposed ORC method compared to two types of voltage control strategies more common in the literature. The first one, denoted active power control method (APCM), consists in a simple active power curtailment proportional to the voltage violation in order to solve voltage rises along the lines. The second one is a decentralized control method (DCM) that uses the sensitivity coefficients proposed in [42], [47], [51] for absorbing/injecting to absorb/inject reactive power to control voltage profiles at the PCC.

The average simulation time to perform the ORC is around 21 s by using the workstation described in Paragraph 3.3. In any case, it is worth noting that the machine has required always less than a minute to give a solution of the implemented optimisation problem. This is fully compatible with the control step time of the time-series simulation, set in 10 minutes. However, the convergence times depend on the case study taken into account. The SQP has been implemented in MATLAB™ setting the maximum number of iterations to 1000, considering a tolerance of $1e^{-3}$ for the step size, $1e^{-6}$ for the objective function and $1e^{-20}$ for the magnitude of any constraint functions.

The starting condition is the same of the CLC method, there are voltage rises on the bus 46 and bus 54. By using one of the three described control methods (APCM, DCM and ORC), it is possible to achieve a correct voltage regulation at bus 54, as illustrated in Figure 28. Voltage issues can be solved indistinctly by using the APCM, DCM and ORC method. Nevertheless, these strategies are characterised by significant differences in terms of active and reactive power usage. In Figure 29 and Figure 30, active and reactive power injections/absorptions for these three methods are illustrated.

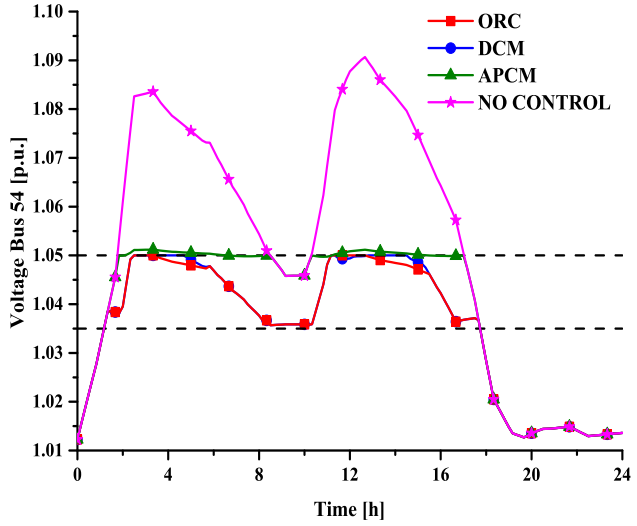

Figure 28. Daily voltage profiles at bus 54 by using different control strategies

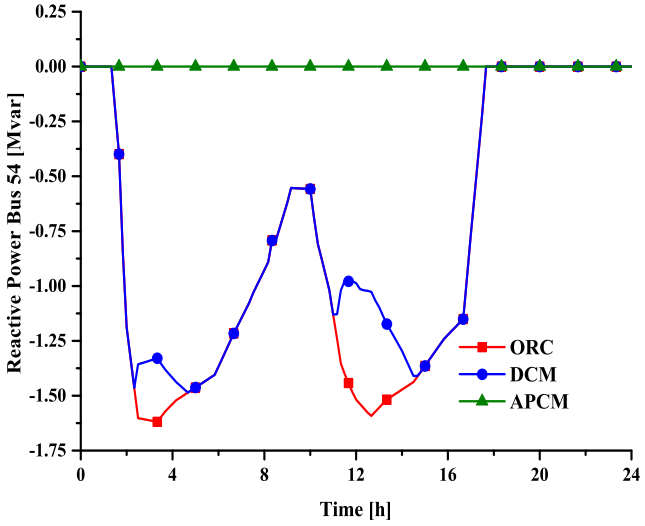

Figure 29. Daily reactive power profiles at bus 54 by using different control strategies

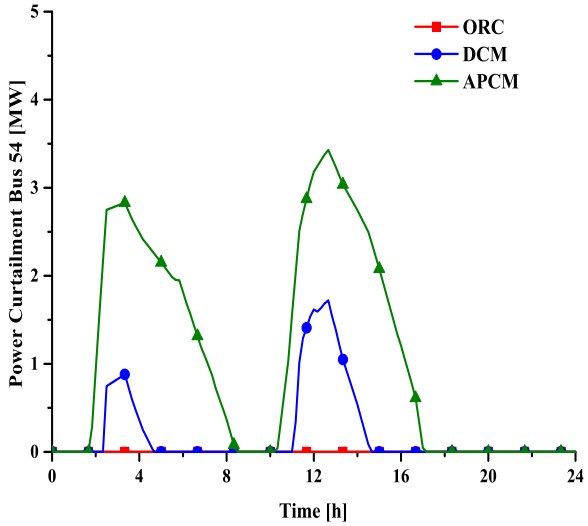

Figure 30. Active power curtailments of DG-54 by using different voltage control strategies

In detail, the DCM compared with the APCM allows reducing active power curtailments during the day by absorbing reactive power up to the limits imposed by the capability curves. As matter of fact, simulation results highlighted an increment of 81.5% in the active power production on a whole day using the DCM instead of the APCM for this specific case study.

Furthermore, as depicted in Figure 30, the coordinated control method (CCM) allows the injection of all the available active power increasing the production of 18.5% compared to the DCM. Figure 31 shows that this result has been obtained increasing the reactive power absorption at the bus 46, which has not already reached the capability curves limits. Nonetheless, CCM requires a daily reactive power absorption of 19.38 Mvarh that is slightly greater than 17.73 Mvarh needed to apply the DCM approach, as showed in Table 5.

Table 5. Comparison between voltage control methods

Control Method	Active Power Curtailment during a day [MWh]	Reactive Power Absorption during a day [Mvarh]
APCM	25.89	0.00 (ind.)*
DCM	5.04	17.73 (ind.)
CCM	0.00	19.38 (ind.)

Comparing Figure 31 and Figure 32, it is possible to see the same behaviour illustrated for the CLC: DG-46 absorbs reactive power supporting the bus 54 in voltage regulation, even though the voltage at bus 46 is within the mandatory limits and out of the range of control (Figure 32). Finally, a further check has been carried out on the capability curves. Indeed, Figure 33 shows the set points elaborated by the IPPCC solving the constrained optimisation problem. Also, in this case, the control works properly: in fact, all the set points are within the standard imposed by national standard (dashed lines) and physical limits (continuous lines).

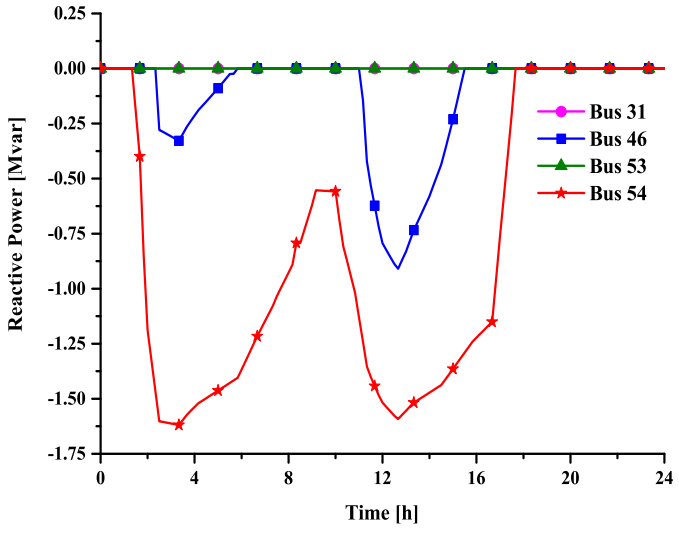

Figure 31. Daily reactive power profiles at the PCC of DG units by using ORC

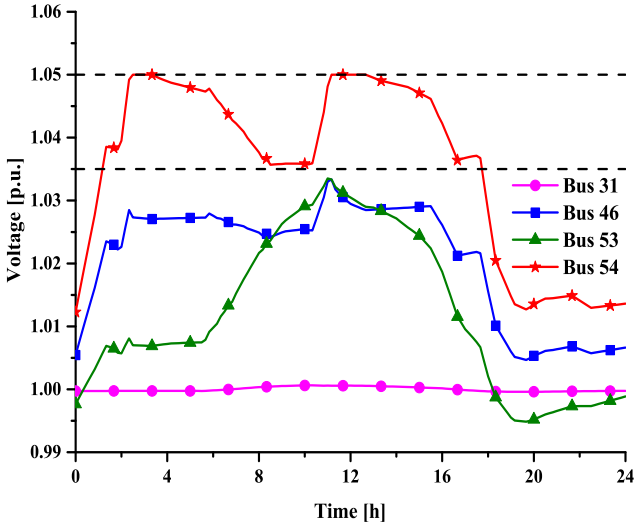

Figure 32. Daily voltage profiles at the PCC of DG units

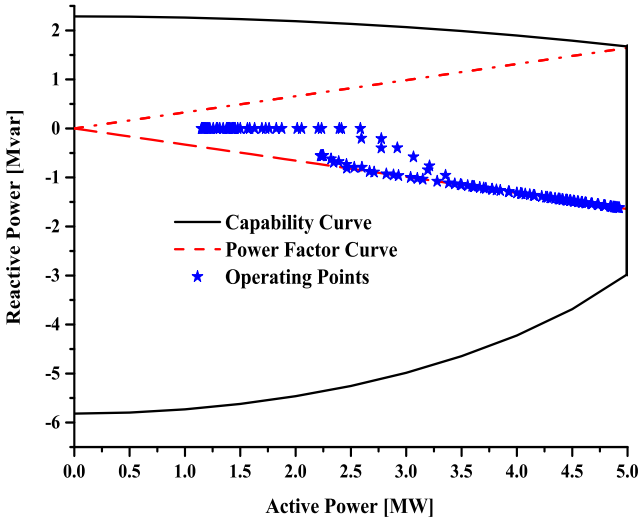

Figure 33. Capability curves of DG-54

Chapter 4

Load as an active energy resource

One of the aspects of the transition towards Smart Grids is the ability to manage demand, particularly given the continuous need to defer investments to expand and reinforce distribution networks. This is mostly seen from the perspective of the infrastructure needed to integrate participants in demand response schemes (typically involving an economic incentive). Organized electricity and ancillary service markets are beginning to support demand response resources for providing ancillary services, as in the United States.

However, the advent of advanced capabilities to manage voltages at different distribution levels has attracted new attention to other possible ancillary services in which the demand is involved. For instance, conservation voltage reduction (CVR) techniques [67] are based on the simple principle that (certain) loads change with voltage, therefore a reduction in voltage can lead to savings in energy consumption (for customers). This technique has been performed to different extents since the '70s [68]. Initially, these methodologies did not have many applications mainly because it was difficult to deploy it over a wide area without causing problems to the network and loads (due to voltage drops below statutory limits). Nevertheless, recent studies on voltage optimisation and *volt-var* control, have drawn more attention on CVR [69], [70], [71], [72], [73] given that they could, in the future, allow the control of voltages accordingly.

From the perspective of a distribution network operator (DNOs) subject to unbundling rules (such as in Europe), it is therefore plausible to envisage an ancillary service based on the active management of voltage regulation devices in order to increase/decrease the demand during certain periods for the benefit of the network (e.g., peak shaving, congestion management) or the whole system (e.g., fast reserves). The

extent to which this voltage-driven demand response can actually help in managing the network is however entirely dependent on the instantaneous load composition – that might have small changes minute by minute but is significantly different from day to night and from season to season. To this end, it is essential to develop accurate load models to analyse and accurately simulate electric power systems and to calculate correctly the effect of voltage modulation both in simulation analysis and in real cases. Improving the modelling of the demand helps to estimate the real impact of control techniques for voltage regulation, such as the ones described in Chapter 3. In the literature, residential and commercial loads are usually modelled considering: i) customer behaviours [74], [75], [76], ii) physical components [77], [78], iii) a combined representation of the previous approaches [79]. A generalised classification identifies two main approaches to build load models: the component-based method [37], [80] and the measurement-based method [37], [81], [82].

Actually, a method to model the steady-state behaviour of the loads is the well-known ZIP model [37], which allows considering active and reactive power variations due to voltage changes by using a simple polynomial formulation. In [83] the authors calculate ZIP coefficients of different appliances by collecting experimental measurements. Afterward, ZIP coefficients are validated by comparing them with actual recordings of load variations due to voltage reductions. An interesting approach to model consumer electronics is shown in [84], [85], where the authors illustrate the impact of electronic appliances on the stability of the network after estimating ZIP parameters of a liquid-crystal display and a light-emitting-diode television. Other studies on ZIP load models are in [86], [87], [88]. In [86] a load component database for household appliances and office equipment is created by Bonneville Power Administration and Pacific Northwest Laboratory; in [87] ZIP coefficients are calculated by using a least-squares (regression) technique and in [88] Sartomme *et al.* estimate the ZIP parameters for four electrical vehicles. It is clear that, generally, the literature tends to estimate a single time-invariant ZIP model for each appliance. Instead, some loads cannot be described by a single triplet of ZIP parameter. For instance, thermostatic loads are loads characterised by different working cycles. Thermostatic loads are controlled by a thermostat and exhibit a periodic behaviour. Wrong results can be achieved if the load

variation of these loads is comparable with the time interval used to run steady-state power system analysis.

To this end, a *time-varying formulation* and a *discrete-time formulation* of the ZIP model are presented, tested and compared with the classic ZIP model formulation.

4.1 Load modelling

The modelling of loads is a difficult task to achieve at the distribution level. A great effort must be done to model the large number and the diversity of devices usually connected to the grid. Also, the exact composition of the load is difficult to estimate: its changes depend on many factors as hours, day, season, weather condition, and state of the economy [37]. Therefore, load representation in power system is usually based on a considerable amount of simplification.

The load models are traditionally classified into two categories: static models and dynamic models. Static models have been investigated to assess load response to voltage changes on the distribution grid. A static load model expresses mathematically the characteristics of the load as a function of the bus voltage magnitude (and frequency). The active power and reactive power are considered separately. Traditionally, two formulations are widely adopted in the literature:

- *exponential model*;
- *ZIP model*.

The exponential load model is defined by the following equations:

$$P = P_0\left(\frac{V}{V_0}\right)^a$$
$$Q = Q_0\left(\frac{V}{V_0}\right)^b \quad \textbf{(26)}$$

where P and Q are the active and reactive power of the load when the bus voltage is V. The subscript 0 identifies the values of the variables at the initial operating condition or usually at the reference voltage (i.e. 230 V). The parameters a and b describe the relationship between the power and the voltage for the specific load: when they assume a value equal to 0, 1, or 2 the model represents constant power, constant current or constant impedance characteristics, respectively.

An alternative model, widely used to represent the voltage dependency of loads is the *ZIP model* (or *polynomial model*):

$$\begin{aligned} P &= P_0\left[Z_P\left(\frac{V}{V_0}\right)^2 + I_P\left(\frac{V}{V_0}\right) + P_P\right] \\ Q &= Q_0\left[Z_Q\left(\frac{V}{V_0}\right)^2 + I_Q\left(\frac{V}{V_0}\right) + P_Q\right] \end{aligned} \quad \textbf{(27)}$$

where Z_P, I_P, and P_P are the active power constant impedance, current and power parameters, respectively; and, Z_Q, I_Q, and P_Q are the reactive power constant impedance, current and power parameters, respectively. Furthermore, the following equalities must hold:

$$\begin{aligned} Z_P + I_P + P_P &= 1 \\ Z_Q + I_Q + P_Q &= 1 \end{aligned} \quad \textbf{(28)}$$

These models need a correct estimation of the parameters (a and b for the exponential and $Z_{P/Q}$, $I_{P/Q}$ and $P_{P/Q}$ for the polynomial) in order to estimate correctly load variations due to voltage changes.

The integration of power electronic components in current devices requires a new investigation of these parameters, indeed, few works in the literature calculate ZIP parameters for current devices. A model able to aggregate and change through time ZIP parameters can help in the evaluation of the impact of technique as CVR. Furthermore, ZIP parameters are considered constant during the whole operating cycle of the appliance. For appliances as washing machines or dishwashers, this assumption can be extremely far from reality. Two formulations able to improve the ability of ZIP model to describe voltage dependency of loads are proposed hereafter.

4.1.1 Time-varying ZIP model

In order to reduce the number of loads to be modelled during a time-series simulation, a polynomial formulation was developed to aggregate ZIP parameters at a given instant.

Considering that the active and reactive power of an aggregation of loads is equal to the sum of the active and reactive power of each single load/appliance connected at a given instant, then it is possible to derive a mathematical formulation of the aggregated ZIP parameters. Equations (29) - (32) extend the polynomial formulation of the traditional ZIP parameters (27) - (28), for multiple loads/appliances. P_{tot} and Q_{tot} are the total active and reactive power of the load aggregation taking into account the actual voltage at the connection point V. Furthermore, $P_{0_{tot}}$ and $Q_{0_{tot}}$ are the amount of active and reactive power, respectively, of the same aggregation measured at nominal voltage. They are obtained by adding the nominal active and reactive power of each load/appliance, P_{0_i} and Q_{0_i} .

To achieve the same formulation of (27) for (29), the aggregated ZIP parameters can be expressed as in (32), where the upper extreme of the summation N_L is the number of the appliances modelled through the ZIP, $Z_{P_i}, I_{P_i}, P_{P_i}, Z_{Q_i}, I_{Q_i}$ and P_{Q_i} are the ZIP parameters of the i^{th} appliance:

$$\begin{aligned} P_{tot} &= P_{0_{tot}}\left[Z_{P_{tot}}\left(\frac{V}{V_0}\right)^2 + I_{P_{tot}}\left(\frac{V}{V_0}\right) + P_{P_{tot}} \right] \\ Q_{tot} &= Q_{0_{tot}}\left[Z_{Q_{tot}}\left(\frac{V}{V_0}\right)^2 + I_{Q_{tot}}\left(\frac{V}{V_0}\right) + P_{Q_{tot}} \right] \end{aligned} \quad \textbf{(29)}$$

$$\begin{aligned} P_{0_{tot}} &= \sum_{i=1}^{N_L} P_{0_i} \\ Q_{0_{tot}} &= \sum_{i=1}^{N_L} Q_{0_i} \end{aligned} \quad \textbf{(30)}$$

$$\begin{aligned} Z_{P_{tot}} + I_{P_{tot}} + P_{P_{tot}} &= 1 \\ Z_{Q_{tot}} + I_{Q_{tot}} + P_{Q_{tot}} &= 1 \end{aligned} \quad (31)$$

$$\begin{cases} Z_{P_{tot}} = \dfrac{\sum_{i=1}^{N_L} P_{0_i} \cdot Z_{P_i}}{P_0} \\ I_{P_{tot}} = \dfrac{\sum_{i=1}^{N_L} P_{0_i} \cdot I_{P_i}}{P_0} \\ P_{P_{tot}} = \dfrac{\sum_{i=1}^{N_L} P_{0_i} \cdot P_{P_i}}{P_0} \end{cases} \cdot \quad (32)$$

$$\begin{cases} Z_{Q_{tot}} = \dfrac{\sum_{i=1}^{N_L} Q_{0_i} \cdot Z_{Q_i}}{Q_0} \\ I_{Q_{tot}} = \dfrac{\sum_{i=1}^{N_L} Q_{0_i} \cdot I_{Q_i}}{Q_0} \\ P_{Q_{tot}} = \dfrac{\sum_{i=1}^{N_L} Q_{0_i} \cdot P_{Q_i}}{Q_0} \end{cases}$$

The proposed formulation allows the creation of a time-varying ZIP models able to reduce considerably the management of data [89].

4.1.2 Discrete-time ZIP model

Starting from a generic profile of an appliance characterised by two working cycles, the analysis conducts to a generalised formulation of the ZIP model able to describe thermostatic and cycling loads. The active power profile in Figure 34 shows the behaviour of a washing machine. Indeed, the first part of the profile represents the water heating phase and it is characterised by a high active power demand P_1 for a short time interval u_1. The second part of the profile u_2 is characterised by a low power absorption P_2 for a long period of time until the end of the full cycle $T_{\max} = k_{max} \cdot T$.

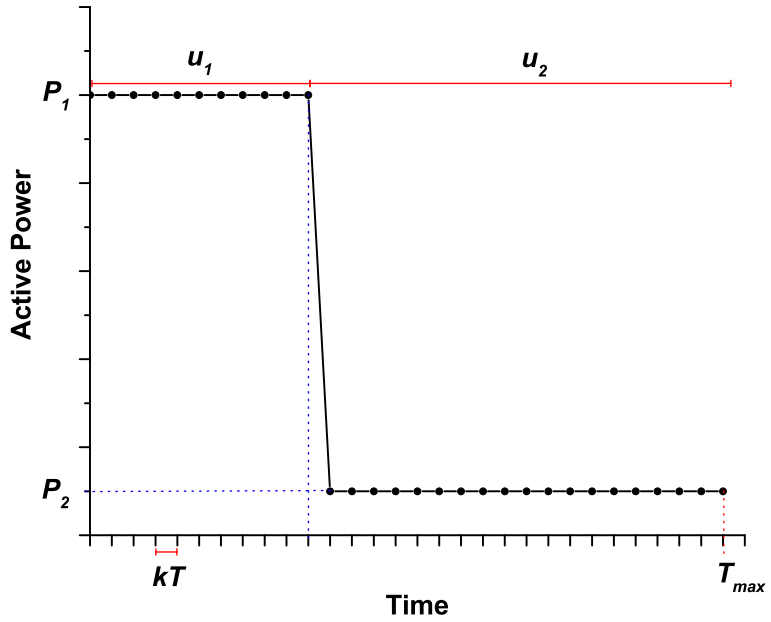

Figure 34. Active power profiles example for an appliance characterised by two different working cycles

Thus, it is possible to split and discretise the active power profiles into two parts taking into account (27) as follows:

$$P_{load}(kT) = \begin{cases} P_1 = P_0\left[Z_{p_1}\left(\frac{V_1}{V_0}\right)^2 + I_{p_1}\frac{V_1}{V_0} + P_{p_1}\right], & 0 \le kT \le u_1 \\ P_2 = P_0\left[Z_{p_2}\left(\frac{V_2}{V_0}\right)^2 + I_{p_2}\frac{V_2}{V_0} + P_{p_2}\right], & u_1 < kT \le T_{\max} \end{cases} \quad (33)$$

where $k = [1, 2, \ldots, k_{max}]$ indicates the minimum step used to discretise the period of time $T_{\max}$. It is possible to rearrange (33) considering:

$$\Delta V_2 = (V_2 - V_1)/V_1 \quad (34)$$

where ΔV_2 is the voltage variation in the percentage of V_2 from V_1. With this rearrangement, it is possible to reformulate (33) as follows:

$$P_{load}(kT) = \begin{cases} P_1 = P_0\left[Z_{p_1}\left(\frac{V_1}{V_0}\right)^2 + I_{p_1}\frac{V_1}{V_0} + P_{p_1}\right] & ,0 \le kT \le u_1 \\ P_2 = P_0\left[Z_{p_2}\left(\frac{V_1(1+\Delta V_2)}{V_0}\right)^2 + I_{p_2}\frac{V_1(1+\Delta V_2)}{V_0} + P_{p_2}\right] & ,u_1 < kT \le T_{\max} \end{cases} \quad (35)$$

The two parts of eq. (35) can be merged into:

$$P_{load}(kT) = P_1 \cdot H(kT) - [P_1 - P_2] \cdot H_{u_1}(kT) \quad , \quad 0 \le kT \le T_{\max} \quad (36)$$

where $H(\cdot)$ is the discrete Heaviside step function, formulated as follows:

$$H(kT) = \begin{cases} 0 , & kT < 0 \\ 1 , & kT \ge 0 \end{cases} \quad (37)$$

$$H_{u_i}(kT) = \begin{cases} 0 , & kT < \sum_{m=1}^{i} u_m \\ 1 , & kT \ge \sum_{m=1}^{i} u_m \end{cases} \quad (38)$$

If the load operation contains more than two separate working cycles, it is possible to generalise (36). In particular, if it is considered a generic case with *N* cycles, it is possible to write the DT-ZIP model:

$$P_{load}(kT) = P_1 \cdot H(kT) - \sum_{i=1}^{N-1} [P_i - P_{i+1}] \cdot H_{u_i}(kT) \quad , \quad 0 \le kT \le T_{\max} . \quad (39)$$

The following equalities (40) – (46) must hold:

$$P_i = P_0\left[Z_{p_i}\left(\frac{V_{ref}(1+\Delta V_i)}{V_0}\right)^2 + I_{p_i}\frac{V_{ref}(1+\Delta V_i)}{V_0} + P_{p_i}\right] \quad (40)$$

$$, \ \sum_{m=0}^{i-1} u_m < kT \le \sum_{m=0}^{i} u_m$$

$$\sum_{i=1}^{N} u_i = T_{\max} \quad (41)$$

$$u_i = u_{i_0} + \Delta u_i \quad (42)$$

$$u_{i_0} = u_i(V_{ref}) \quad (43)$$

$$\Delta u_i = \alpha_i \cdot \Delta V_i \quad (44)$$

$$\Delta V_i = \left(V_i - V_{ref}\right)/V_{ref} \quad (45)$$

$$V_{ref} = \max[V_1,...,V_i,...,V_N] \quad (46)$$

where (40) indicates the active power P_i in each sub-interval u_i; eq. (41) expresses the equality between the whole cycle T_{max} and the sum of each sub-interval u_i; eqs. (42) – (46) formulate the relationship between the duration of each sub-interval u_i and the voltage variation ΔV_i from the reference voltage $V_{ref.}$; ΔV_i indicates the voltage variation in percentage compared to V_{ref}; Δu_i is the time variation due to a voltage change of the reference sub-interval u_{i_0} (duration of the cycle i at the reference voltage V_{ref}). Δu_i is obtained by multiplying ΔV_i and the parameter α_i, which is calculated by using real measurements. Finally, V_{ref} represents the maximum measured voltage between the voltage values acquired during a full working cycle of the appliance under test. The representation is able to consider the typical behaviour of thermostatic loads, which require more time to reach a reference temperature when the active power decreases.

4.2 Case studies

Two case studies are illustrated in this paragraph. The first one wants to proof the benefits of implementing the *time-varying ZIP model* in a massive data analysis without losing information about the characteristics of loads during the process of aggregation. The study is conducted on a UK distribution network (HV and LV network) and the load response to voltage changes are measured. The second case study is a laboratory experience performed in real condition to estimate the ZIP parameters and to validate the *discrete-time ZIP model* for a washing machine.

4.2.1 Estimate the load response to voltage changes on a DN

From the perspective of a DSO, it is, therefore, plausible to envisage the active management of voltage regulation devices in order to increase/decrease the demand during certain periods for the benefit of the network (e.g., peak shaving, congestion management) or the whole system (e.g., fast reserves). The extent to which this voltage-driven demand response can actually help in managing the network is however entirely dependent on the instantaneous load. On the other hand, the boundaries to which voltage changes can be applied will also depend on how load changes and the corresponding final voltages downstream, particularly for low voltage connected consumers. Such final voltages should remain within statutory limits and be compliant with standards such as the EN50160 [20].

4.2.1.1 Description of the case study

In order to assess the feasibility of the scheme above, this work first estimates the domestic load response to voltage changes whilst complying with voltage limits at low voltage. This is carried out on a UK HV-LV distribution network in the North West of England with 351 residential, 2 commercial and 1 industrial customers, with a total peak demand of 932 kW. The UK HV-LV distribution network is

operated by Electricity North West Limited. The single-line diagram is shown in Figure 35: there are four feeders connected to the busbar of the on-load tap changer-enabled primary substation (33 kV/6.6 kV). The topological diagram of the Landgate LV network is presented in Figure 36. It has six radial feeders and supplies power to 351 residential loads. The corresponding OLTC transformer (blue dot in Figure 36) is set to have a 5.75% boost (i.e., 6.6 kV/423 V).

In order to achieve a time-series simulation, the profiles of industrial and commercial customers are obtained through a historic, aggregated half-hourly yearly load profiles (produced by Elexon [90]). Figure 37 shows the estimated profiles for 19 December 2011 (with a peak demand of 394 kW for the industrial load and respectively 132 kW and 66 kW for the commercial loads and a power factor of 0.96). On this same day, the peak demand of the residential loads is approximately 500 kW (Figure 38). This particular day will be used in the simulations. OpenDSS (OpenDSS - EPRI Distribution System Simulator, n.d.) and MATLAB™ were used in this study to implement the *time-varying ZIP parameters* and assess the corresponding impacts when changes in voltages are made.

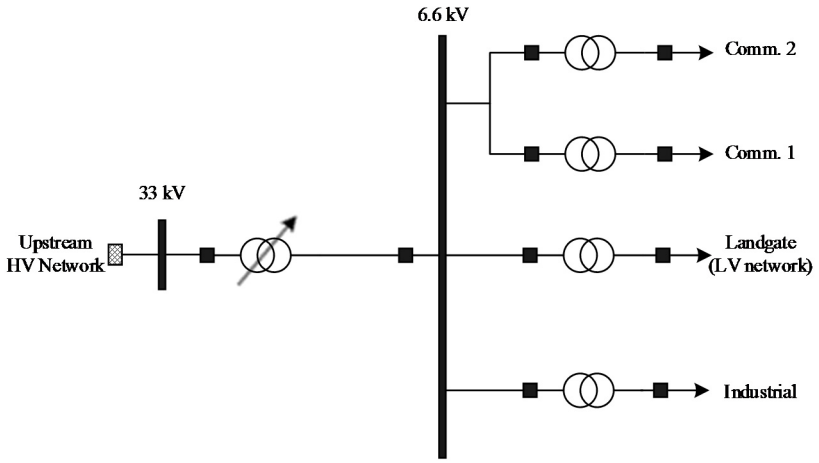

Figure 35. Diagram of the HV-LV network

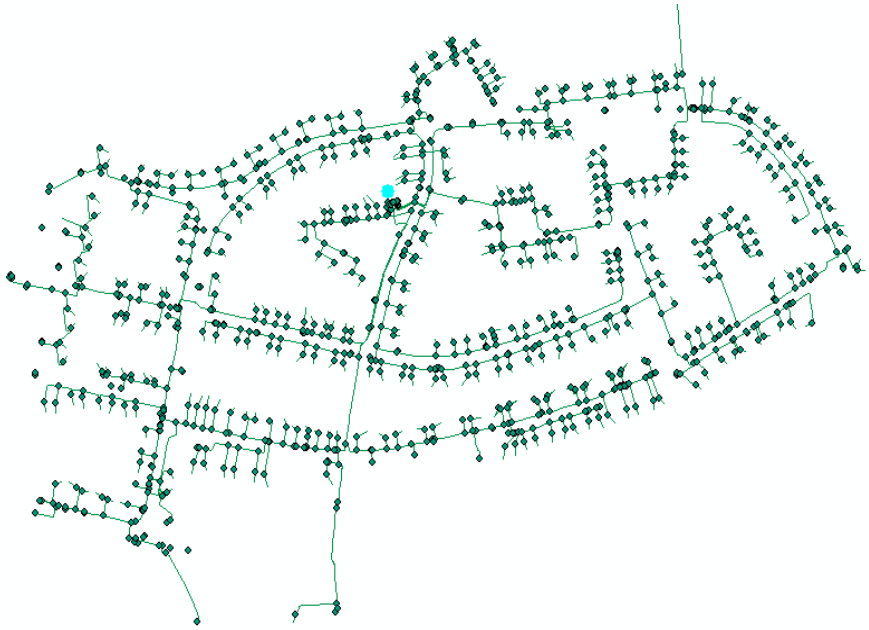

Figure 36. Diagram of Landgate LV network

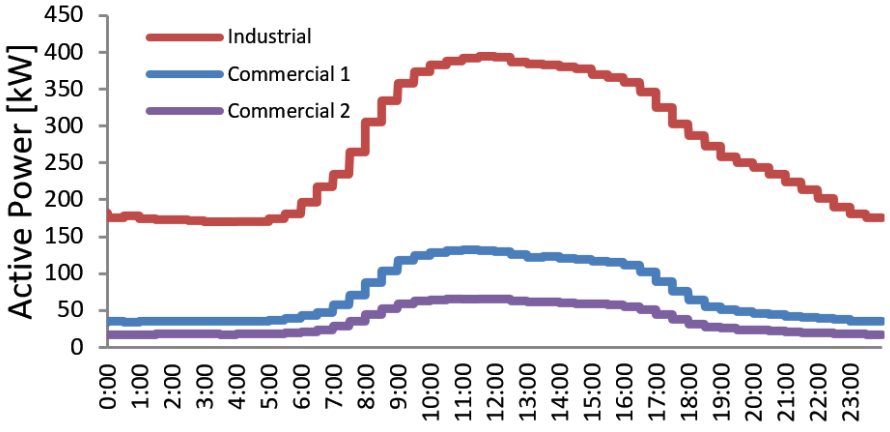

Figure 37. Commercial and Industrial Profiles (19 December 2011)

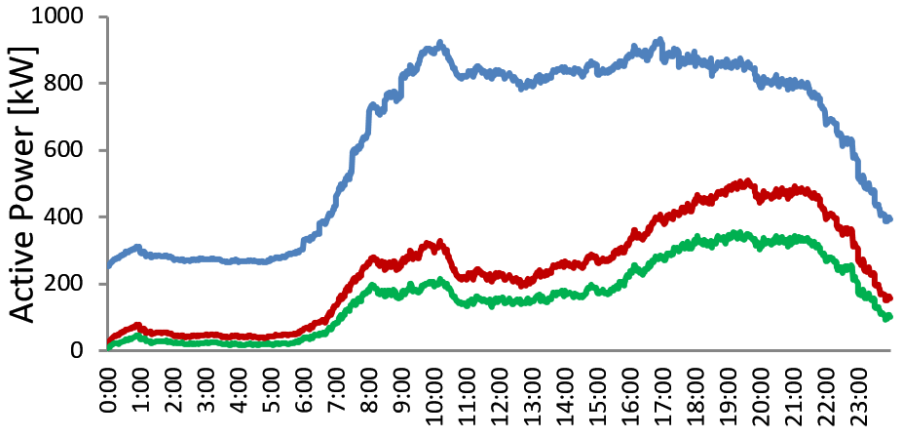

Figure 38. Aggregated active power of the network (blue), aggregated residential demand (red), and aggregated residential demand modeled with ZIP parameters (green)

Focus has been given to residential loads of which certain appliances have been modelled aggregating the corresponding ZIP parameters for each customer. This, combined with the corresponding load profiles, allowed the creation of *time-varying ZIP models* per residential customer. Based on the ZIP parameters available in the literature (see Table 6), it was possible to model approximately 70% of the residential (active power) peak demand. This represents around 40% of the whole peak demand (as shown in Figure 38) and will be the only part of the load that will respond to changes in voltages. The profiles of the residential customers are produced using a high-resolution (e.g., minute by minute) model developed by Centre for Renewable Energy Systems Technology [74] at Loughborough University. In addition, UK National Statistics were adopted to determine the occupancy of households (29% with 1, 35% with 2, 16% with 3 and 20% with 4 people) [92]. A typical daily profile of a UK residential customer (4 people) for a weekday in December is shown in Figure 39. The voltage target for the secondary of the primary substation was changed (0.01 p.u. steps) in order to assess how the *time-varying ZIP model* responds and to quantify the final voltages for residential customers. The British version of the standard EN50160 was adopted to determine whether voltage excursions happened. This

standard (adapted for UK LV networks) states that the 10-minute rms phase to neutral voltages should not exceed 10% of nominal (230 V).

Table 6. ZIP parameters

Appliance Data				Zip Parameters					
Name	S0 (VA)	pf	%	Active Power			Reactive Power		
				Z%	*I%*	*P%*	*Z%*	*I%*	*P%*
Tv(Crt)	150	0.99	0.48	0.00	1.24	-0.24	0.00	0.00	-1.00
Tv(Plasma)	470	0.99	0.50	-0.27	0.44	0.83	-1.95	2.32	-1.37
Dishwasher	1500	0.80	0.34	0.10	0.10	0.80	1.54	-1.43	0.89
Oven	2500	1.00	0.62	1.00	0.00	0.00	0.00	0.00	0.00
Kettle	2000	1.00	0.98	1.00	0.00	0.00	0.00	0.00	0.00
Wash.Machine	1065	0.61	0.93	0.06	0.31	0.63	-0.56	2.20	-0.64
Fridge	225	0.84	0.99	1.19	-0.26	0.07	0.59	0.65	-0.24
PC	150	1.00	0.77	0.00	0.00	1.00	0.00	0.00	0.00
Microwave	1300	1.00	0.85	-2.78	6.06	-2.28	0.00	0.00	0.00
Hob	2500	1.00	0.46	1.00	0.00	0.00	0.00	0.00	0.00
Heater	1500	1.00	0.50	1.00	0.00	0.00	0.00	0.00	0.00
Light Bulb	70	1.00	1.00	0.57	0.43	0.00	0.00	0.00	0.00

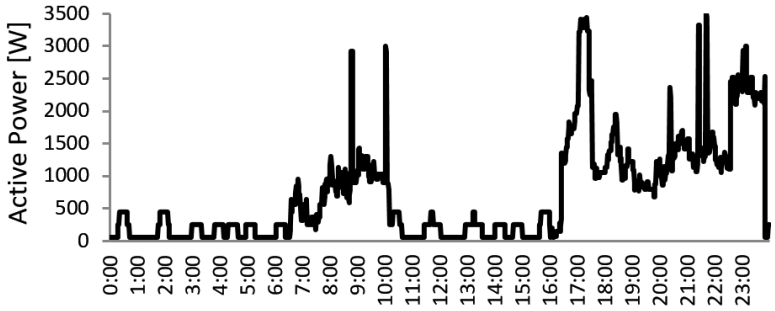

Figure 39. Typical 4-people residential profile (December, weekday)

In addition, 95% of measurements should not be below 6% of nominal and never below 15% of nominal. Although the standard considers a week, here it will be used for a day.

4.2.1.2 Simulation results

The results from the simulations showed that the minimum and maximum feasible voltage targets at the primary substation are 0.97 and 1.02 p.u., respectively. Values outside these limits could result in voltage issues to customers and non-compliance with BS EN50160.

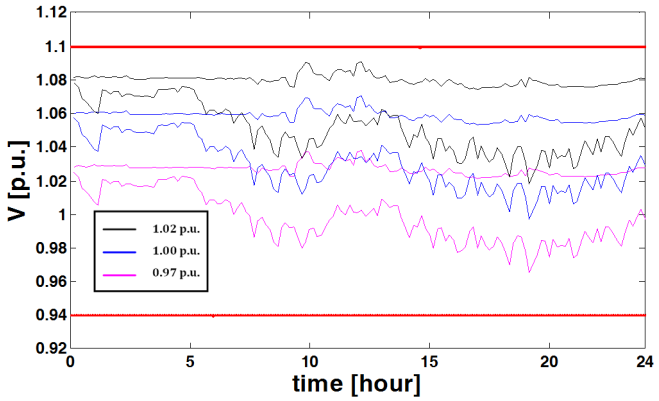

a) phase 1 to neutral voltage profile (10-minute average)

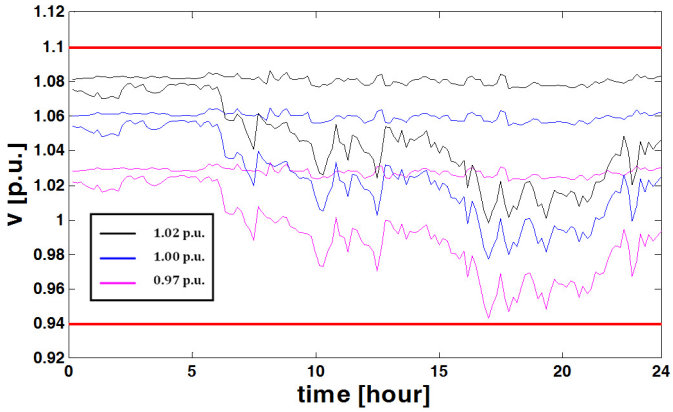

b) phase 2 to neutral voltage profile (10-minute average)

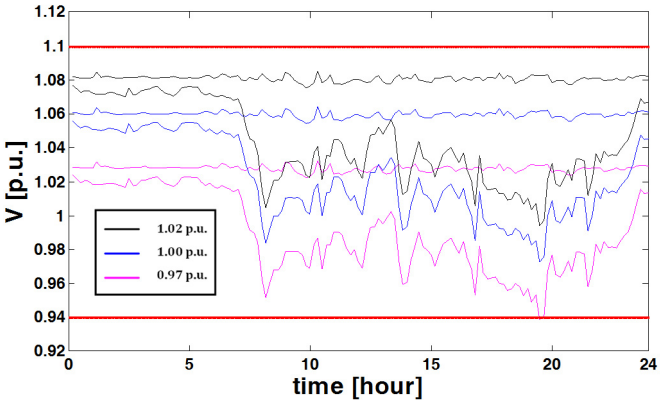

c) phase 3 to neutral voltage profile (10-minute average)

Figure 40. Maximum and minimum voltages found in the LV network for different voltage targets at the primary substation.

The corresponding results for three voltage targets (1.02, 1.00 and 0.97 p.u.) are presented in Figure 40. It is important to highlight that, although voltage targets of 1.03 and 0.96 p.u. did result in a limited number of excursions (around the 2% of the daily), a more conservative range was adopted given that the simulations were limited to a day only. In Figure 41 it is shown the period during the studied day with the largest load responses (in kW) to voltage changes. This period corresponds to 6 pm to 7 pm (peak load).

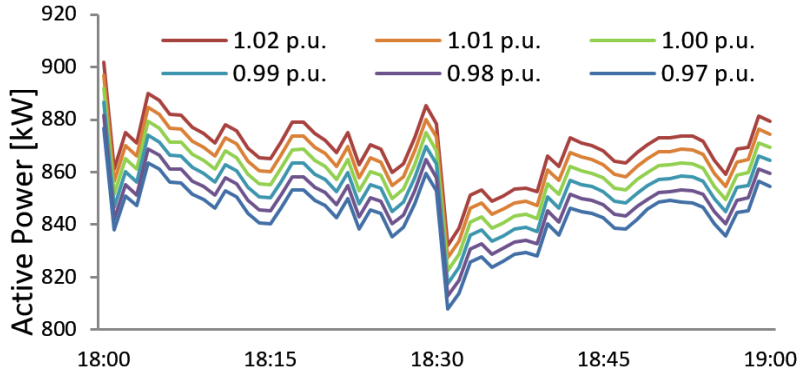

Figure 41. Period with largest load response to voltage changes

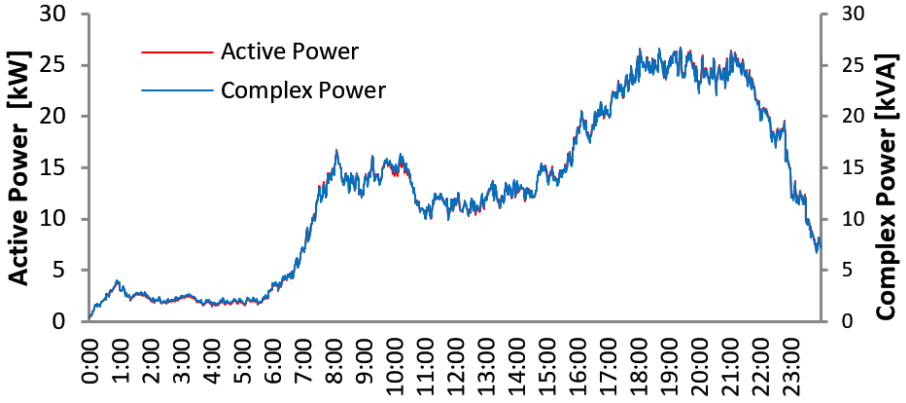

Figure 42. Total load response for a voltage target change of 0.05 p.u. (from 1.02 p.u. to 0.97 p.u.)

Considering that typically primary substations in the UK have target voltages above nominal, it can be said that the maximum feasible change in the target voltage for this network is 5%, i.e., from 1.02 to

0.97 p.u. The total load response (both active and complex power) throughout the day or such a change in the voltage target at the primary substation is shown in Figure 42. The average (active power) load response throughout the day compared to the total load of the network is 1.75% with a maximum of 3.24%, as summarized in Table 7.

Table 7. Load response summary

Values	%Total	%Residential	%ZIP
Minimum (daily)	0.17	1.96	5.31
Maximum (daily)	3.24	5.66	9.73
Average (daily)	1.75	4.65	8.01
Average (6-7pm)	2.88	5.06	7.62
Average (4-5am)	0.67	4.07	9.37

However, if the average response is compared to the total residential load, this figure goes up to 4.65%. More interesting is the percentage compared to the part of the residential load modelled with the ZIP parameters, with an average of 8.01%. This highlights the importance of adequately modelling most of the load with ZIP parameters to truly quantify the potential effects. During the peak load alone (at 4.56pm), the corresponding figures were 2.22, 4.78 and 7.30%, respectively. The complex power showed a similar trend.

4.2.2 Experimental validation of discrete-time ZIP model

The analysis starts by collecting a set of measurements of a washing machine in real operating conditions. The washing machine used is an Ariston Hotpoint Aqualtis AQXXD 169 h (7.5 kg). To emulate real working conditions of the appliance, the measurements are performed in an apartment connected to the LV network in different days of the week, different hours and different laundry loads.

4.2.2.1 Description of the portable measurement station

A portable measurement station has been set-up for on-site measurements (Figure 43). The portable station is composed by:

- a single-phase auto-transformer HSG 0302 Metrel;
- an electronic power and energy meter Schneider Power Logic TM PM5561 and
- a current transformer (CT) TAQB50B150 IME.

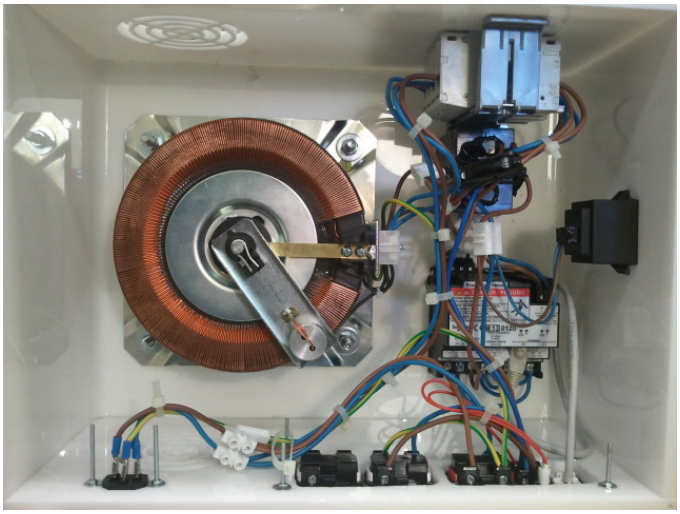

a)

b)

Figure 43. Portable measurement station

Security is guaranteed by two 16 A circuit breakers installed downstream and upstream of the auto-transformer. A bipolar switch allows the disconnection of the load and performing no-load measurements of voltage on the secondary side of the autotransformer. The measurements are saved in the data logger integrated into the meter and downloaded by using an Ethernet port.

4.2.2.2 Stochastic analysis

Ten full operating cycles have been acquired for three different voltage levels: -5%, +0%, and +5%. The reference voltage is $V_0 = 230$ V. The average duration of one full cycle of the washing machine under test is about 120 minutes. Thus, each measurement cycle consists of 120 signal acquisitions with a time-step of 1 minute. Measurements of active power, energy and voltage have been collected.

In Figure 44 are depicted ten full operating cycles acquired at the reference voltage level V_0. The identification of a specific pattern able to model the active power absorption of the washing machine is difficult to capture. The complexity is due to the uncertainty and the variability of working cycles: a statistical analysis can help in approaching this challenging task. To point out possible similarities among the active power profiles, the Pearson coefficients has been calculated, which are formulated as follows:

$$\rho_{p_i p_j} = \frac{\sigma_{p_i p_j}}{\sigma_{p_i} \sigma_{p_j}} \quad (47)$$

where the subscript p_i and p_j indicate two of the ten active power profiles, and $\sigma_{p_i p_j}$, σ_{p_i} and σ_{p_j} are the standard deviations associated with them.

In Figure 45, the correlation coefficients for the ten measurements at 230 V are represented on a colour map. Except for case 4, there is a high correlation between the different measurements. The existing correlation allows looking for a general representative model able to simulate active power profiles of the washing machine under test.

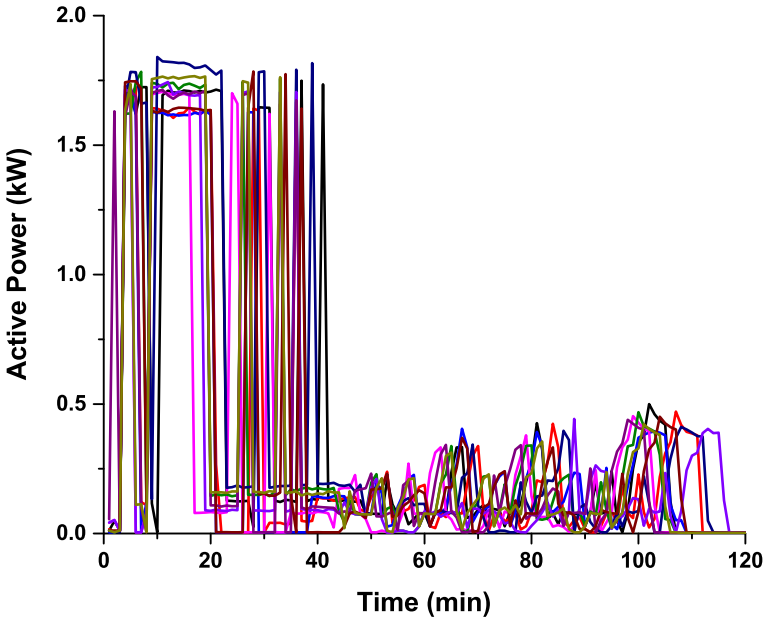

Figure 44. Active power measurements at reference voltage level (230 V)

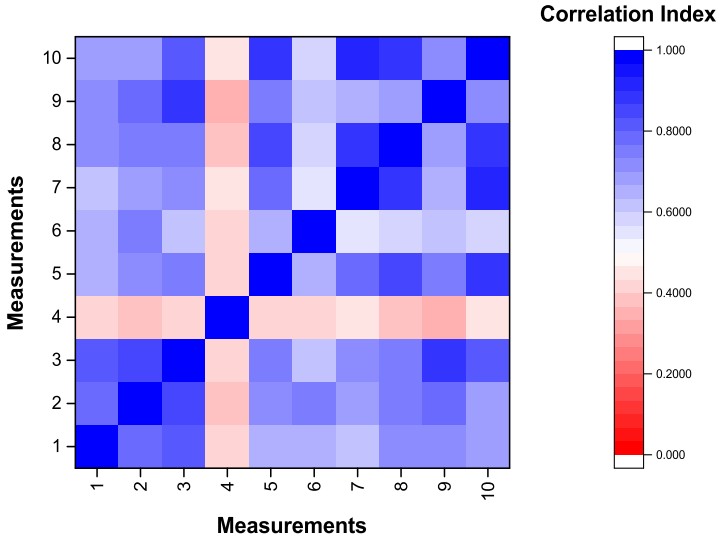

Figure 45. Visual map of the correlation matrix

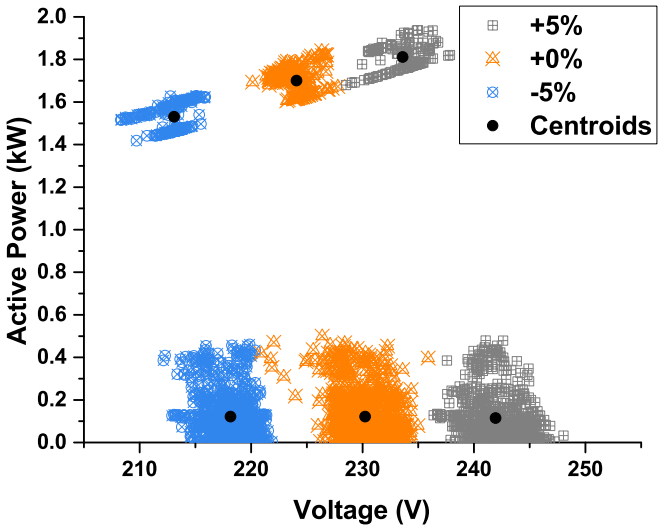

Figure 46. Full cycle measurements with different voltage settings

In Figure 46 are shown all the operating points collected (10 full cycles measurement for three different voltage levels) on a power-voltage plane. High absorption of active power occurs during the water heating phase. On the other hand, the bottom of the graph is characterised by lower active power consumption (rinsing and spinning phase), which does not exceed 500 W. The working phases of the washing machine can be easily classified into two groups referring to the y-axis of Figure 46. The two parts are well distinguishable and six clusters are easily identifiable (two for each voltage level). Thus, the coordinates of the centroids of each cluster (V_c , P_c) are calculated by averaging the coordinates of the *N* elements of each cluster as follows:

$$\begin{cases} V_c = \frac{1}{N}\sum_{i=1}^{N} V_{c_i} \\ P_c = \frac{1}{N}\sum_{i=1}^{N} P_{c_i} \end{cases} . \quad (48)$$

In Table 8 the coordinates of the centroids are reported.

Table 8. Centroids coordinates

		Voltage Values		
		-5%	**+0%**	**+5%**
P_C **(kW)**	**Top**	1.53	1.70	1.81
	Bottom	0.12	0.12	0.12
V_C **(V)**	**Top**	213.09	224.08	233.60
	Bottom	218.15	230.23	241.94

It is worth noting that due to real operating conditions of the washing machine, the voltage is subject to change during the full operating cycle (120 minutes). This behaviour is emphasised when the operation moves from the heating phase to the rinsing and spinning phase; for instance, when the washing machine is heating the water, there is a reduction of voltage compared to the voltage reference or to the one measured in low load conditions as shown in Figure 47. The voltage reduction is due to an increase of the active power flow on the lines.

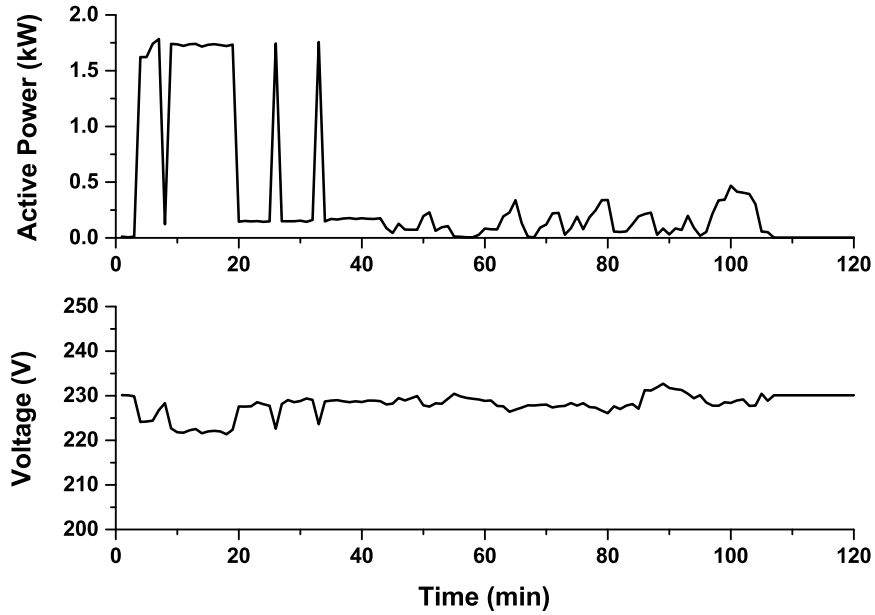

Figure 47. Active power and voltage profile of a full cycle (230 V)

Starting from the achieved results, it is possible to implement a methodology to calculate the ZIP parameters before moving to the DT-

ZIP. The classic formulation of the ZIP model in (27) is based on the knowledge of P_0 and V_0 to represent active power variations due to voltage changes. As stated before, the uncertainty and the variation of the supply voltage due to real operating conditions (Figure 47) makes it difficult to identify a reference value P_0. A recursive procedure is implemented to overcome the problem and calculate the reference value for the active power P_0. The algorithm can be summarised in the following steps:

1. choose a guess value P_0^g and set $V_0 = 230$ V;

2. calculate the ZIP parameters by solving the following constrained optimization problem:

$$\min_{Z_p, I_p, P_p} \sum_{i=1}^{M} \left\| P_{c_i} - P_0^g \left[Z_p \left(\frac{V_{c_i}}{V_0} \right)^2 + I_p \frac{V_{c_i}}{V_0} + P_p \right] \right\|_2^2 \qquad \textbf{(49)}$$
$$s.t. \quad Z_p + I_p + P_p = 1$$

where M is the number of measurements cycles used to calculate ZIP parameters (for this case study $M = 3$, because the measurements are collected at three different voltage levels) and P_{c_i} and V_{c_i} are the coordinates of the centroids at each voltage level i (Table 8);

3. update the value of P_0 by using Z_p, I_p and P_p evaluated in the previous step as follows:

$$P_0 = \frac{1}{M} \sum_{i=1}^{M} \frac{P_{c_i}}{\left[Z_p \left(\frac{V_{c_i}}{V_0} \right)^2 + I_p \frac{V_{c_i}}{V_0} + P_p \right]} \qquad \textbf{(50)}$$

4. calculate the difference between P_0 and P_0^g : if the difference is lower than the maximum allowable error ε (for this case study $\varepsilon = 0.001$) the cycle ends; otherwise, the procedure restarts from step 2.

4.2.2.3 Validation of the model and experimental results

The evaluation of P_0 allows the implementation of a second order polynomial interpolation based on the formulation (27) to calculate the triplet of ZIP parameters of the washing machine in the two different operating cycles. In blue (top line) is depicted the interpolation of the centroids during the heating phase, while in red (bottom line) the same relationship is shown for the rinsing-spinning phase. ZIP coefficients are extremely different for the two working phases, the appliance reacts differently to voltage changes. The calculated ZIP coefficients are in Table 9. The model and the calculated ZIP parameters (Table 8) accurately fit the trends illustrated in Figure 48 and described by the centroids in Table 8, pointing out the goodness of the achieved solution.

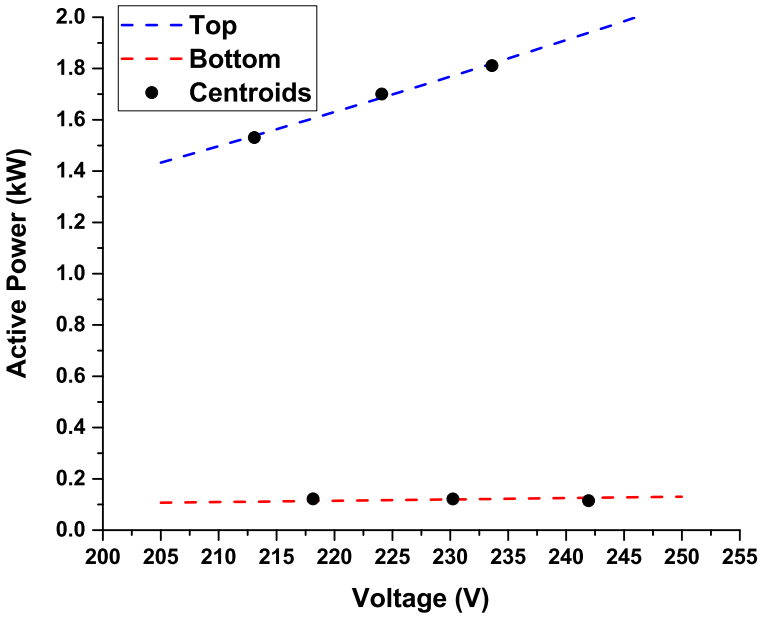

Figure 48. Polynomial interpolation of the centroids

Table 9. Washing machine ZIP coefficients

	P_0	Z_P	I_P	P_P
Top	1.77	0.741	0.343	-0.084
Bottom	0.12	0.334	0.333	0.333

The DT-ZIP formulation requires the estimation of additional parameters, which are shown in Table 10 and have been calculated starting from the measurements of the washing machine. The duration of the cycle u_1 is calculated by averaging the measured time periods of the heating cycle. ΔV_1 is the result of averaging voltage variations in the first working cycle. To explain the need of introducing a parameter Δu_1, the case where $\Delta u_1 = 0\%$ is depicted in Figure 49. $\Delta u_1 = 0\%$ means that the duration of the heating phase is not affected by voltage variations. In contrast, the measurements have pointed out that the duration changes with an average $\Delta u_1 = 12\,\%$ (Figure 50). The voltage reference for the case study is $V_{ref} = \max [V_1, V_2] = V_2$, as a consequence $\Delta V_2 = 0\%$.

Table 10. DT_ZIP parameters of the washing machine

	ΔV_1 (%)	ΔV_2 (%)	Δu_1 (%)	α_1	u_1 (min)	T_{max} (min)
Washing Machine	3	0	12	4	25	120

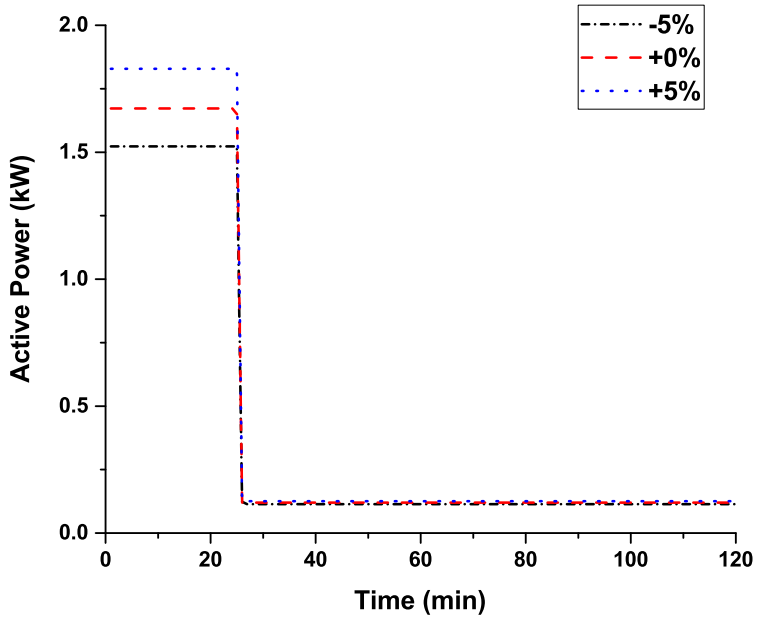

Figure 49. DT-ZIP of the washing machine with $\Delta u_1 = 0\%$

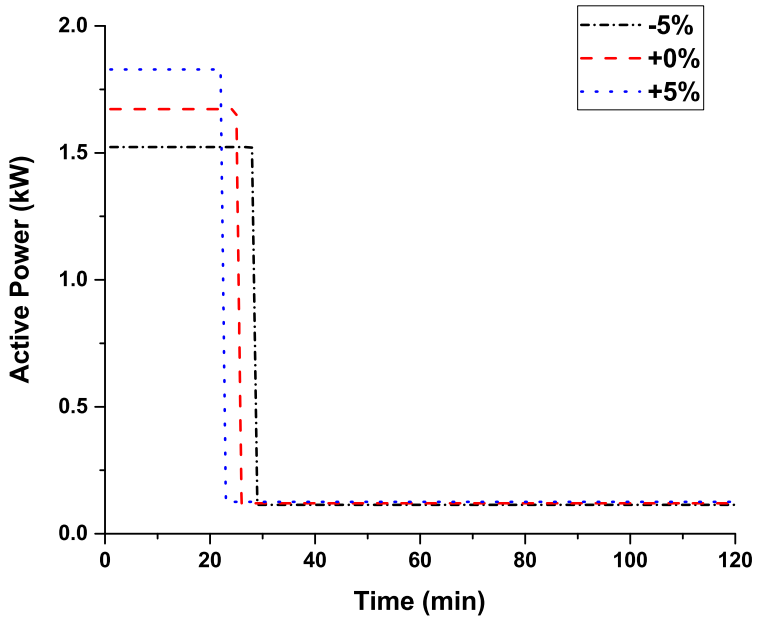

Figure 50. DT-ZIP of the washing machine with $\Delta u_1 = 12\%$

The proposed DT-ZIP model has been compared with the ZIP model of a washing machine presented in [93] that suggests: $Z_p = 0.05$, $I_p = 0.31$ and $P_p = 0.63$. In the same work, it is specified also a constant value of P_0 for the full cycle. The value of P_0 is pertinent only to the washing machine used in the case study of [93]. In fact, the average power absorption calculated by Hajagos *et al.* could be different from the one obtained in our case study at the reference voltage of 230 V.

For the above-mentioned reason, the results achieved with the DT-ZIP are compared with the ones obtained with the ZIP model formulated by using three different constant values of P_0 and the triplet of ZIP parameters in [93]. In detail, in the first case, the value of P_0 is set to 1.67 kW, which is the average of the active power measured at the reference voltage during the heating phase. In the second case, P_0 is set to 0.12 kW that is equal to the average active power measured at the reference voltage during the rinsing-spinning phase. In the third case, P_0 is equal to 0.89 kW, which is the average of the previous two values. The results achieved by using the DT-ZIP model are compared with the results pointed out by the classic ZIP model for the three cases

previously mentioned. Results are summarised in Table 11 in terms of energy consumption, where the real case indicates the energy measured during the test experience.

Table 11. Energy consumptions

	Real case	**DT-ZIP**	**ZIP 1** $P_0 = 1.67$ **kW**	**ZIP 2** $P_0 = 0.12$ **kW**	**ZIP 3** $P_0 = 0.89$ **kW**
Energy (kWh)	0.70	0.74	3.2	0.23	1.71

The proposed DT-ZIP method better describes the real energy consumption of the washing machine compared to the classic ZIP model, which overestimates or underestimates energy consumption. However, if the average value of energy needed for a full cycle of the washing machine (E) is available, a better estimation of P_0 for the ZIP model can be obtained simply from its definition:

$$P_0 = \frac{E}{T}. \quad (51)$$

By using (51), assuming $E = 0.70$ kWh, as in Table 11, it is possible to calculate the active power $P_0 = 0.35$ kW. In this way, the ZIP model emulates well the consumption of the washing machine even if the active power profile is flat during the whole cycle T, as shown in Figure 51. Furthermore, this flat profile is not able to represent any temporal pattern typical of cyclic loads or any peak in the consumption of the appliance. Another benefit of the DT-ZIP model can be observed when loads are aggregated. The typical diversity of residential appliances has been reproduced by a random aggregation of active power profiles of washing machines. In Figure 52, the aggregated demand of washing machines is depicted. The level of aggregation represented in Figure 52 is different and it is expressed by the letter k.

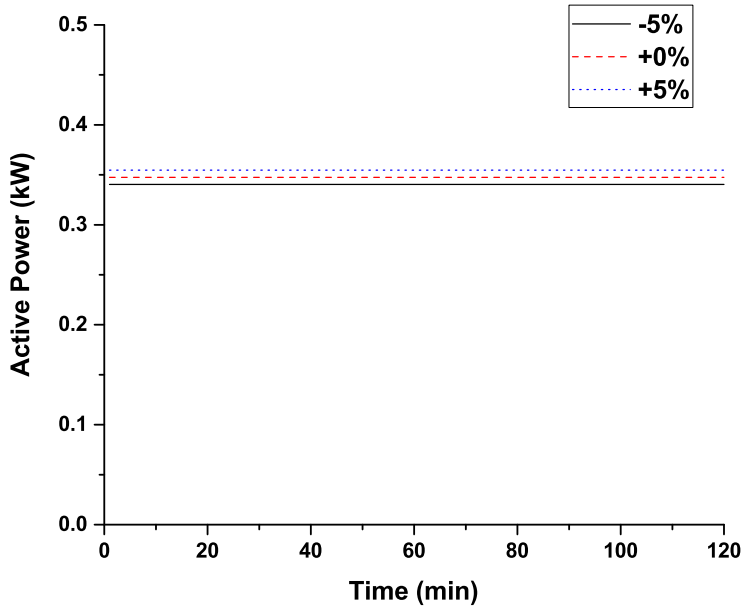

Figure 51. Washing Machine profiles by using the ZIP formulation and P0=0.35 kW

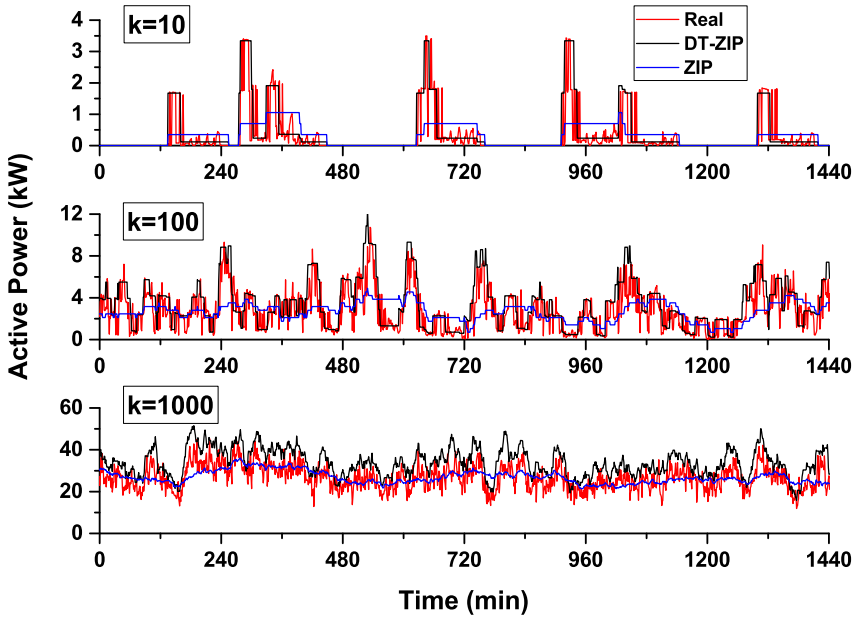

Figure 52. Aggregated demand of washing machines

From the top graph to the bottom graph, the number k of washing machines increases from 10 to 1000. The model pointed out and the classic ZIP model are compared with the real case, which has been simulated by choosing randomly the measured profiles depicted in Figure 44. The DT-ZIP model, in contrast with the classic ZIP formulation, fittingly emulates the variation of the aggregated demand of the washing machines. By drastically increasing the number of appliances, the DT-ZIP model may overestimate the real power consumption, as it is possible to observe in Figure 52 for the case of 1000 washing machines.

Contrariwise, the classic ZIP model tends to average the active power profiles resulting in a good estimation of the energy consumption but failing in the representation of possible demand peak. Anyway, if the number of appliances is not too high as for the case of a building or a district, the proposed method better describes the active power behaviours and the energy consumptions compared to the classic ZIP model. The proposed formulation allows the improvement of the estimation of the active power absorption of a single customer, an aggregation of customers or the active power at a MV/LV substation. The effect of shifting loads (as washing machines or dishwashers) for demand-side management purposes can be better estimated by modelling cyclic or thermostatic appliances with the proposed DT-ZIP. The ability to model thermostatic load behaviour allows the calculation of accurately energy consumption of the appliances during simulation analysis.

Chapter 5

The dire need for storage

In recent years, several DERs have been developed and made viable even for small-scale distribution systems. The integration of these resources, in particular DGs, in the distribution grid requires the development of new solutions and new control techniques as widely explained in the previous chapters. For instance, DSO is forced to deal with new challenges to obtain higher performances from unpredictable RESs (i.e. wind and solar) [94]. New ancillary services based on storage systems are needed to improve power and voltage quality, reducing losses and deferring investments.

As a matter of fact, storage systems are an undeniable opportunity for DSOs to make these generation resources predictable, programmable and dispatchable. To this end, energy storage resources (ESRs) have the ability to play multiple roles in power system due to their versatility, flexibility, quick response times and the ability to act either as a generator or as a load or to be in the idle phase. ESRs can store and subsequently release energy, effectively transferring energy from a period to another. An ESR is the only power system resource able to capture technical and economic opportunities created by shifting energy over periods of time. However, ESRs are causal choices in the sense that they can release energy only after that energy has been charged. An ESR can be deployed at the transmission level, distribution level or at the customer side of the meter. Our objective is to analyse the roles that ESRs take on in various power system deployment, including those in a competitive market environment. At this stage, wholesale electricity markets operate only at the bulk transmission grid level. The deepening penetrations of RESs, the development of microgrids with various DERs, including RESs, and the growing

penetration of electric vehicles lead to the vision of an analogous market structure at the distribution grid level.

By shifting energy consumption from one period to another, ESRs can assist the grid in solving operational problems such as relief overloads at a primary substation or in increasing supplies in electricity helping in the avoidance of high electricity prices. Moreover, ESRs can be deployed to delay the start-up of cycling units with the effect of reductions in overall energy prices due to shorter operations of cycling units. The power electronic, which interfaces battery energy storage system (BESSs) to the grid, is able to provide fast response times and ramping capabilities in addition to the ability to operate with a power factor different than 1.

These characteristics allow the ESRs to provide a wide range of ancillary services including spinning reserves, frequency regulation, voltage support, as well as black start capability. Additionally, ESRs can provide virtual inertia to replace the missing inertia in grids with RESs or in microgrids.

5.1 Voltage support by PV and BESS in DNs

As the number of installation of PV units is continuously increasing, the intermittent and stochastic production poses also technical and economic challenges for DSOs [94]. In particular, if the PV generation exceeds the local demand, the surplus of power may cause reverse power flows in the feeder and, in some cases, voltage rises [95]. On the other hand, if the power demand is high while the PV production is low or absent, voltage drops can be consistent. In both cases, voltage violations occur in the network [38]. Distributed generation units can locally support the grid in addressing these challenges providing an ancillary service. Thanks to the development of the new BESSs, which provide a unique opportunity for dramatic increases in asset utilisation of many types of currently underutilised distribution equipment, numerous services can provide benefits to utilities, DG owners and customers [96].

In the literature, active power curtailments and reactive power controls are proposed to solve voltage violations [47], also considering coordination strategies between independent power producers and DSOs [97]. The specific role of PV units in developing ancillary services in distribution systems by using reactive power is described in [98]. Solutions based on ESSs in LV networks are implemented in [99], where a scenario-based method to define the minimum capacity of ESSs in LV networks to prevent voltage rises has been proposed. However, the study is tested on a balanced LV three-phase system and without considering the possibility that users can control ESSs. In [100], in order to improve the voltage quality in an LV network, the authors present an innovative management strategy for distributed battery storages that increases the capability of distribution networks to exploit PV generation. Each battery cycle is optimised to minimise battery losses and costs and to improve voltage profiles. The work considers only one random allocation of 26 ESSs: a small radial LV network and a daily time simulation are carried out for testing the strategy. Thus, the solution cannot be generalised. Monte Carlo (MC) simulations are typically used to tackle the stochasticity in distribution systems as in [101]. In [12] a coordinated control strategy of PV with co-located ESS is presented and a MC analysis is performed in order to evaluate the possible benefits in supporting the DSO in controlling voltage profiles.

Although economic analyses still show several barriers to the deployment of ESSs, the introduction of an economy of scale together with a forecasted capital cost reduction of the assets make this solution more and more feasible for the distribution network. Benefits result from using energy storage systems to provide ancillary services such as load following, load shifting, peak shaving, capacity firming, reactive power support and power quality [102], [103], [104]. In fact, storage systems are becoming of interest to both utilities and energy power producers or prosumers, because of their ability to optimize energy management increasing self-consumption of energy [105], [106], [107] to integrate small-scale renewable energy sources into commercial and residential sectors [108], [109], [110], [111], [112], [113] and to increase the efficiency of supply maintaining the required PQ in the power system [114]. To this end, ancillary services by using BESSs co-

located with PV units in MV and LV network are proposed in this chapter.

In this paragraph, two ancillary services able to support DSO by using co-located PV/BESS systems are described. The first strategy is a voltage regulation method for MV network based on the following characteristics [95], [96]:

- the presence of BESS co-located with PV systems able to store part of PV production for voltage regulation;
- local reactive power injection/absorption for voltage control as a backup solution;
- the modulation of PV production, if BESSs and reactive power are not able to support voltage profile.

The second ancillary is able to support the DSO in solving voltage issues on LV network. The strategy implements the following features [97], [98], [99]:

- an analysis that takes into account two different seasons (summer and winter) in which the PV profiles are randomly chosen from a database of real profiles of a PV farm located in the south of Italy;
- a focus on the effect due to changing the BESS capability rather than the capacity;
- an enhanced analysis with historical data of the coordinated charging/discharging control (CCD) strategy and a comparison with an uncoordinated charging/discharging (UCD) strategy.

5.1.1 Model of the energy storage system

In the literature, different models that reproduce the characteristic of ESSs are described. Several techniques, such as Fuzzy Logic, Kalman Filtering, Neural Networks and recursive, self-learning methods are employed to improve the accuracy of the state of charge (SoC) estimation [100]. Some models are very detailed and represent well the different operations of the battery, but the use of them in power

system simulations is computationally expensive and often not justified by the level of approximation that characterizes the other data of the problem. The Coulomb counting method is used to estimate the SoC of ESSs on long observation periods, reducing the computational complexity of the simulations. The mathematical formulation of the Coulomb counting method is:

$$SoC(T+\Delta T) = SoC(T) \pm \frac{I(T)\times \Delta T}{3600 \times C_{ESS}} \quad (52)$$

where C_{ESS} [Ah] is the BESS's capacity, I indicates the BESS's current, obtained by dividing the charge/discharge power of the BESS to its constant voltage and ΔT is the time interval of the control. In Figure 53 is depicted the connection scheme of the co-located PV/BESS at the PCC of the DN.

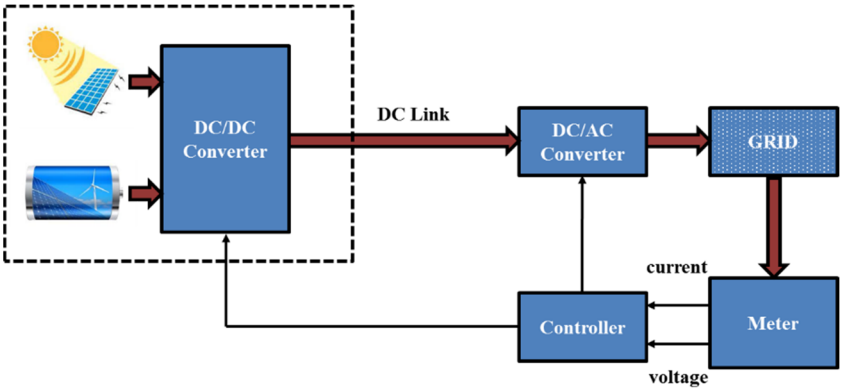

Figure 53. Layout of the co-located PV generator and BESS

The BESS is connected with the PV unit at a DC/DC converter and, through a DC-Link, interfaced to the distribution system by an inverter. The controller acquires current and voltage values from the network by means of meters. Data are processed in the control unit and the reference signals are sent to the DC/DC converter and the DC/AC converter to control the reactive/active power exchange with the DN, according to capability curves (see §3.1.1).

5.1.2 Co-located PV/BESS voltage control in DNs

A high PV production could cause voltage rises in distribution networks due to possible gaps between consumption and supply of electricity. The maximum admissible deviation from nominal system voltage at the PCC is typically 5% for the MV network [101], which allows having 5% of voltage margin on the LV network. However, these limits require the development of proper control techniques, able to realise regulation actions and to offer ancillary services for the distribution systems. Typically, PV units are interfaced to the grid by means of inverters that are able to inject or absorb reactive power. According to inverter characteristics, in some Countries, the DSO can receive reactive power support from IPPs when voltage problems occur (i.e. in Italy [102]). The integration of a BESS can increase the ability of PV systems in providing voltage support by reducing the need for reactive power. At the same time, active power curtailments are reduced.

5.1.2.1 Control method to improve voltage profiles on MV networks

The voltage regulation strategy is a decentralised control performed by the co-locate PV/BESS. Voltage problems usually occur when the difference between generation and demand is consistent. BESSs can support PV unit operations reducing active power curtailments. BESS store PV production during the period of over-generation and release the energy when voltage profiles are within a safe region or during peak demand periods to avoid voltage drops along the lines. However, BESSs might not solve the problem due to technical limits (limited capacity and capability of the battery). In this case, it is possible to support the network providing reactive power support to keep the voltage within mandatory limits. Nevertheless, due to the capability of the inverter, which limits the maximum injection/absorption of reactive power, also this control might fail forcing the PV unit to reduce the production. This strategy is applied locally at the PCC of each PV/BESS unit to regulate the voltage (decentralised approach). In details, the control is based on the sensitivity coefficients described in §3.2.1.1. By using the sensitivity coefficients, it is possible to calculate

the amount of active power to store or inject into the grid and, if necessary, the exchange of reactive power. The BESS is charged and discharged according to two control bands delimited by the coefficients $\varepsilon_{BESS\_charge}$ and $\varepsilon_{BESS\_discharge}$, as depicted in Figure 54.

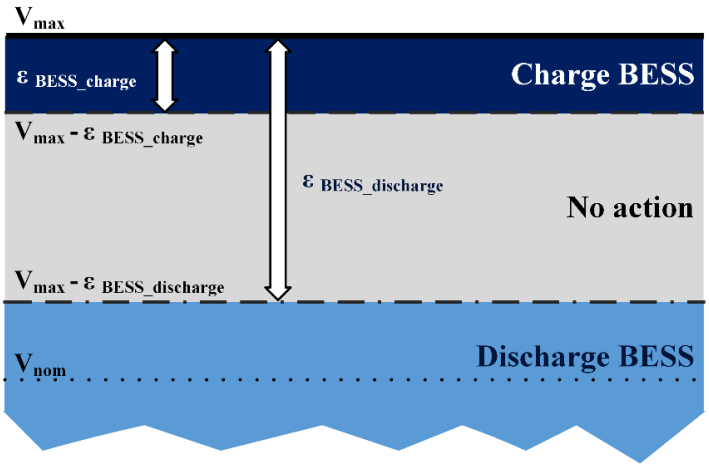

Figure 54. BESS voltage control bands

The flow chart in Figure 55 describes each single step of the control in case of voltage rise issues. The control algorithm starts measuring the voltage at the PCC of the PV unit, then the control time step, that is the minimum indecomposable time interval during the analysis, is ΔT. If the voltage is within the range [V_{max} - $\varepsilon_{BESS\_charge}$, V_{max}], the control carries out the value of active power $P_{BESS}(T)$ at which the PV energy is stored in the BESS, taking into account the maximum capacity (P_{BESS_max}) and capability (E_{BESS_max}). $P_{BESS}(T)$ is calculated by using the sensitivity coefficients. If the BESS energy $E_{BESS}(T)$ exceeds the maximum capability E_{BESS_max}, the control limits the charging power to the maximum capacity P_{BESS_max}. Battery physical limits might not allow keeping the voltage within safety values. In this case, the control applies a decentralised reactive control to reduce the voltage and, if necessary, curtails part of the active power production. Both these controls are applied as described in [47], where the sensitivity coefficients are used to calculate the amount of reactive power and, in case, active power curtailments to control the voltage.

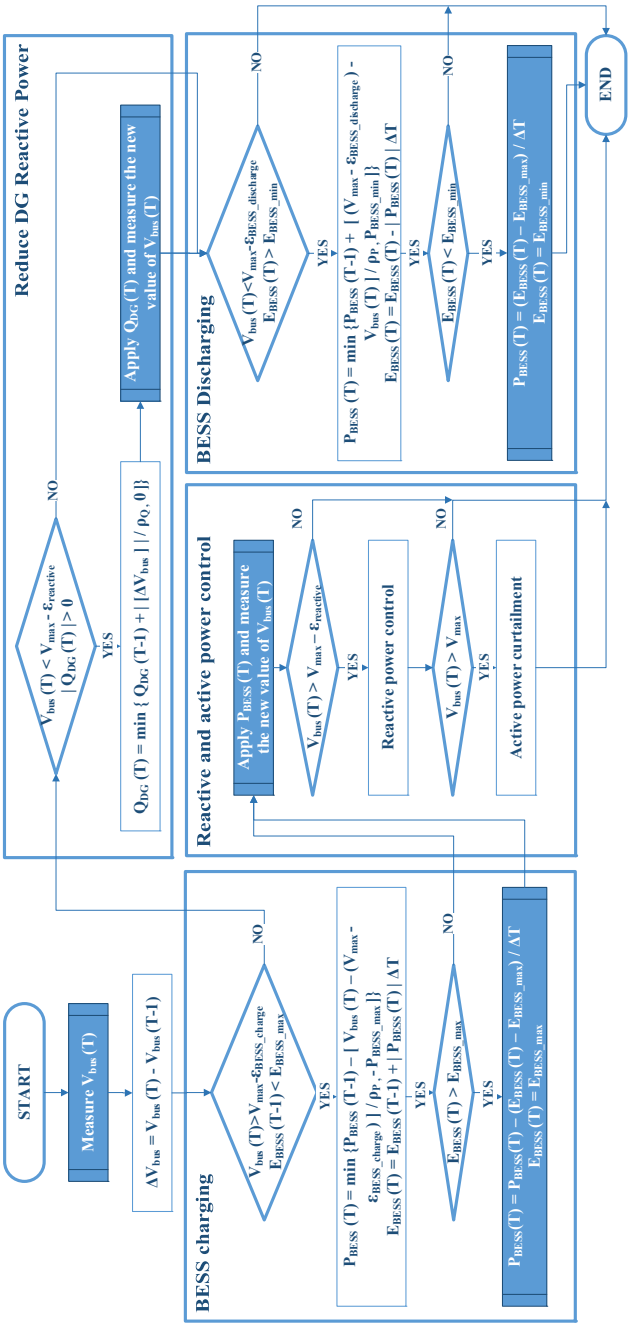

Figure 55. Flow chart of the voltage control algorithm

If the voltage at the PCC is in a safe area [V_{max} - $\varepsilon_{reactive,}$ V_{max}], the control reduces the reactive power of the system, if it is not already equal to zero. In case the voltage is lower than (V_{max} - $\varepsilon_{BESS\_discharge}$) and $\varepsilon_{reactive} > \varepsilon_{BESS\_discharge}$, the battery is discharged providing energy to the system. All the previous steps take into account SoC limits, maximum and minimum BESS capacity and capability, and the inverter capability curves.

5.1.2.2 Voltage control ancillary service in LV networks

Two BESS control strategies are implemented in order to evaluate the impact of BESS on LV voltage profiles. The interconnection with the main grid is 1-phase and is implemented by means of an inverter.

UCD control consents to increase the energy that can be self-consumed from a residential PV unit. Considering a single PV/BESS and the residential demand of the customer that owns the PV/BESS, the control can be synthetised in the following steps:

- the BESS is charged when the PV production is greater than the customer demand and the battery is not full;
- the BESS is discharged when the demand exceeds the generation and the battery is not empty;
- otherwise, the BESS is in idle mode.

Each residential customer independently controls its PV/BESS, thus the DSO is not involved in the process of charging/discharging the BESSs.

On the other hand, CCD control charges/discharges the BESS, according to the indications coming from the DSO in terms of time intervals. The DSO is able to roughly estimate when generation and demand peaks occur during the day by means of historical data and forecast analysis. In these periods of the day, the possibility of having voltage rises and voltage drops increases. As such, it is possible to envisage a control strategy where the DSO indicates charging (ΔT_c) and discharging (ΔT_d) time intervals of the residential BESS. In particular, ΔT_c is in correspondence of the daylight hours characterised by PV generation peak, while ΔT_d is in correspondence of the demand peak hours, where no generation comes from the PV units and there is a high

demand to satisfy (evening time). The BESS is charged if the following inequalities are verified:

$$\begin{cases} T_c^{\min} \le T \le T_c^{\max} \\ P_{PV_i}(T) \ge P_{load_i}(T) \\ SoC_{BESS_i}(T) \le SoC_{BESS_i}^{\max} \end{cases} \quad (53)$$

and it is discharged if:

$$\begin{cases} T_d^{\min} \le T \le T_d^{\max} \\ P_{PV_i}(T) \le P_{load_i}(T) \\ SoC_{BESS_i}(T) \ge SoC_{BESS_i}^{\min} \end{cases} \quad (54)$$

where $\Delta T_c = [T_c^{\min}, T_c^{\max}]$ and $\Delta T_d = [T_d^{\min}, T_d^{\max}]$, $P_{PV_i}(T)$, $P_{load_i}(T)$ and $SoC_{BESS_i}(T)$ are the power generated by the *i*-th PV unit, the load demand of the *i-th* customer and the SoC of *i*-th BESS at the time step *T*, respectively. Furthermore, $SoC_{BESS_i}^{\min}$ and $SoC_{BESS_i}^{\max}$ are the minimum and maximum values of the SoC related to *i*-th BESS. The storage system is in *idle* phase when eq. (53)-(54) are not verified.

5.2 Case studies

The control methodologies illustrated in the previous paragraph are tested on two distribution network characterised by different voltage levels. The control described in §5.1.2.1 is developed on a real MV distribution network, while the ancillary services proposed in §5.1.2.2 are applied to a typical Italian LV network.

Case studies are described before showing the results achieved in the simulation process.

5.2.1 Support DSO in solving voltage issues on MV networks by using co-located PV/BESS

The validation of the control proposed in §5.1.2.1 is performed on a real Italian MV distribution network. Simulations are carried out on an annual basis with real profiles for PV solar systems and considering different size for the BESSs.

5.2.1.1 Description of the case study

The MV distribution network considered is described in detail in Paragraph 3.3. Four PV plants, each with a rated power of 5 MVA, are connected to buses 31, 46, 53 and 54. Three different lithium-ion battery sizes are considered in the study: the first one, denoted as BESS1, has a size of 0.5 MW/1.5 MWh; the second one, named BESS2, considers a 1 MW/3 MWh battery; the last one, indicated as BESS3, is a 2 MW/6 MWh battery. In all cases, the SoC is limited to 20% and 90%.

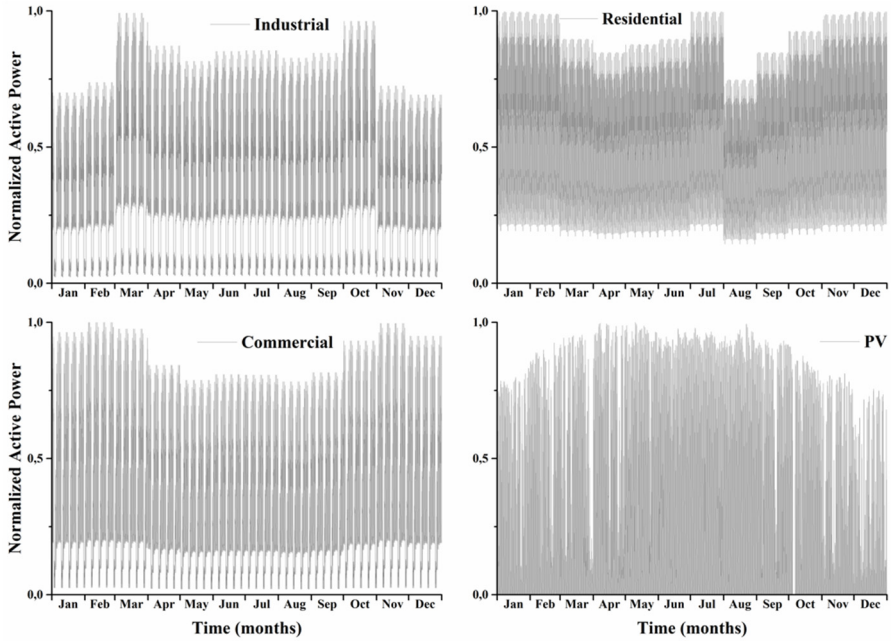

Figure 56. Normalised active power annual profiles

The annual normalised profiles used to model the PV production and the demand are depicted in Figure 56. PV production is based on real measurements on the site where the distribution network is located (south of Italy) [103]. The demand is built considering the work in [104]. A time-series simulation is carried out on a year, from January to December, with a time step of 15 minutes, so that the annual time series simulation is carried out on 35040 points. The parameters are set as follows: $\varepsilon_{BESS\_charge} = \varepsilon_{reactive} = 0.01$ and $\varepsilon_{BESS\_discharge} = 0.05$. Italian standard CEI 0-16 [102] is considered. Voltage profiles without applying any control at the PCC of the PV units are shown in Figure 57. Buses 46 and 54 are affected by voltage issues. In detail, voltage rises occur in summer days when the PV units production increases.

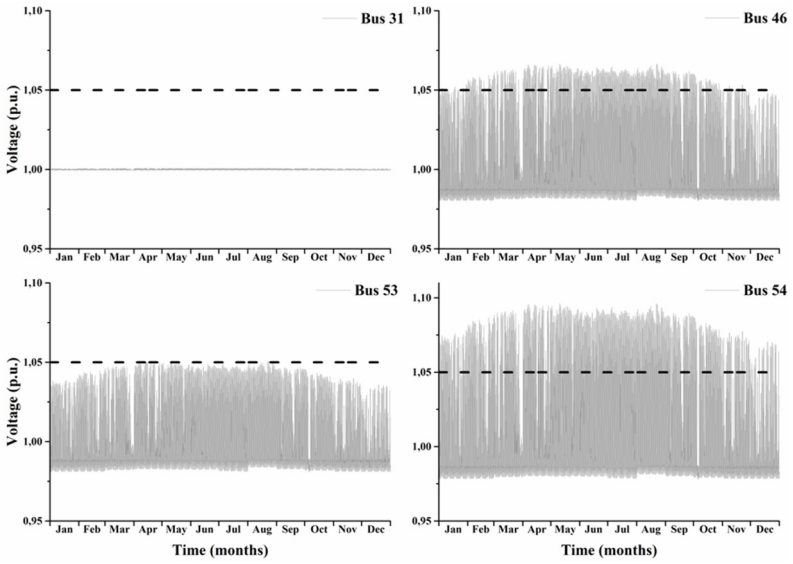

Figure 57. Voltage profiles at the PCC of the PV units without control

5.2.1.2 Simulation results

In Figure 58, the results achieved by applying the reactive power control as in [47] and the proposed control methodology are compared. Box charts representation has pointed out that all the control strategies achieve a correct control. Furthermore, a reduction of the maximum, the mean and the range of voltage variation on the whole year is

achieved. Nevertheless, same results are achieved with a different use of the distributed resources in terms of reactive power. For instance, in Table 12 are reported the annual energy consumption of the PV unit connected to bus 54, which is the most sensible to voltage issues.

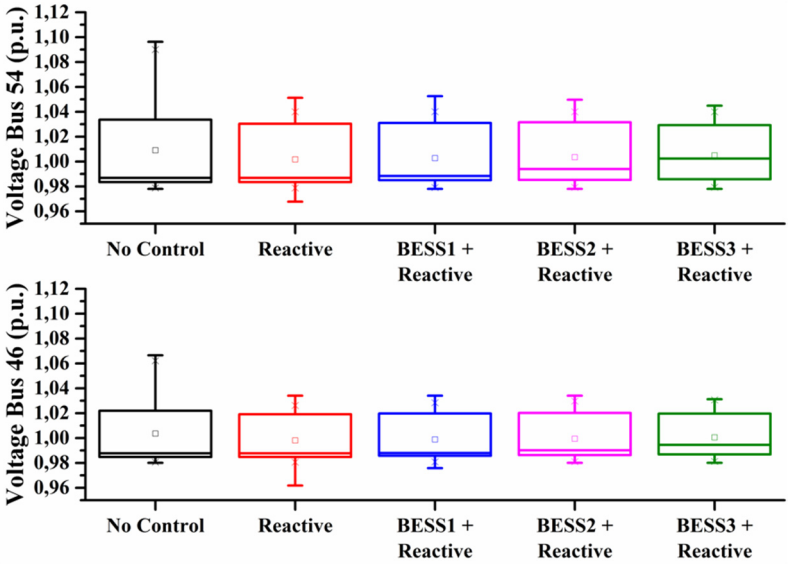

Figure 58. Voltage profiles at buses 46 and 54 in different scenarios

Table 12. Summary of annual energy consumption of PV unit at bus 54

Cases	$E_{reactive}$ (MVArh)	$\Delta E_{reactive}$	E_{stored} (MWh)
Reactive control	3469	0%	-
BESS1 + Reactive	3068	-12%	443
BESS2 + Reactive	2784	-20%	893
BESS3 + Reactive	2263	-35%	1767

A reduction of reactive power usage is visible with the installation of a BESS. The reduction of reactive energy consumption varies from a minimum of 12% (BESS1 scenario) to a maximum of 35% (BESS3 scenario). Furthermore, in the third column is reported the annual energy stored by the BESS from the co-located PV unit: this amount of energy can be used to support the network during demand peak hours providing an ancillary service to the DSO. Voltage profiles for different

scenarios of the PV/BESS at bus 54 are depicted in Figure 59. To illustrate the BESS effect on voltage profiles, a zoom of 9 days is shown in Figure 60. The grey curve is the voltage when no control actions are applied, while the red curve shows the effect of the BESS when the proposed control is implemented. A peak shifting action due to the action of the BESS is distinguishable. In Figure 61, the capability curves and the operating points of the applied control strategies are shown. No violations occur during the whole analysis. The installation of a BESS with a PV system brings several benefits to the IPP. For instance, in summer BESS allows the reduction of possible disconnections or power curtailments when generation exceeds the demand. Furthermore, the stored energy can be released during peak demand hours to support the network in case of voltage drops. Another paramount aspect is the possibility to reduce the size of the inverter (nominal apparent power) without incurring in active power curtailments when the PV units provide reactive power support at nominal power.

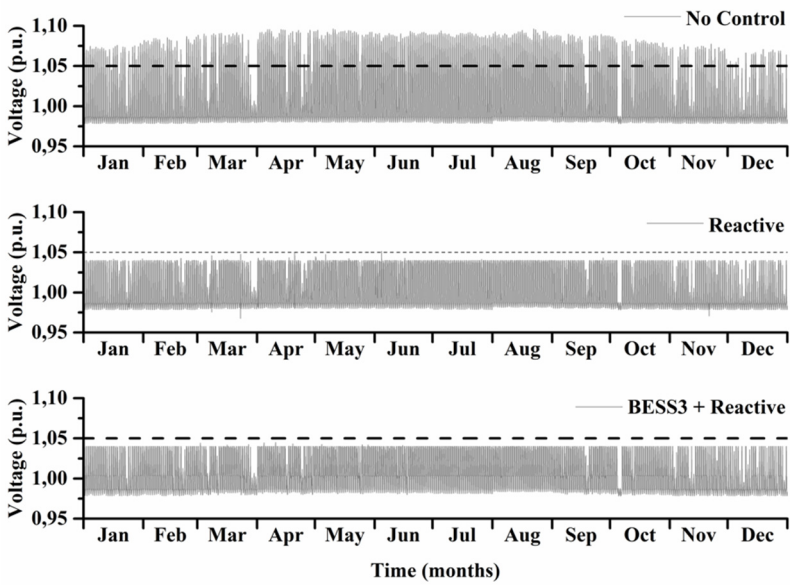

Figure 59. Voltage profiles at bus 54 in different scenarios

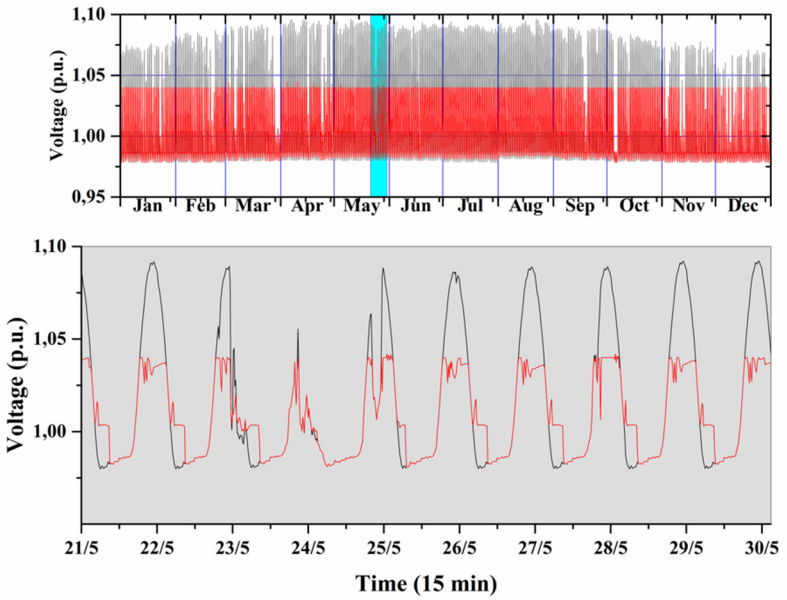

Figure 60. Effect of the proposed control on voltage profiles

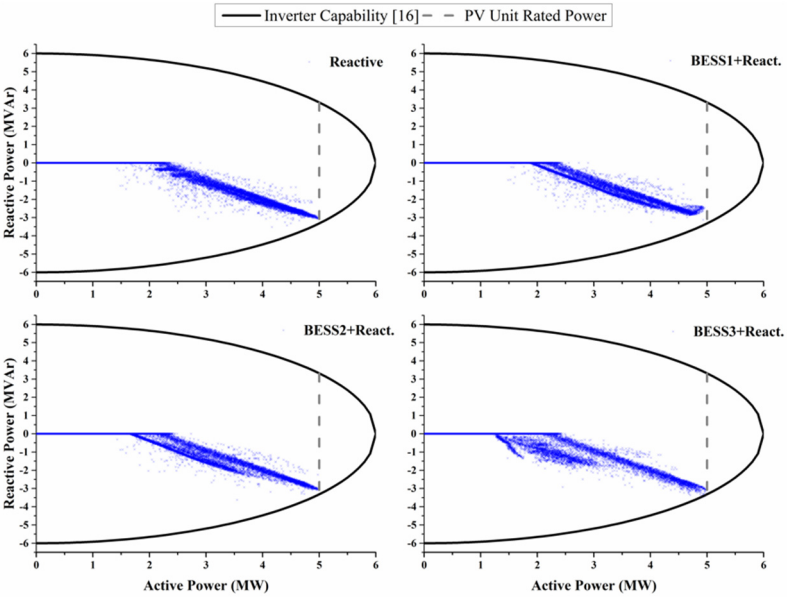

Figure 61. Capability curves of PV units at bus 54 in different scenarios

In fact, the BESS can manage this behaviour by storing the excess power and releasing it when voltage issues are solved. Instead, in case the BESS is not installed, a reduction of the inverter size reduces the ability of the PV unit to inject/absorb reactive power at the rated power of the PV system. This means that the IPP must cut off the production or disconnect the PV unit during periods of high generation. However, it is worth noting that, usually, the IPP might be not interested in developing an ancillary service without remuneration. If the IPP has a quantifiable benefit in solving voltage rises along the lines, he cannot be interested in supporting the DSO in case of voltage drops if no incentives or remuneration mechanisms are implemented.

5.2.2 Assess PV/BESS integration in residential unbalanced LV network to support voltage profiles

Time-series simulations on a typical LV network are developed to assess the benefits of the ancillary service described in §5.1.2.2. In real-life systems, the integration of co-located PV/BESSs can have different effects depending on the specific scenario, control strategy, customer needs, irradiance and local demand. To this end, the stochasticity at this voltage level is tackled by implementing a Monte Carlo analysis as in [105], [106]. In detail, simulations are carried out for summer and winter days by varying generation profile, customer demand and penetration level, location, capacity and capability of the PV/BESS.

Thus, the massive data analysis consents to understand under different conditions the possible benefits achievable in terms of voltage quality and energy self-consumption. The achieved results are an important indication of the possibility that BESSs have in providing ancillary services in LV network. Based on that, DSO could implement incentive or remuneration mechanisms to sustain BESS installations in distribution systems.

5.2.2.1 Stochastic analysis

The stochasticity at this voltage level is analysed by applying a Monte Carlo simulation with different penetration levels and locations of PV/BESSs on the LV network as well as different generation and

load profiles. The objective is to estimate the impact of BESS when these are involved in providing an ancillary service able to reduce voltage issues. Results are a function of locations, penetration levels, ESS capability, PV unit capacity, load and generation profiles. A classical Monte Carlo approach estimates the mean and the variance of the output variables expressed as follows:

$$\langle x \rangle = \frac{1}{N} \sum_{i=1}^{N} x_i \quad \textbf{(55)}$$

$$s^2(x) = \frac{N}{N-1} \left[\langle x^2 \rangle - \langle x \rangle^2 \right] \quad \textbf{(56)}$$

where x_i is the number of occurrences of the event and N is the number of cases. Furthermore, the standard error of the mean ($SE_{\langle x \rangle}$) can be defined formulated as:

$$SE_{\langle x \rangle} = \frac{s}{\sqrt{N}}. \quad \textbf{(57)}$$

Simulations are carried out for two seasons: winter (scenario I) and summer (scenario II). Although EN50160 suggests a weekly analysis, only two days that present critical characteristics in terms of voltage profiles are analysed. On the basis of other studies (e.g.: [105]), this analysis is sufficient to achieve accurate results. For each scenario and for each control strategy (UCD and CCD), the space of solutions is examined by applying a Monte Carlo analysis, as described in the following step-by-step procedure.

1. set the PV penetration level, defined as the percentage of PV units in the network compared to the total number of residential customers (from a minimum value of 0% to a maximum value of 100% with steps of 10%);
2. perform a random allocation of PV units on the residential buses of the LV network;
3. associate to each bus a load profile chosen randomly from a database created by means of a high-resolution software;

4. associate to each PV unit a generation profile chosen randomly from a database of real PV profiles;
5. perform a random choice of PV units capacity;
6. perform a random choice of BESSs capability from a list of different models;
7. perform three different daily unbalanced power flows: the first considering only the PV units (Step 2), the second taking into account also the co-located BESSs controlled by using the UCD strategy, and the third one by applying the CCD control to the previous case;
8. repeat the Steps from 2 to 7 up to the maximum number of cases (k_{MAX});
9. come back to the Step 1 and increase the PV penetration level up to 100% (with steps of 10%).

A flow chart is depicted in Figure 62. A statistical analysis of voltage violation occurrences and energy self-consumption is performed for each PV penetration level considering three different scenarios:

- only PV units connected to the buses;
- co-located PV/BESSs controlled with UCD control;
- CCD control.

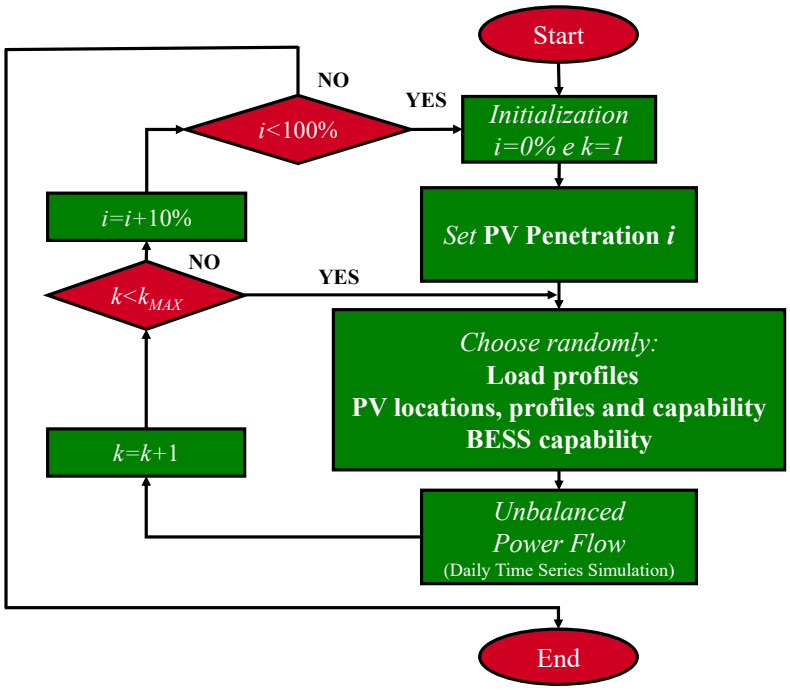

Figure 62. Flowchart of the Monte Carlo procedure used to simulate different sources of uncertainty in the distribution network

5.2.2.2 Description of the case study

The diagram of the LV network is shown in Figure 63: it is a typical LV Italian distribution network [104] with 3 LV feeders (A, B, C) connected to the MV network through a 10/0.4 kV Δ/Yg transformer with rated power equal to S_T = 250 kVA and V_{cc} = 4%. The transformer tap is fixed to 1.00 p.u. The network consists of 68 buses with 136 mono-phase residential loads and 9 three-phase between industrial and commercial loads. Taking into account the rated power of each customer, it is possible to divide the demand as in [104]: 43% in the feeder A, 44% in the feeder B and 13% in the feeder C.

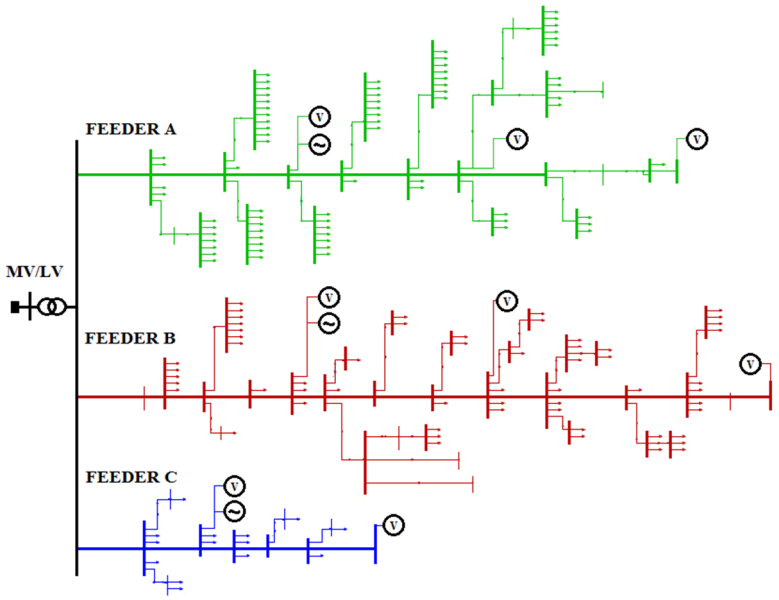

Figure 63. LV Network diagram

Single-phase residential profiles are simulated by using a modified version (customised for the Italian case) of the software elaborated by the CREST [74], which allows the creation of a database of high resolution domestic profiles (in this case, the resolution is 5 minutes) for specific periods of the year, load compositions and number of family members. A database of 250 different daily residential load profiles has been created for the Monte Carlo analysis. To this end, three-phase loads are characterised by typical commercial and industrial profiles [61].

Mono-phase PV systems are randomly allocated at each Monte Carlo iteration. PV penetration level changes from 0% to 100% of the demand, with steps of 10%. The rated power of residential PV systems changes randomly at each iteration from 2 to 6 kW. The power factor is set to 1 in order to be independent from possible effects of the reactive power on voltage profiles. 3 three-phase PV units with a rated power of 15 kW and a unitary power factor are connected to the LV network as showed in Figure 63. The size and location of these PV units do not change during the Monte Carlo analysis; moreover, PV profiles are randomly chosen from a database of 10 real Italian PV generation

profiles of a winter day (scenario I) and 10 real Italian PV generation profiles of a summer day (scenario II) [107]. BESSs, co-located with PV systems, have a capacity of 3 kW and a capability chosen randomly among one of the three possible solutions illustrated in Table 13.

Table 13. BESSs Characteristics

Capacity (kW)	Capability (kWh)	SoC limits (%)
3	5.25	20-90
3	7.00	20-90
3	8.75	20-90

By applying the UCD control, the BESSs can be charged or discharged during the day, depending only on customers' behavior. In order to enhance the peak shaving capacity of BESSs, the charging and discharging periods can be constrained in two time intervals, during higher generation and demand periods, by means of CCD control. Here, the choice of ΔT_c and ΔT_d is not the result of an optimisation process but it is based on historical data and on a day-ahead forecast of the demand and generation profiles. ΔT_c and ΔT_d are estimated considering the historical and the irradiation data of the PV site located in the south of Italy [107] both with the database of demand profiles. The charging time interval results to be ΔT_c = [12:00, 18:00], while the discharging time interval is ΔT_d = [18:00, 24:00], both for the summer scenario. For the winter scenario, ΔT_c = [10:00, 16:00] and ΔT_d = [16:00, 24:00]. DSO communicates the set-points to the residential customers through an information layer. Time intervals are wide enough to take into account possible forecast errors due to the variability and uncertainty of residential demand and PV generation. The aim of fixing two time intervals to charge and discharge the ESSs is to support the network during peak period (generation and demand). In the next sub-paragraph, it will be shown how the provision of the ancillary service to the DSO has a limited impact in terms of energy self-consumption. Furthermore, by limiting the charging and discharging period of the ESS it is possible to increase the cycling life of the batteries (the battery cycle is limited to 1 per day).

Unbalanced power flow problems are solved monitoring each phase of the network by using OpenDSS [91]. The location of the meters used

to monitor the voltage in the network is depicted in Figure 63. $N = 1000$ cases are simulated for each PV penetration level. Whereas two scenarios with 11 PV penetration levels are analysed, a total number of 22000 cases are simulated: three power flows (without BESSs, with BESSs controlled with UCD and with BESSs controlled with CCD) every 5 minutes for a whole day. 19.008×10^6 unbalanced power flows are solved during the analysis. Thermal limits are checked to verify the technical feasibility of the solution.

5.2.2.3 Simulation results

CEI EN50160 is considered as the standard reference to determine voltage violations in the feeders [20]. The analysis is carried out considering two different scenarios:

- Scenario I represents a typical Italian winter day. One of the PV generation profiles depicted in Figure 64a is randomly picked by the algorithm. The peak demand is forecasted to be in the early evening;
- Scenario II represents a typical Italian summer day characterised by a high PV production in the mid of the day, as visible in Figure 64b. Peak demand is slightly shifted towards late evening. The network is highly affected by voltage rises, so that the possibility to limit the maximum ESS charging power to 1.5 kW for each ESS residential system (when the CCD control is applied) is considered.

The results of the Monte Carlo analysis show that feeders A and B are subjected to voltage issues in both scenarios, while feeder C does not incur in any voltage problem.

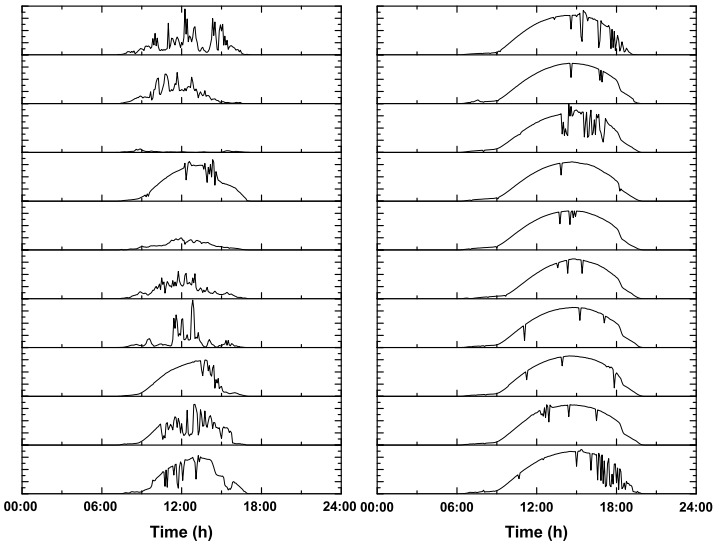

(a) (b)

Figure 64. Real Italian normalised PV generation profiles for winter (a) and summer (b)

Scenario I: winter

Figure 65 compares voltage drops occurrences both for feeder A (Figure 65a) and B (Figure 65b) as a function of PV penetration levels. In blue, results without ESSs are depicted, while in red and in green are shown the daily mean of voltage drops with BESSs considering UCD and CCD control, respectively. BESSs are able to reduce voltage drops at each penetration level. It is clear that the benefits grow with the PV/ESS penetration. This behavior depends on the increasing capacity that the PV/ESS have in supplying locally the residential demand. Moreover, CCD control achieves in most cases better results compared to the UCD control. Furthermore, voltage rises are negligible for Scenario I, because PV production is not so high in winter; for these reasons simulation results for voltage rises are not shown. Figure 66 shows that the CCD slightly reduces self-consumption of energy coming from PV systems compared to the UCD. Both controls increase local energy consumption, compared to the case where no BESSs are installed. In Table 14 the means, variances and standard errors of voltage drops for feeder A are shown. Standard Error (*SE*) confirms that the solution is stable because the variability of the mean is low (*SE* is less than 0.21 for each penetration level).

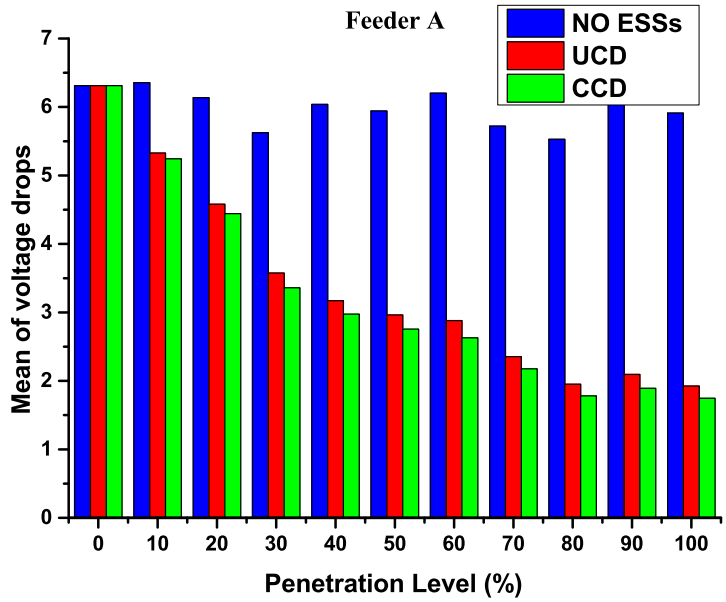

(a)

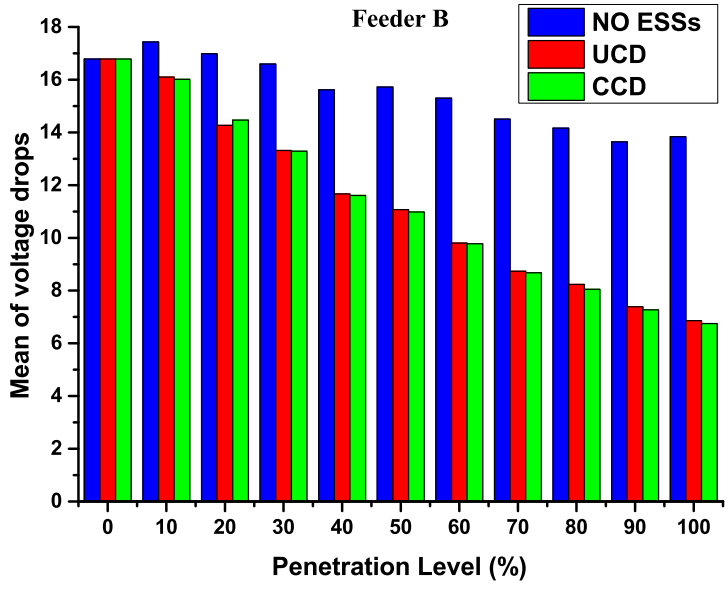

(b)

Figure 65. Mean of voltage drop issues for feeder A (a) and feeder B (b) - Scenario I (winter)

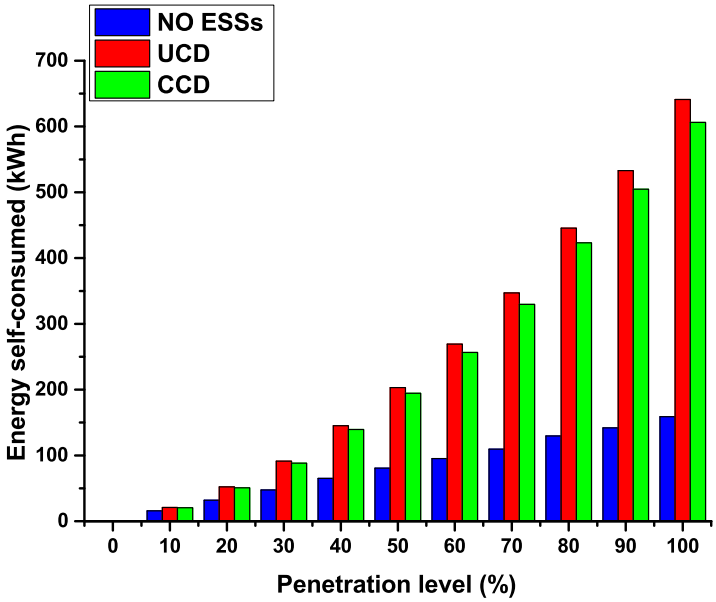

Figure 66. Daily mean of aggregated energy self-consumption - Scenario I (winter)

Table 14. Statistical results of Scenario I: voltage drops in feeder A

Penetration	UCD			CCD		
	‹x›	$s^2(x)$	*SE*	‹x›	$s^2(x)$	*SE*
0%	6.31	6.52	0.21	6.31	6.52	0.21
10%	5.32	5.80	0.18	5.24	5.78	0.18
20%	4.58	5.93	0.19	4.44	5.85	0.19
30%	3.57	5.01	0.16	3.36	4.81	0.15
40%	3.17	4.94	0.16	2.98	4.74	0.15
50%	2.96	4.55	0.14	2.76	4.32	0.14
60%	2.88	4.89	0.15	2.63	4.64	0.15
70%	2.35	4.39	0.14	2.18	4.20	0.13
80%	1.95	3.88	0.12	1.78	3.66	0.12
90%	2.09	4.16	0.13	1.89	3.90	0.12
100%	1.92	3.90	0.12	1.75	3.69	0.12

Scenario II: Summer

The increase of PV production in summer consents to exploit the ability of battery systems to provide voltage support by shifting energy

from a period to another. Voltage drops are conspicuously reduced with the introduction of BESSs, as in Scenario I. Voltage drops are almost independent from the PV penetration level when no BESSs are installed into the grid because, usually, they occur during demand peak when PV generation is very low or zero. Also, in this case, there is not a substantial difference between UCD and CCD controls, as shown in Figure 67. If the results obtained by using CCD control are promising by analysing voltage drop issues, they are noteworthy when voltage rises are analysed. Figure 68 shows the reduction of voltage rise problems in the network achieved by applying the CCD control at different PV/BESS penetration level. This result may be explained considering that the integration of a BESS with a PV system can solve, in most of the cases, voltage rise violations by flattening the net demand in the network. The UCD control limits the possibility to support the network during demand and generation peak because the ESS can be charged or discharged independently by the state of the network. Furthermore, the continuous alternation of charging and discharging phases of the UCD control increases the number of BESS cycles in a day reducing the life of the battery system. It has also been exploited the possibility of implementing the CCD control by reducing the maximum charging power of the ESS to 1.5 kW. This allows spreading the ability to store energy for a longer time period. This choice does not reduce energy self-consumption compared to the CCD control without a capacity limit. Moreover, in summer, the battery need less time to fully charge because of the high PV production during the mid of the day. The reduction of the maximum charging power has also a positive effect on the battery life obtained by reducing the C-rate. It is worth noting that the CCD control with a capacity limit configuration allows the reduction of considerably voltage rise occurrences in both feeders increasing the hosting capacity. Voltage rise occurrences greater than 1 are taken as the limit to identify the hosting capacity of the network. CCD control with maximum 1.5 kW during the charging phase increases the hosting capacity compared to the UCD control from 40% to around 80% in the feeder A and from 30% to around 60% in the feeder B (Figure 68).

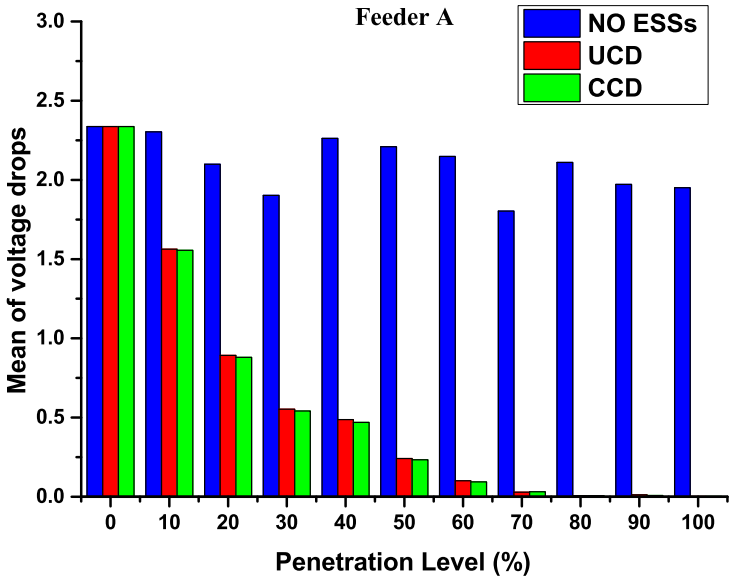

(a)

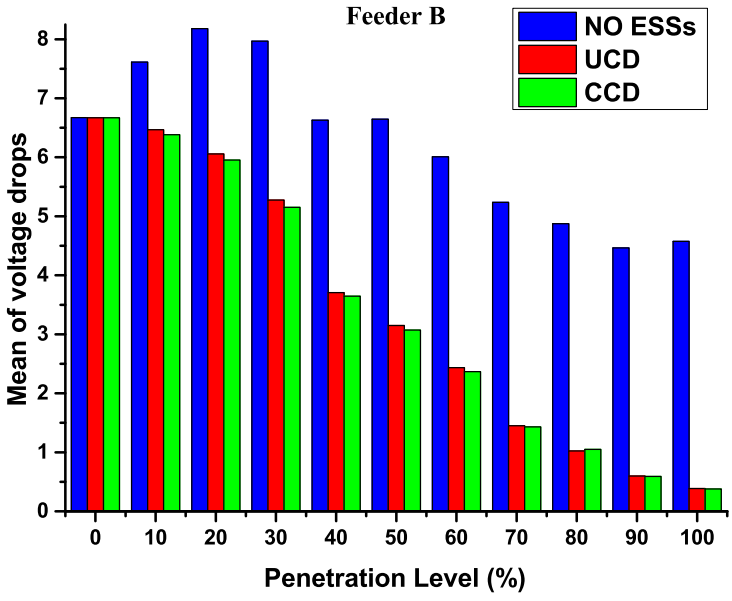

(b)

Figure 67. Mean of voltage drop issues for feeder A (a) and feeder B (b) - Scenario II (summer)

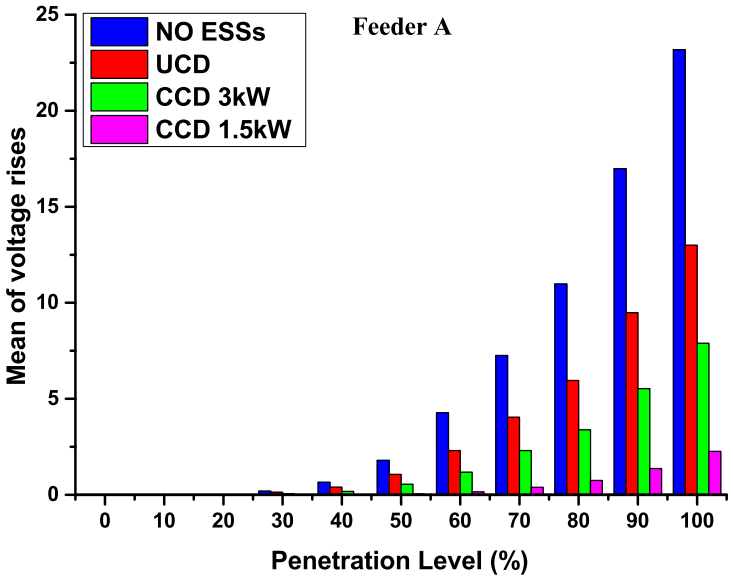

(a)

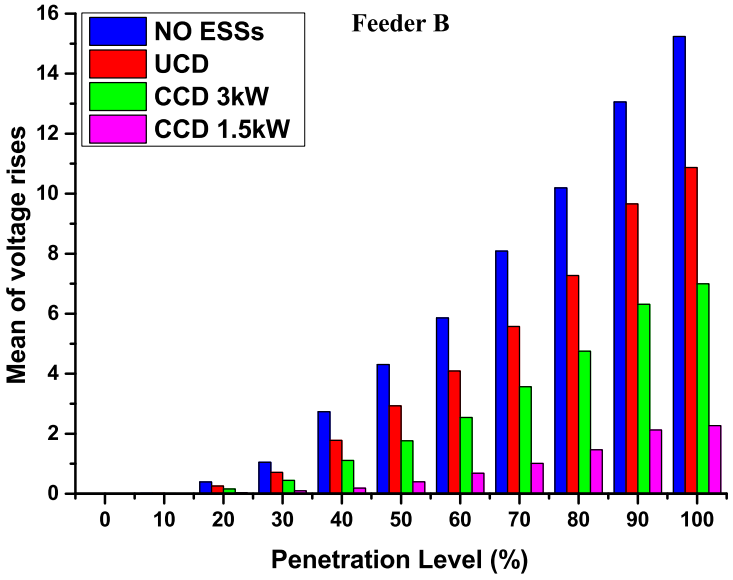

(b)

Figure 68. Mean of voltage rise issues for feeder A (a) and feeder B (b) - Scenario II (summer)

Having less voltage rise issues, it is possible to have a reduction in PV systems disconnections or active power curtailments. Figure 69 shows the daily self-consumption of solar energy of all residential customers equipped with a PV/BESS. The CCD does not reduce significantly energy self-consumption compared to UCD control. Moreover, the CCD with a limited charging capacity of 1.5 kW shows similar self-consumption to the case without any capacity limit.

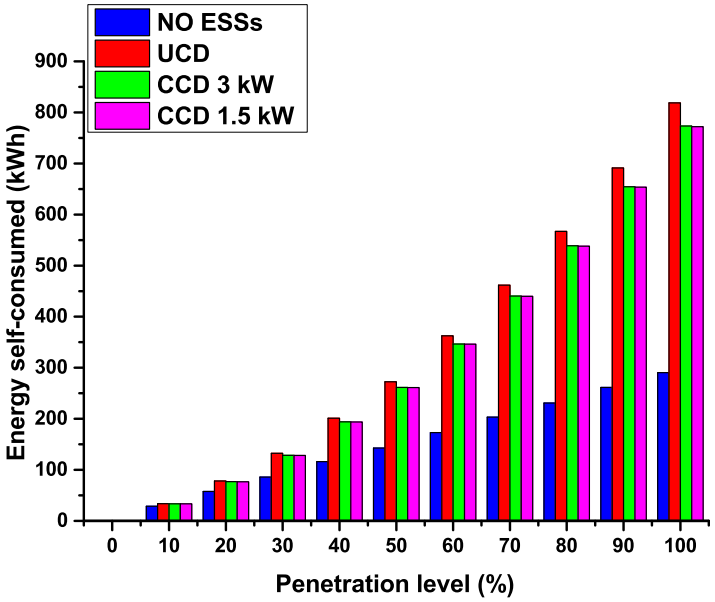

Figure 69. Daily mean of aggregated energy self-consumption - Scenario II (summer)

In Table 15 and Table 16, the statistical results of the MC analysis are summarised. It is worth noting that the average of voltage problems of feeder A is lower than 1 up to 60% of penetration level by using the 3 kW-CCD control. Similar conditions are reached in feeder B up to 30%. The 1.5kW-CCD control further reduces voltage rise occurrences at each penetration level. In Figure 70 the robustness of the solution after 1000 cases is proven by illustrating the moving average of voltage drops for feeder B without and with the ESSs. The Monte Carlo analysis gives stable solutions after 250 iterations. Finally, a snapshot of the three-phase daily voltage profiles at 100% of PV penetration for feeder

A is depicted in Figure 71, in order to show how the integration of storage systems with PV units allows keeping the voltage within the mandatory limits of 0.9 p.u. and 1.1 p.u.

Table 15. Statistical results of Scenario II: voltage rises in feeder A

Penetration	UCD			CCD (3 *kW*)			CCD (1.5 *kW*)		
	‹*x*›	$s^2(x)$	*SE*	‹*x*›	$s^2(x)$	*SE*	‹*x*›	$s^2(x)$	*SE*
0%	0.00	0.00	0.00	0.00	0.00	0.00	0.00	0.00	0.00
10%	0.00	0.00	0.00	0.00	0.00	0.00	0.00	0.00	0.00
20%	0.01	0.16	0.01	0.01	0.13	0.00	0.00	0.00	0.00
30%	0.13	1.00	0.03	0.06	0.48	0.02	0.00	0.00	0.00
40%	0.39	1.88	0.06	0.17	0.99	0.03	0.01	0.11	0.00
50%	1.06	3.45	0.11	0.55	2.09	0.07	0.04	0.38	0.01
60%	2.31	5.04	0.16	1.18	3.06	0.10	0.15	1.03	0.03
70%	4.04	6.68	0.21	2.31	4.40	0.14	0.39	1.76	0.06
80%	5.95	7.59	0.24	3.38	5.12	0.16	0.75	2.83	0.09
90%	9.49	8.49	0.27	5.53	6.12	0.19	1.37	3.93	0.12
100%	12.99	7.94	0.25	7.89	6.42	0.20	2.26	4.42	0.14

Table 16. Statistical results of Scenario II: voltage rises in feeder B

Penetration	UCD			CCD (3 *kW*)			CCD (1.5 *kW*)		
	‹*x*›	$s^2(x)$	*SE*	‹*x*›	$s^2(x)$	*SE*	‹*x*›	$s^2(x)$	*SE*
0%	0.00	0.00	0.00	0.00	0.00	0.00	0.00	0.00	0.00
10%	0.01	0.14	0.00	0.00	0.07	0.00	0.00	0.00	0.00
20%	0.26	1.86	0.06	0.16	1.27	0.04	0.03	0.47	0.01
30%	0.71	2.99	0.09	0.45	2.10	0.07	0.10	0.90	0.03
40%	1.78	4.52	0.14	1.11	3.04	0.10	0.19	1.10	0.03
50%	2.93	5.93	0.19	1.76	3.98	0.13	0.40	2.18	0.07
60%	4.09	7.08	0.22	2.54	4.90	0.15	0.69	2.65	0.08
70%	5.57	7.78	0.25	3.57	5.57	0.18	1.01	3.04	0.10
80%	7.27	8.40	0.27	4.75	6.12	0.19	1.47	4.28	0.14
90%	9.66	9.10	0.29	6.31	6.69	0.21	2.12	4.97	0.16
100%	10.87	8.71	0.28	6.99	6.51	0.21	2.27	5.32	0.17

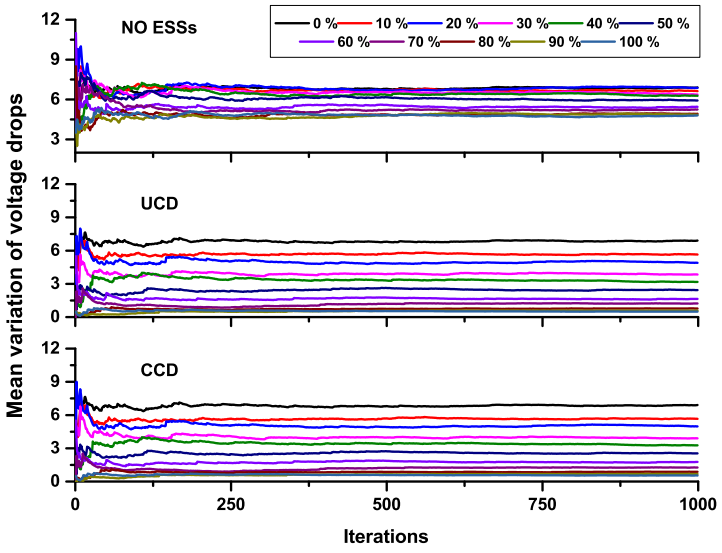

Figure 70. Moving average of voltage drops for feeder B

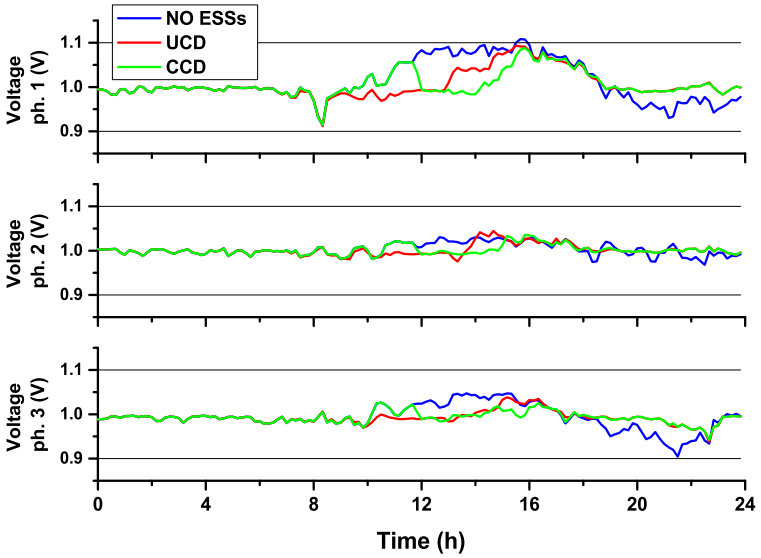

Figure 71. 3-phase voltage profiles

5.3 A conceptual framework to assess the economics of grid-integrated energy storage resources

A conceptual framework able to represent the unique ESR features and to monetise ESR deployment in a broad range of cases – a variety of roles and applications – is presented. The economic evaluation of the operation of ESRs must be undertaken through a comprehensive approach, which must be able to account for all the benefits of the integration of ESRs, and must be generic, and thus, have the capability to be utilized for different scenarios. Hence, in order to take into account all the primary and the supplementary services of ESRs in different scenarios, it is indispensable to develop a conceptual framework which must take into account all the operational, regulatory, financial, and environmental aspects of ESR integrations. A key requirement of the framework is to have the ability to represent different scenarios and applications in which the ESR can be deployed within a market environment. Apart from the operational paradigm of different ESR applications, the framework must be able to incorporate also the business models of these applications. The aim is to incorporate relevant policy issues and appropriate policy alternatives as well as to implement new market products to effectively harness ESR features. To this end, the structure and a preliminary formulation of the framework are presented in this paragraph.

5.3.1 Energy storage systems comprehensive framework

The framework must evaluate the environmental impacts of ESRs and it must have the ability to represent various contractual agreements between ESRs and other resources via instruments such as power purchase agreements and contract for differences. The framework must be able to represent the physical grid, the ESR embedding environment, if any, all resources/loads; the interchange of control signals, market information/forecasts/data, environmental attributes and sensor measurements; the physical/financial/information flows between

physical resources, market players, asset owners and resource and grid operators. To meet these requirements, an interconnected four-layer framework structure consisting of a physical layer, an information layer, a market layer and an environmental layer has been designed. The framework comprehensively describes all the interactions among the embedding environment in which the ESR is deployed and other players/stakeholders in the grid and markets. Two specific operators are identified in the structure:

- the independent grid operator (IGO), which operates the grids and the wholesale markets;
- the embedding environment operator, which operates and is in charge of submitting bids/offers of the physical assets of the embedding environment.

The embedding environment is able to generalise the wide range of ESR applications. The aim is to emphasise and to represent the interactions between different elements of the layer whatsoever are the used models to describe them. The structural modularity of the framework provides enough flexibility for its applications in several studies and analysis regarding ESRs. The models inside each layer are for this reason only mentioned but not fully described. Multiple designs may be accommodated by the general structure depicted in Figure 72. The framework is comprehensive as it includes all the necessary modules and interactions to describe storage deployment and operations under a wide range of settings. The implementation of the various layers can be done through the development of different models and tools in order to assess the different aspects associated with the deployment of ESRs and their operation in a given setting.

5.3.1.1 Physical layer and ESR embedding environment

The need of defining an embedding environment relies on the willingness to divide the interactions inside the embedding environment with the interactions of the embedding environment with the grid and the electricity market. The embedding environment is, at the same time, embedded into the power system. The embedding environment includes the physical assets of the specific applications.

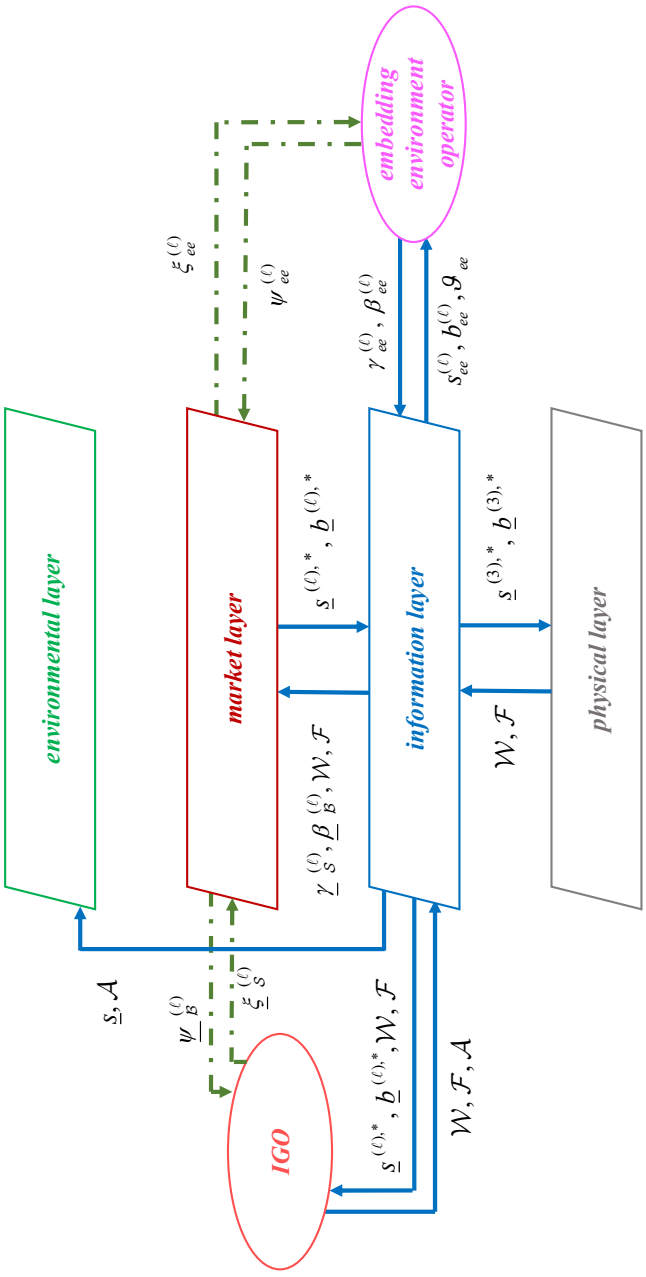

Figure 72. Structure of the comprehensive framework

For instance, in the case of a benefit/cost analysis of an ESR installed in a wind farm to reduce the energy spillage, the embedding environment is the system wind farm - energy storage. Analogously, the embedding environment in the case of deferring the investment in a primary substation is the same substation. In some applications, the embedding environment could incorporate only the ESR: this is the case of an IPP which owns an ESR for speculative purposes. By using an embedding environment, it is possible to represent an aggregation of ESRs playing in the energy markets. Hence, this framework allows also the study of the benefits of the implementation of a vehicle-to-grid/vehicle-to-microgrid structure in which an aggregator of electric vehicles sells/buys energy in the energy market.

The physical assets of the embedding environment are represented by three different entities, as depicted in Figure 73: a load resource, a generation resource and an ESR. The three entities can represent either a single asset or an aggregation of multiple assets.

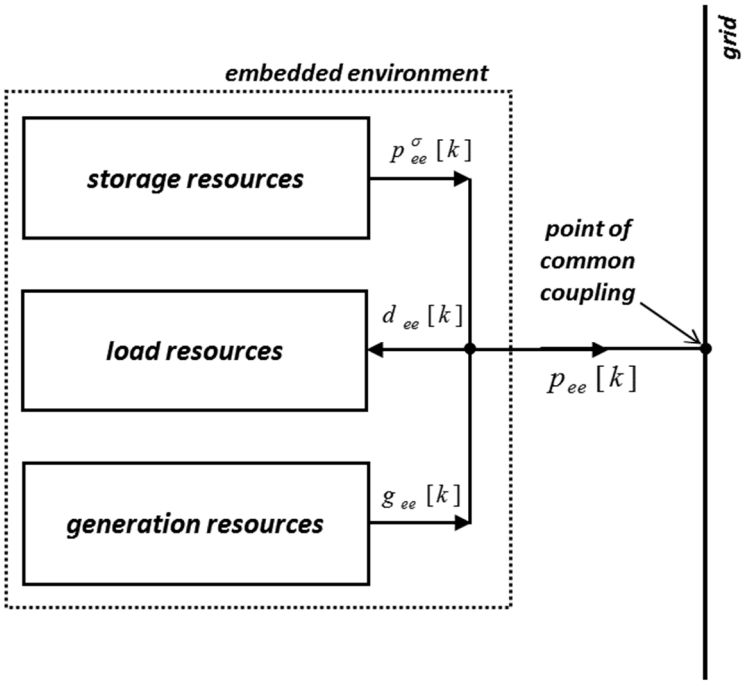

Figure 73. Embedding environment – grid interactions

In the figure above, $x\,[k]$ is the variable x in the k-th discrete time period. The power flows between the embedded environment and the power grid are represented in Figure 73. The power exchange with the grid is:

$$p_{ee}[k] = g_{ee}[k] - d_{ee}[k] + p_{ee}^{\sigma}[k]. \qquad (58)$$

The ESR σ acts either as a load or as a generation resource or remains idle with no impact on the side-by-side power system and market operations. The operational state of the ESR – charge, discharge or idle – together with its associated output $p_{ee}^{\sigma}[k]$ remains unchanged over the time period k. Under this assumption, let $e_{ee}^{\sigma}[k]$ be the stored energy of the ESR resource σ at the close time period k, or at the start of the time period $[k + 1]$. The discharge and charge efficiency of ESR σ by the factor η_d^{σ} and η_c^{σ}, respectively. The round-trip efficiency is $\eta^{\sigma} = \eta_d^{\sigma}\eta_c^{\sigma}$. The relation between $e_{ee}^{\sigma}[k]$ and $p_{ee}^{\sigma}[k]$ can be formulated as follows:

$$e_{ee}^{\sigma}[k] = e_{ee}^{\sigma}[k-1] + p_{ee}^{\sigma}[k]\left(u_d^{\sigma}[k]\,\eta_d^{\sigma} + u_c^{\sigma}[k]\frac{1}{\eta_c^{\sigma}}\right). \qquad (59)$$

The binary variables $u_d^{\sigma}[k], u_c^{\sigma}[k] \in \{0, 1\}$ are used to specify the operational state of each *ESR* σ in the time period k. Binary variable $u_d^{\sigma}[k]$ ($u_c^{\sigma}[k]$) assumes the value 1 if *ESR* σ discharges (charges) during the time period k; 0 otherwise.

The capacity and capability limits of each ESR σ are taken into account in (60) and (61). $[p_{ee}^{\sigma}]^{M}$ and $[p_{ee}^{\sigma}]^{m}$ denote the minimum and maximum capacity both for the charging and discharging state. $[e_{ee}^{\sigma}]^{m}$ and $[e_{ee}^{\sigma}]^{M}$ are the minimum and maximum capability of the resource σ. To consider that an ESR cannot charge and discharge at the same time, physical constraints are enforced through eq. (62). ESR is said to be idle when it neither discharges nor charges,

$u_d^{\sigma}[k]=u_c^{\sigma}[k]=0$. Equations (63) and (64) allow the output $p_{ee}^{\sigma}[k]$ to be consistent with the binary variables $u_d^{\sigma}[k]$ and $u_c^{\sigma}[k]$. $p_{ee}^{\sigma}[k]$ is negative during the discharging phase ($u_d^{\sigma}[k]$) and positive during the charging phase ($u_c^{\sigma}[k]$)

$$[p_{ee}^{\sigma}]^m \le \left| p_{ee}^{\sigma}[k] \right| \le [p_{ee}^{\sigma}]^M \quad (60)$$

$$[e_{ee}^{\sigma}]^m \le \left| e_{ee}^{\sigma}[k] \right| \le [e_{ee}^{\sigma}]^M \quad (61)$$

$$u_c^{\sigma}[k] + u_d^{\sigma}[k] \le 1 \quad (62)$$

$$u_c^{\sigma}[k]\, p_{ee}^{\sigma}[k] \ge 0 \quad (63)$$

$$u_d^{\sigma}[k]\, p_{ee}^{\sigma}[k] \le 0. \quad (64)$$

5.3.1.2 Market layer

The framework allows the simulation of multi-settlement market structures. The market layer has the aim to model the wholesale electricity markets including day ahead market, intra-day market, real-time market and ancillary services market. The entities that are interfaced with the market layer are the IGO and the *embedding environment operator*, and the market layer handles the dollar flows of the payments/incomes that occur between the IGO and each player of the market, such as the embedding environment operator ($\psi_{ee}^{(\ell)}$, $\xi_{ee}^{(\ell)}$).

Let $\mathcal{L} = \{\ell : \ell = 1, 2, 3\}$ be the set of the electricity markets, where ℓ represents the single market structure. This structure allows the simulation of different market architectures, market products and market payments. $\ell = 1$ identifies the day-ahead market, $\ell = 2$ the intraday energy market and $\ell = 3$ the real-time market. Depending

on the aim of the study, it is possible to implement a specific model or neglect some specific parts of the main structure. For instance, if the aim is to solve a planning problem, the implementation of a day-ahead market structure can be exhaustive.

A transmission network with $N + 1$ buses and J lines is considered. Let $\mathcal{N} = \{ n : n = 1, \ldots, N \}$ be the set of buses, with the bus 0 being the slack bus. $\mathcal{F} = \{ f_1, f_2, \ldots, f_F \}$ is the set of transmission lines and transformers that connect buses in the set $\mathcal{N}$. At each element $f \in \mathcal{F}$ is associated the ordered pair (i, j). $\underline{\gamma}_S^{(\ell)}$ and $\underline{\beta}_B^{(\ell)}$ are the energy sale offers and bids, respectively. The IGO collects all the pool offers/bids and communicates them to the market layer. In the bids/offers pool, it is possible to represent also bilateral contracts and virtual bids/offers. For bilateral customers, the same formulation developed in [108] has been considered. All transactions are assumed to be basic and are represented by the set $\Phi = \{\phi^1, \ldots, \phi^F\}$, with each element denoted by the ordered triplet $\phi^f = \{m^f, n^f, r^f\}$. The triplet represents a transaction with receipt point m^f (*from* node) to the delivery point (*to* node) n^f in the amount of r^f. The customer requests the corresponding grid services to the IGO for each transaction (i.e. transmission rights). These transactions can be introduced as an active power injection p_n^f at each node n as follows:

$$p_n^f = \sum_{f=1,\ m^f=n}^{F} r^f - \sum_{f=1,\ n^f=n}^{F} r^f, \quad n \in \mathcal{N}. \qquad (65)$$

The market engine must receive from the information layer the grid configuration in terms of lines and transformers $\mathcal{F}$ and the state of the grid $\mathcal{W}$, which includes the estimation/measurements of grid parameters as voltage angles $\underline{\theta} = [\theta_1, \theta_2, \ldots, \theta_N]$. Offers and the bids cleared in the market ℓ are denoted, respectively, by $\underline{s}^{(\ell),*}$ and $\underline{b}^{(\ell),*}$. The outcomes of the market ℓ are sent to the market settlement

tool and to the information layer. The information layer communicates the schedules to the operators of the grid resources and to the IGO. The market settlement tool calculates the incomes of each seller *s* and the payments to each buyer *b* in each market ℓ. Total payments are denoted by $\underline{\xi}_{\mathcal{S}}^{(\ell)}$ and total incomes by $\underline{\psi}_{\mathcal{B}}^{(\ell)}$. In the case of a multi-settlement structure, total payments/incomes will be a linear combination of the payments/incomes calculated for each market ℓ. The difference $\sum_{b \in \mathcal{B},\, s \in \mathcal{S}} \psi_b^{(\ell)} - \xi_s^{(\ell)}$ indicates the merchandise surplus.

5.3.1.3 The Environmental Layer

The environmental layer captures the impacts of the storage deployment on GHG emissions. It is necessary to estimate the environmental impacts due to the integration of ESRs because some policies incentivise their installations only if ESRs are able to reduce GHG emissions. For instance, *California Public Utilities Commission* (*CPUC*) has mandated a target by 2020 of 1,325 MW of ESRs to be installed by the three major jurisdictional *investor owned utilities* (*IOUs*) by 2024 [109]. One of the requirements of the new ESR installations is the reduction of GHG emissions. A layer able to estimate the environmental impacts of the ESR in a wide range of applications is therefore needed.

The environmental layer evaluates specific emission-related attributes of the various resources in the power system including the *ESR*s. As is quite widely known, the environmental impacts in terms of GHG emissions of ESRs is case and application specific in terms of GHG emission quantities. For instance, an ESR installed to reduce wind curtailments can reduce GHG emissions by displacing polluting resources later in the day. By contrast, if the ESR is charged during periods of low demand and discharged during peak hours it can increase the GHG emissions. The same problem arises when an ESR that takes advantage of differences in energy prices during the day (so-called arbitrage) is considered; in this case, the impact in terms of GHG emissions can be negative.

For the above-mentioned reasons, our framework allows the calculation of GHG emissions and represent potential carbon taxes in

various ways with which ESRs can be deployed. These policies are applied with different impacts to reduce GHG emissions.

The environmental layer needs to receive the characteristics of the generation units $\mathcal{A}$ and the power injections $\underline{s}$. The information is sent to the environmental layer from the IGO by means of the information layer.

5.3.1.4 Information layer

The layer consists of computer/communication/control infrastructures to receive/send, collect and elaborate all the information flows needed to operate the power system. In detail, the embedding environment operator collects the measurements $\mathcal{G}_{ee}$ and sends the output setting $p_{ee}^{\sigma}[k]$ to the physical assets. Moreover, the *embedding environment operator* sends to the IGO his bids/offers that will be subsequently forwarded to the market layer. The IGO sends the collected bids $\underline{\beta}_{\mathcal{B}}^{(\ell)}$ and offers $\underline{\gamma}_{\mathcal{S}}^{(\ell)}$ to the market layer both with the state of the grid $\mathcal{W}$ and the configuration of the line/transformers $\mathcal{F}$. The results cleared in the market layer will be communicated to each resource operators and the IGO. The amount of power cleared in the market ℓ is denoted by $\underline{s}^{(\ell),*}$ for generator resources (included the *ESR*s acting as generators) and $\underline{b}^{(\ell),*}$ for demand resources (included the *ESR*s acting as load resources). $\underline{s}^{(3),*}$ and $\underline{b}^{(3),*}$ are sent to the physical layer. the generation unit characteristics $\mathcal{A}$ and $\underline{s}$ are communicated to the environmental layer to calculate the GHG emissions. Furthermore, the IGO sends the state of the grid $\mathcal{W}$ and his configuration $\mathcal{F}$. The *embedded environment operator* uses the monitored values to calculate parameters as the state of charge and state of health of the *ESR*. In the same way, the IGO monitors and controls the grid. The environmental layer receives the measurements needed to calculate the emission coefficients directly from information layer. The information flows serve to interconnect the three layers and the operators into the proposed comprehensive framework.

Chapter 6

Conclusions

The dissertation aimed to investigate the impact of ancillary services provided by DERs in DNs. In particular, distributed generators, energy storage systems and active demand are considered as service providers to reduce or avoid network constraints and increase the hosting capacity. This chapter tries to summarise the achieved results and draws some conclusions about the research contribution of this dissertation.

6.1 Contributions of the thesis

DGs, in particular the one feed by green energy, are a key ingredient in energy policy aiming at the decarbonisation of the energy sector. The integration of DG units in distribution systems brings several direct and indirect benefits to system operators and customers. Anyway, there may be technical, economic and regulatory challenges that must be addressed in order to increase the penetration of these technologies into the grid. Major technical issues related to the connection of DG units involve voltage control, power quality and grid protection system. Ancillary services can help system operator in dealing with some of these. From an economic point of view, policies such as feed-in tariff programs are needed to make viable projects aimed at integrating renewable technologies in the distribution system. Furthermore, because of the structure of existing electricity markets, the identification of new market products/mechanisms is needed in order to recognise direct but also indirect benefits of RESs.

To support DERs integration in future DNs, a transition of DNOs to DSOs in the next few years is required. Distributor operators must assume more active roles and implement new services. These services allow the solution of technical issues and the implementation of new market structure/products able to exploit efficiently DERs characteristics and defer infrastructural investments. Key services become the so-called ancillary services, usually deployed at transmission level, that are becoming of interest at lower voltage levels due to the changing paradigm of DNs from *networks follow demand* to *networks follow power flow, both active and passive*. Ancillary services can be provided by network assets as well as DERs. Aim of the thesis is to deploy and show the potential of some of these services, with a focus on voltage control ancillary service, by exploiting three different typologies of DERs: distributed generators, energy storage systems and active demand. The aim is not only to support DSO in solving network constraints, but also to increase the hosting capacity that often is limited by voltage violations and thermal issues along the lines.

The following are the main research contributions of this dissertation, in the reference context described above.

- **Providing voltage support in DNs by using DGs.**

  Two coordinated voltage control methods have been proposed in Chapter 3 and tested on a real MV distribution network. Both methodologies allow an increasing of power production from WF and PV systems supporting at the same time the DSO in solving voltage issues along the lines. The methods gave approximately the same results in terms of control even though each of them presents different advantages and disadvantages. The CLC method is very fast to perform the active and reactive power set point of DG units but in order to be applied, it is necessary to calculate the mixed sensitivity matrix at the PCC of each DG. Furthermore, the CLC could not give the best solution in terms of reactive power injection/absorption when many DG units are involved in the control because the algorithm calculates the active and reactive power set points independently without considering the problem as global. For these reasons, CLC could not give the best solution in terms of active power production. When the IPP deal

with multiple DG units on the grid, the coordination could be simplified and optimised applying the ORC, which automatically calculates the correct set points for each DG unit reducing the overall reactive power injection/absorption needed to control the voltage. In contrast, as this method requires a cooperation of data transfer between DSO and IPPs in order to calculate the status of the grid, monitoring and acquisition systems (i.e. Smart Meters) are necessary.

The increasing installations of Smart Meters in the distribution networks allow the ORC to be a good solution in a Smart Grid. On the contrary, the CLC can be easily applied in a distribution network lacking of equipment for a simultaneous metering. Finally, both control strategies achieve similar results in different ways and the choice can be done only referring to a specific case.

- **Improve load modelling and estimate demand response to voltage changes.**

  In Chapter 4, two alternative formulations of the ZIP model have been proposed to improve the ability to describe the dependency of demand to voltage changes in steady condition on the distribution network. Starting from the classic ZIP model the following models are proposed:

  - *time-varying ZIP model* able to reduce the number of loads to be modelled through a polynomial formulation that aggregates and makes time-varying the triplet of ZIP parameters;
  - *discrete-time ZIP model* able to describe the characteristics of cyclic and thermostatic loads such as washing machines.

  By using these models, it is possible to make a correct estimation of load response to voltage changes in distribution networks; this is important in the context of CVR as well as for the potential usage controllable demand resource if aggregated (e.g., congestion management, peak shaving or provision of reserves). Results of the first case study have

suggested that, even considering voltage constraints, there is considerable load response that can be unlocked from residential loads. However, this is highly dependent on the time of the day. For this particular case study, the active power reductions also presented a linear behaviour compared to voltage change. This depends on the appliances and their ZIP models. Furthermore, results achieved for the DT-ZIP formulation are extremely promising and they show that the model accurately reproduces profiles of cyclic loads giving good expectations for the analysis of electrical systems. For instance, it allows designing new simulation tools, simulating appropriately control techniques in the context of CVR or developing new functions (e.g. new ancillary services for DSO) in distribution systems.

- **Estimate the potential of energy storage systems in providing ancillary services in DNs.**

Lastly, in Chapter 5, two ancillary services able to exploit the unique characteristics of energy storage systems have been presented and tested on two distribution network: a MV network and a LV network. The aim of the proposed control strategy is to support the DSO in solving voltage issues along the lines.

The first approach is a decentralized strategy able to control a BESS integrated with a PV unit. The control has been compared with a decentralized reactive power control in order to show the reduction of reactive power that is possible to achieve. The BESS, indeed, is able to store the power during maximum PV generation avoiding active power curtailments or disconnections reducing the needs of reactive power. The stored energy could be used to support the network during peak demand providing an ancillary service to the DSO. Furthermore, the BESS allows reducing the size of the inverter preserving the ability to support the network during voltage issues. The decentralized control can be applied locally by the IPP by using the same meters used to monitor the PV units.

The second strategy has been tested on a typical LV Italian network. Simulations have pointed out the benefits that

the integration of BESSs with PV units has in improving voltage quality. Thus, the BESS control has not only increased self-consumption but also reduced the risk of possible PV disconnections due to voltage infringements. Results show that an indirect voltage support can be reached by BESS installations to support both local consumptions of energy and the DSO. Co-located systems have been locally monitored by residential customers without adding other meters in the grid. The possibility to provide ancillary services by means of residential BESSs can help to deploy battery systems making them more attractive and economically sustainable. Furthermore, CCD control increases the life of battery systems by reducing the number of cycles in a day without a significant impact on self-consumptions.

A preliminary design of a conceptual framework for the analysis of ESR deployment operations and economics is presented. Further studies are needed to make this part exhaustive.

6.2 Future works

The research developed in the Thesis has successfully achieved all the research objectives defined by the Ph.D. at the beginning. Nevertheless, the work has highlighted new opportunities for research that, starting from the achieved results, will make a further contribution to the development of research in the field of planning and control of the distribution networks.

In detail, the control strategies presented in Chapter 3 are both based on a sensitivity analysis of the network. In practice, IPPs are not always allowed to have the sensitivity coefficients of the networks. To apply the proposed control strategies, a regulatory framework should be developed to set the rules for the exchange of this information between the DSO and IPPs. Contrariwise, IPPs should be able to develop a methodology to estimate the sensitivity coefficients at the PCC. Another aspect regards the possibility to coordinate the proposed

voltage control approaches with the OLTC, the capacitor banks and other equipment in the network capable to control the voltage along the feeders. This requires to coordinate the control actions of the DSO and IPPs to maintain the voltage within mandatory limits.

In Chapter 4, the *discrete-time ZIP model* has been carried out by analysing a set of measurements of a washing machine. The analysis must be extended to all the domestic appliances to improve the proposed model and identify a set of new ZIP parameters for modern appliances. Furthermore, the analysis can be extended to calculate the ZIP parameters related to the reactive power.

The conceptual framework introduced in Chapter 5 should be extended and tested in different scenarios to assess the economics of storage as well as other resources in the provision of ancillary services in a distribution network. To this end, in the future a great effort should be make for the development of an electricity market structure for distribution systems.

List of publications

- **F. Lamberti**, V. Calderaro, V. Galdi, G. Graditi, *Massive data analysis to assess PV/ESS integration in residential unbalanced LV networks to support voltage profiles*, Electric Power Systems Research, vol. 143, February 2017
- **F. Lamberti**, V. Calderaro, V. Galdi, G. Graditi, *Assessing the Performances of Residential ESSs Control by Means of a Monte Carlo Analysis*, IEEE ISGT Europe 2016, Ljubljana, Slovenia, October 2016
- **F. Lamberti**, V. Calderaro, V. Galdi, A. Piccolo, G. Gross, *Long-Term Performance in Providing Voltage Support by PV and Storage Systems in Distribution Networks*, IEEE General Meeting 2016, Boston, Massachusetts, United States of America, July 2016
- V. Calderaro, V. Galdi, **F. Lamberti**, A. Piccolo, *Co-located Storage Systems with Renewable Energy Sources for Voltage Support in Distribution Networks*, IEEE General Meeting 2015, Denver, Colorado, United States of America, July 2015
- **F. Lamberti**, V. Calderaro, V. Galdi, A. Piccolo, G. Graditi, *Impact Analysis of Distributed PV and Energy Storage Systems in Unbalanced LV Networks*, Powertech 2015, Eindhoven, Holland, June 2015
- V. Calderaro, V. Galdi, **F. Lamberti**, A. Piccolo, *A Smart Strategy for Voltage Control Ancillary Service in Distribution Networks*, IEEE Transactions on Power Systems, vol. 30, n. 1, January 2015
- V. Calderaro, V. Galdi, G. Graditi, **F. Lamberti**, A. Piccolo, *Voltage Support Control of Unbalanced Distribution Systems by Reactive Power Regulation*, IEEE ISGT Europe 2014, Istanbul, Turkey, October 2014
- V. Calderaro, V. Galdi, G. Graber, G. Graditi, **F. Lamberti**, *Impact assessment of Energy Storage and Electric Vehicles on Smart Grids*,

IEEE Electric Power Quality and Supply Reliability 2014, Tallinn, Estonia, June 2014

- V. Calderaro, V. Galdi, G. Graditi, **F. Lamberti**, *Comparison of Voltage Control Methods for Incrementing Active Power Production*, IEEE ENERGYCON 2014, Dubrovnik, Croatia, May 2014
- V. Calderaro, V. Galdi, **F. Lamberti**, A. Piccolo, *Coordinated local reactive power control in smart distribution grids for voltage regulation using sensitivity method to maximize active power*, Journal of Electrical Systems, vol. 9, n. 4, December 2013
- **F. Lamberti**, D. Cuicai, V. Calderaro, L.F. Ochoa, *Estimating the Load Response to Voltage Changes at UK Primary Substations*, IEEE ISGT Europe 2013, Copenhagen, Denmark, October 2013

References

[1] EPA - United States Environmental Protection Agency. Global Greenhouse Gas Emissions Data. [Online]. https://www.epa.gov/ghgemissions/global-greenhouse-gas-emissions-data

[2] IEA - International Energy Agency. (2016, Mar.) https://www.iea.org/newsroom/news/2016/march/decoupling-of-global-emissions-and-economic-growth-confirmed.html.

[3] "G7 Ise-Shima Leaders' Declaration," Ise-Shima, 2016.

[4] "G20 Energy Efficiency Leading Programme," China, 2016.

[5] United Nations Framework Convention on Climate Change (UNFCCC), "Paris Agreement," Paris, 2015.

[6] IEA - Internation Energy Agency, "Energy Matters - How COP21 can shift the energy sector onto a low-carbon path that supports economic growth and energy access," 2015.

[7] IEA - International Energy Agency, "World Energy Outlook," 2015.

[8] MIT, The future of natural gas, 2011.

[9] D. J. Frame, C. Huntingford, C. D. Jones, J. A. Lowe, M. Meinshausen, N. Meinshausen M. R. Allen, "Warming caused by cumulative carbon emissions towards the trillionth tonne," *Nature*, vol. 458, pp. 1163-1166, April 2009.

[10] IPCC, "Climate Change - Mitigation of Climate Change," Cambridge University Press, 2014.

[11] IRENA, "REthinking Energy: Accelerating the global energy," International Renewable Energy Agency, Abu Dhabi, 2017.

[12] European Commission, "EU climate and energy package ," 2007.

[13] European Commission, "A 2030 framework for climate and energy policies," 2013.

[14] European Commission, "A Roadmap for moving to a competitive low carbon economy in 2050," 2011.

[15] E. F. El-Saadany Y. M. Atwa, "Reliability Evaluation for Distribution System With Renewable Distributed Generation During Islanded Mode of Operation," *IEEE Trans. on Power Systems*, vol. 24, no. 2, pp. 572-581, May 2009.

[16] N. Mithulananthan, R. C. Bansal D. Q. Hung, "A combined practical approach for distribution system loss reduction," *Int. Journal Ambient Energy*, vol. 36, no. 15, pp. 123-131, 2015.

[17] E. F. El-Saadany, Y. M. Atwa R. S. Al Abri, "Optimal Placement and Sizing Method to Improve the Voltage Stability Margin in a Distribution System Using Distributed GenerationUsing Distributed Generation," *IEEE Trans. on Power Systems*, vol. 28, no. 1, pp. 326-334, February 2013.

[18] Lazard, "Lazard's Levelized Cost Of Energy Analysis - v.10.0," December 2016.

[19] J. M. A. Myrzik, Bas Kruimer, W. L. Kling E. J. Coster, "Integration Issues of Distributed Generation in Distribution Grids," *Proceedings of the IEEE* , pp. 28-39, September 2010.

[20] CEI EN 50160 - Voltage Characteristics of electricity supplied by public electricity networks, 2015.

[21] N. Hatziargyriou, J. Mutale, P. Djapic, N. Jenkins J.A. Pec¸as Lopes, "Integrating distributed generation into electric power systems: A review of drivers, challenges and opportunities," *Electric Power System Res.*, vol. 77, pp. 1189-1203, 2007.

[22] L. Bryans, D. Flynn, N. Jenkins, D. Milborrow, M. O'Malley, R. Watson, O. Anaya-Lara B. Fox, *Wind Power Integration: Connection and System Operational Aspects*. London, U.K.: IET, 2013.

[23] "Renewable distributed generation: The hidden challenges – A review from the protection perspective," *Reneable and Sustainable Energy Reviews*, vol. 58, pp. 1457-1465, 2016.

[24] A. A. Girgis S. M. Brahma, "Development of Adaptive Protection Scheme for Distribution Systems With High Penetration of Distributed Generation," *IEEE Trans. on Power Delivery*, vol. 19, no. 1, pp. 56-63, January 2004.

[25] "Current Status and Issues of Concern for the Integration of Distributed Generation Into Electricity Networks," *IEEE System Journal*, vol. 9, no. 3, pp. 933-944, September 2015.

[26] J. Szolgayova, S. Fuss, M. Obersteiner W. H. Reuter, "Renewable energy investment: policty and market impacts," *Applied Energy*, vol. 97, pp. 249-254, 2012.

[27] F. Pilo, A. Keane, P. Cuffe, G. Pisano L. N. Ochoa, "Embracing an Adaptable Flexible Posture," *IEEE Power & Energy Magazine*, pp. 16-28, September/October 2016.

[28] T. Jamasb R. Poudineh, "Distributed generation, storage, demand response and energy efficiency as alternative to grid capacity enhancement," *Energy policy*, vol. 67, pp. 222-231, 2014.

[29] D. Flynn, M. O'Malley E. Lannoye, "Evaluation of Power System Flexibility," *IEEE Trans. on Power Systems*, vol. 27, no. 2, pp. 922-931, May 2012.

[30] D. Flynn, M. O'Malley E. Lannoye, "Transmission, Variable Generation, and Power System Flexibility," *IEEE Trans. on Power Systems*, vol. 30, no. 1, pp. 57-66, January 2015.

[31] Eurelectric, "Active Distribution System Management - A key tool for the smooth integration of distributed generation," 2013.

[32] Council of European Energy Regulators (CEER), "The Future Role of DSOs," Brussels, Belgium, 2015.

[33] (2016) evolvDSO project - Development of methodologies and tools for new and evolving DSO roles for efficient DRES integration in distribution network. [Online]. http://www.evolvdso.eu

[34] International Electrotechnical Commission, "Organisation/market of electricity," 2008.

[35] REserviceS Project, "Ancillary services: technical specifications, system needs and costs - Deliverable D2.2," November 2012.

[36] Martin Braun, Provision of Ancillary Services - Technological and Economic Perspective, 2008, PhD Thesis.

[37] P. Kundur, *Power System Stability and Control*. Palo Alto, California: Electric Power Research Institute, 1994.

[38] R. Saint, R. C. Dugan, J. Burke, L. A. Kojovic R. A. Walling, "Summary of distributed resources impact on power delivery systems," *IEEE Trans. Power Del.*, vol. 23, no. 3, pp. 1636-1644, July 2008.

[39] J. Driesen, D. Haeseldonckx, R. Belmans, W. D'haeseleer G. Pepermans, "Distributed generation: definition, benefits and issues," *Energy Policy*, vol. 33, no. 6, pp. 787-798, April 2005.

[40] N. Hatziargyriou, J. Mutale, P. Djapic, N. Jenkins J.A. Peças Lopes, "Integrating distributed generation into electric power systems: A review of drivers, challenges and opportunities," *Electric Power Systems Research*, vol. 77, no. 9, pp. 1189–1203, July 2007.

[41] R. Allan, P. Crossley, D. Kirschen, G. Strbac N. Jenkins, *Embedded generation*.: The Institution of Electrical Engineers, 2000.

[42] H. Mokhlis, K. Naidu, S. Uddin, A.H.A. Bakar M. Karimi, "Photovoltaic penetration issues and impacts in distribution network – A review," *Renewable and Sustainable Energy Reviews*, vol. 53, pp. 594-605, January 2016.

[43] H. Assari M. Rahimi, "Addressing and assessing the issues related to connection of the wind turbine generators to the distribution grid," *International Journal of Electrical Power & Energy Systems*, vol. 86, pp. 138–153, March 2017.

[44] M. Oshiro, S. Toma, A. Yona, T. Senjyu, T. Funabashi, C.H. Kim K. Tanaka, "Decentralised control of voltage in distribution systems by distributed generators," *IET Gener. Transm. Distrib.*, vol. 4, no. 11, pp. 1251-1260, November 2010.

[45] R. Kavasseri R. Aghatehrani, "Reactive power management of a DFIG wind system in microgrids based on voltage sensitivity analysis," *IEEE Trans. Sustain. Ener.*, vol. 2, no. 4, pp. 451-458, 2011.

[46] G. Conio, V. Galdi, A. Piccolo V. Calderaro, "Reactive power control for improving voltage profiles: A comparison between

two decentralized approaches," *Elec. Power Syst. Res.*, vol. 83, pp. 247-254, 2012.

[47] G. Conio, V. Galdi, G. Massa, A. Piccolo V. Calderaro, "Optimal Decentralized Voltage Control for Distribution Systems with Inverter-Based Distributed Generators," *IEEE Trans. Power Systems*, vol. 29, no. 1, pp. 230-241, 2014.

[48] V. Vahidinasab, M. S. Ghazizadeh A. Abessi, "Centralized Support Distributed Voltage Control by," *IEEE Trans. on Smart Grid*, vol. 7, no. 1, pp. 178-188, January 2016.

[49] K. Tanaka, A. Uehara, T. Senjyu, Y. Miyazato, A. Yona, T. Funabashi M. Oshiro, "Optimal voltage control in distribution systems with coordination of distribution installations," *Int. Journal of Electrical Power & Energy Systems*, vol. 32, no. 10, pp. 1125-1134, December 2010.

[50] G. Franzè, D. Menniti, N. Sorrentino A. Casavola, "Voltage regulation in distribution networks in the presence of distributed generation: A voltage set-point reconfiguration approach," *Elec. Power Syst. Res.*, vol. 81, no. 1, p. 25.34, January 2011.

[51] L. F. Ochoa, E. Vittal, C. J. Dent, G. P. Harrison A. Keane, "Enhanced Utilization of Voltage Control Resources With Distributed Generation," *IEEE Trans. Power Syst.*, vol. 26, no. 1, pp. 252-260, 2011.

[52] R. Angelino, G. Carpinelli, M. Mangoni, D. Proto A. Bracale, "Dispersed generation units providing system ancillary services in distribution networks by a centralised control," *IET Renewable Power Generation*, vol. 5, no. 4, pp. 311-321, July 2011.

[53] A Padilha-Feltrin A.C. Rueda-Medina, "Distributed Generators as Providers of Reactive Power Support - A Market Approach," *IEEE Trans. Power Systems*, vol. 28, no. 1, pp. 490-502, February 2013.

[54] J.A. Peças Lopes A.G. Madureira, "Ancillary services market framework for voltage control in distribution networks with microgrids," *Elec. Power Syst. Res.*, vol. 86, pp. 1-7, May 2012.

[55] E. De Tuglie, M. Liserre, R.A. Mastromauro A. Cagnano, "Online Optimal Reactive Power Control Strategy of PV Inverters," *IEEE Trans. Industrial Electronics*, vol. 58, no. 10, pp. 4549-4558, October 2011.

[56] J. L. Kirtley, L. K. Norford Y. J. Kimm, "Reactive Power Ancillary Service of Synchronous DGs in Coordination With Voltage Control Devices," *IEEE Trans. on Smart Grid*, pp. 1-13, in press.

[57] T. Undeland, and W. Robbins N. Mohan, *Power Electronics Converters, Apllications and Design,* , 3rd ed. Hoboken, NJ: Wiley, 2003.

[58] N. Ansari Chun-Hao Lo, "Decentralized Controls and Communications for Autonomous Distribution Networks in Smart Grids," *IEEE Trans. on Smart Grids*, vol. 4, no. 1, pp. 66-77, March 2013.

[59] K. Bhattacharya N. R. Ullah, *Wind Farms as Reactive Power Ancillary Service Providers-Technical and Economic Issues*.: IEEE Trans. Energy Convers., 2009, vol. 24.

[60] V. Galdi, G. Graditi, F. Lamberti V. Calderaro, "Comparison of voltage control methods for incrementing active power production," in *ENERGYCON 2014*, Dubrovnik, 2014.

[61] V. Galdi, F. Lamberti, A. Piccolo V. Calderaro, "Coordinated local reactive power control in smart distribution grids for voltage regulation using sensitivity method to maximize active power," *Journal of Electrical Systems*, 2013.

[62] V. Galdi, F. Lamberti, A. Piccolo V. Calderaro, "A Smart Strategy for Voltage Control Ancillary Service in Distribution Networks," *IEEE Trans. Power Syst.*, vol. 30, no. 1, pp. 494-502, 2015.

[63] J.A. Momoh, *Electric Power System Application of Optimization*. Boca Raton, FL: CRC Press, 2009.

[64] R. Zhou, Y. Zhang, and J. Liu, "Reactive Power Optimization Algorithm Based on Trust-Region Global SQP," in *2nd International Conference on Electrical and Electronics Engineering*, 2005.

[65] A. M. Greco S. Conti, "Innovative voltage regulation method for distribution networks with distributed generation," in *International Conf. on Electricity Distrib. (CIRED)*, 2007.

[66] Carlos E. Murillo-Sánchez & others Ray D. Zimmerman. MATPOWER - MATLAB Power System Simulation Package. [Online]. http://www.pserc.cornell.edu/matpower/

[67] K. K. Lee P. K. Sen, "Conservation Voltage Reduction Technique: An Application Guideline for Smarter Grid," *IEEE Trans. on Industry Applications*, vol. 52, no. 3, pp. 2122-2128, 2016.

[68] R. F. Preiss and V. J. Warnock, "Impact of Voltage Reduction on Energy and Demand," *IEEE Trans. on Power Apparatus and Systems*, vol. PAS-97, no. 5, pp. 1665-1671, 1978.

[69] J. Sandraz, R. Macwan, F. de Leòn, D. Czarkowski, C. Comack, D. Wang M. Diaz-Aguiló, "Field-Validated Load Model for the Analysis of CVR in Distribution Secondary Networks: Energy Conservation," *IEEE Trans. on Power Delivery*, vol. 28, no. 4, pp. 2428-2436, 2013.

[70] F. K. Tuffner, J. C. Fuller, and R. Singh K. P. Schneider, "Evaluation of conservation voltage reduction (CVR) on a national level," Richland, WA, USA, 2010.

[71] J. Wang Z. Wang, "Time-Varying Stochastic Assessment of Conservation Voltage Reduction Based on Load Modeling," *IEEE Trans. on Power Systems*, vol. 29, no. 5, pp. 2321-2328, 2014.

[72] L. F. Ochoa L. Gutierrez-Lagos, "CVR assessment in UK residential LV networks considering customer types," in *IEEE Innovative Smart Grid Technologies - Asia* , 2016, pp. 1-6.

[73] L. F. Ochoa A. Ballanti, "Initial assessment of voltage-led demand response from UK residential loads," in *IEEE Innovative Smart Grid Technologies Conference (ISGT)*, 2015, pp. 1-5.

[74] M. Thomson, D. Infield, and C. Clifford I. Richardson, "Domestic electricity use: A high-resolution energy demand model," *Energy and Buildings*, vol. 42, pp. 1878-1887, 2012.

[75] E. Wackelgard J. Widen, "A high resolution stochastic model of domestic activity patterns and electricity demand," *Appl. Energy*, vol. 87, pp. 1880–1892, June 2010.

[76] M. Kuzlu, S. Rahman, Y. Teklu M. Pipattanasomporn, "Load Profiles of Selected Major Household Appliances and Their Demand Response Opportunities," *IEEE Trans. on Smart Grid*, vol. 5, pp. 742-750, March 2014.

[77] C. E. Cresswell, S. Z. Djokic A. J. Collin, "Harmonic Cancellation of Modern Switch-Mode Power Supply Load," in *14th IEEE Int. Conf. Harmonics and Quality of Power*, 2010, pp. 1-9.

[78] M. Pipattanasomporn, and S. Rahman S. Shao, "Development of physical-based demand response-enabled residential load models," *IEEE Trans. Power Syst.*, vol. 28, no. 2, pp. 607–614, May 2013.

[79] G. Tsagarakis, A.E. Kiprakis, S. McLaughlin A.J. Collin, "Development of Low-Voltage Load Models for the Residential Load Sector," *IEEE Trans. on Power Syst.*, vol. 29, pp. 2180-2188, September 2014.

[80] K. A. Wirgau, A. Murdoch, J. V. Mitsche, E. Vaahedi, M. A. El-kady W. W. Price, "Load modeling for load flow and transient stability computer studies," *IEEE Trans. Power Syst.*, vol. 3, pp. 180–187, February 1988.

[81] H. D. Jiang, C. L. Chang, A. H. Liu J. C. Wang, "Development of a frequency-dependent composite load model using the measurement approach," *IEEE Trans. Power Syst.*, vol. 9, pp. 1546–1556, August 1994.

[82] B. Danai L. M. Hajagos, "Laboratory measurements and Models of Modern Loads and Their Effect on Voltage Stability Studies," *IEEE Trans. on Power Syst.*, vol. 13, pp. 584-592, May 1998.

[83] A. Alkan, R. Dogan, M. Diaz-Aguilo, F. de Leon, D. Czarkowski, Z. Zabar, L. Birenbaum, A. Noel, R.E. Uosef A. Bokhari, "Experimental Determination of the ZIP Coefficients for Modern Residential, Commercial, and Industrial Loads,"

IEEE Trans. on Power Delivery, vol. 29, pp. 1372-1381, June 2014.

[84] Wei-Jen Lee, J. Jativa-Ibarra F.L. Quilumba, "Load Models for Flat-Panel TVs," *IEEE Trans. on Industry Applications*, vol. 50, pp. 4171-4178, Nov.-Dec. 2014.

[85] Wei-Jen Lee, Heng Huang, D.Y. Wang, R.L. Szabados F.L. Quilumba, "Load model development for next generation appliances," in *IEEE Industry Applications Society Annual Meeting (IAS)*, 2011, pp. 1-7.

[86] Yulong Xie, Zhenyu Huang, F. Puyleart, S. Yang Ning Lu, "Load component database of household appliances and small office equipment," in *IEEE Power and Energy Society General Meeting*, 2008, pp. 1-5.

[87] A. Ellis, and J. Mechenbier S.J. Ranade, "The development of power system load models from measurements," in *IEEE/PES Transmission and Distribution Conference and Exposition*, 2011, pp. 201-206.

[88] A.I. Negash, S.S. Venkata, D.S. Kirschen E. Sortomme, "Voltage dependent load models of charging electric vehicles," in *IEEE Power and Energy Society General Meeting*, 2013, pp. 1-5.

[89] D. Cuicai, V. Calderaro, L.F. Ochoa F. Lamberti, "Estimating the Load Response to Voltage Changes at UK Primary Substations," in *IEEE ISGT Europe 2013*, Copenaghen, Denmark, 2013.

[90] Load Profiles and their use in electricity settlement. [Online]. http://www.elexon.co.uk

[91] OpenDSS - EPRI Distribution System Simulator. [Online]. http://electricdss.sourceforge.net/

[92] UK Office for National Statistics, "Families and households, 2001 to 2011," 2012.

[93] B. Danai L. M. Hajagos, "Laboratory measurements and Models of Modern Loads and Their Effect on Voltage Stability Studies," *IEEE Trans. on Power Syst.*, vol. 13, pp. 584-592, 1998.

[94] I. Dincer, B.V. Reddy A.S. Joshi, "Performance analysis of photovoltaic systems: a review," *Renew. Sustain. Energy Rev.*, vol. 13, no. 8, pp. 1884–1897, 2009.

[95] V. Calderaro, V. Galdi, A. Piccolo, G. Gross F. Lamberti, "Long-Term Performance in Providing Voltage Support by PV and Storage Systems in Distribution Networks," in *IEEE General Meeting 2016*, Boston, Massachusetts, July 2016.

[96] V. Galdi, F. Lamberti, A. Piccolo V. Calderaro, "Co-located Storage Systems with Renewable Energy Sources for Voltage Support in Distribution Networks," in *IEEE General Meeting 2015*, Denver, Colorado, July 2015.

[97] V. Calderaro, V. Galdi, G. Graditi F. Lamberti, "Massive data analysis to assess PV/ESS integration in residential unbalanced LV networks to support voltage profiles," *Electric Power Systems Research*, vol. 143, pp. 206-214, February 2017.

[98] V. Calderaro, V. Galdi, G. Graditi F. Lamberti, "Assessing the Performances of Residential ESSs Control by Means of a Monte Carlo Analysis," in *IEEE ISGT Europe 2016*, Ljubljana, October 2016.

[99] V. Calderaro, V. Galdi, A. Piccolo, G. Graditi F. Lamberti, "Impact Analysis of Distributed PV and Energy Storage Systems in Unbalanced LV Networks," in *Powertech 2015*, Eindhoven, Holland, June 2015.

[100] P. Weicker, *Lithium-Ion Battery management*.: Norwood: Artech House, 2014.

[101] IEEE Std. 1547.2-2008, IEEE Standard for Interconnecting Distributed Resources with Electric Power Systems, 2009.

[102] Comitato Elettrotenico Italiano, CEI 0-16, Reference technical rules for the connection of active and passive consumers to the HV and MV electrical networks of distribution Company, 2016.

[103] Solar Energy Services for Professionals. SoDa - Solar Radiation Data. [Online]. http://www.soda-pro.com/web-services/typical-years/normal-year-global-radiation-temperature

[104] Progetto Atlantide - Archivio TeLemAtico per il riferimento Nazionale di reTi di Distribuzione Elettrica. [Online]. http://www.progettoatlantide.it

[105] L. F. Ochoa A. Navarro-Espinosa, "Probabilistic Impact Assessment of Low Carbon," *IEEE Trans. on Power Syst.*, vol. 31, no. 3, pp. 2192-2203, 2016.

[106] F. Pilo, A. Navarro-Espinosa, L. F. Ochoa A. Ballanti, "Assessing the benefits of PV var absorption on the hosting capacity of LV feeders," in *Innovative Smart Grid Technologies Europe (ISGT Europe)*, Copenhagen, 2013.

[107] PVOutput. [Online]. http://pvoutput.org/list.jsp?p=5&id=33436&sid=30648&v=0&o=date&d=desc

[108] G. Gross M. Liu, "Framework for the design and analysis of congestion revenue rights," *IEEE Trans. on Power Systems*, vol. 19, no. 1, pp. 243 - 251, 2004.

[109] California Public Utilities Commission, Decision D.13-10-040, 2013.

[110] D. Turcotte, T. H. M. El-Fouly R. Tonkoski, "Impact of high PV penetration on voltage profiles in residential neighborhoods," *IEEE Trans. Sustain. Energy*, vol. 3, pp. 518-527, 2012.

[111] L. Giaccone, F. Spertino, M. Tartaglia A. Canova, "Electrical impact of photovoltaic plant in distributed network," *IEEE Trans. Ind. Appl.*, vol. 45, pp. 341-347, 2009.

[112] J. Volland, T.S. Schmidt, V. H. Hoffmann J. Hoppmann, "The economic viability of battery storage for residential solar photovoltaic systems – A review and a simulation model," *Renew. Sustain. Energy Rev.*, vol. 39, pp. 1101–1118, 2014.

[113] N.D. Hatziargyriou P.S. Georgilakis, "Optimal Distributed Generation Placement in Power Distribution Networks: Models, Methods, and Future Research," *IEEE Trans. Power Syst.*, vol. 28, no. 3, pp. 3420-3428, 2013.

[114] R. Procopio, M. Rossi, G. Ronda F. Delfino, "Integration of large-size photovoltaic systems into the distribution grids: a p-

q chart approach to assess reactive support capability," *IET Renewable Power Generation*, vol. 4, pp. 329-340, 2010.

[115] J. Østergaard, G. Yang S. Hashemi, "A Scenario-Based Approach for Energy Storage Capacity Determination in LV Grids With High PV Penetration," *IEEE Trans. Smart Grid*, vol. 5, pp. 1514-1522, 2014.

[116] P. Wolfs, M. A.S. Masoum N. Jayasekara, "An optimal management strategy for distributed storages in distribution networks with high penetrations of PV," *Electric Power Systems Research*, vol. 116, pp. 147-157, 2014.

[117] M. Pan, Y. Fang, P. P. Khargonekar Y. Guo, "Decentralized Coordination of Energy Utilization for Residential Households in the Smart Grid," *IEEE Trans. Smart Grid*, vol. 4, pp. 1341-1350, 2013.

[118] X. Zhang, H. Chen, Y. Xu, C. Tan X. Yan, "Techno-economic and social analysis of energy storage for commercial buildings," *Energy Conversion and Management*, vol. 78, pp. 125-136, 2014.

[119] A. Davigny, F. Colas, Y. Poste, B. Robyns H. Zhang, "Fuzzy logic based energy management strategy for commercial buildings integrating photovoltaic and storage systems," *Energy and Buildings*, vol. 54, pp. 196-206, 2012.

[120] E. Wäckelgård, J. Paatero, P. Lund J. Widén, "Impacts of distributed photovoltaics on network voltages: Stochastic simulations of three Swedis low-voltage distribution grids," *Electric Power Systems Research*, vol. 80, pp. 1562-1571, 2010.

[121] K. M. Muttaqi, and D. Sutanto M. J. E. Alam, "Mitigation of Rooftop Solar PV Impacts and Evening Peak Support by Managing Available Capacity of Distributed Energy Storage Systems," *IEEE Trans. Power Syst.*, vol. 28, pp. 3874-3884, 2013.

[122] G. Yang, C. Traeholt, J. Ostergaard, E. Larsen Marra, "A Decentralized Storage Strategy for Residential Feeders With Photovoltaics," *IEEE Trans. Smart Grid*, vol. 5, pp. 974-981, 2014.

[123] Y. Mishra, G. Ledwich, Z. Y. Dong, K. P. Wong M. N. Kabir, "Coordinated Control of Grid-Connected Photovoltaic Reactive Power and Battery Energy Storage Systems to Improve the Voltage Profile of a Residential Distribution Feeder," *IEEE Trans. Industrial Informatics*, vol. 10, pp. 966-977, 2014.

[124] T. Stetz, M. Braun, A. Schmiegel J. v. Appen, "Local Voltage Control Strategies for PV Storage Systems in Distribution Grids," *IEEE Trans. Smart Grid*, vol. 5, pp. 1002-1009, 2014.

[125] X. Lin, M. Pedram Y. Wang, "Adaptive Control for Energy Storage Systems in Households With Photovoltaic Modules," *IEEE Trans. Smart Grid*, vol. 5, pp. 992-1001, 2014.

[126] R. Pawelek, R. Mienski I. Wasiak, "Energy storage application in low- voltage microgrids for energy management and power quality improvement," *IET Generation, Transmission & Distribution*, vol. 8, pp. 463-472, 2014.

[127] R. Larke, and G. C. Tarnowski P. C. Kjaer, "Ancillary services provided from wind power plant augmented with energy storage," in *Power Electronics and Applications Int. Conf*, 2013.

[128] G. Huff, A. B. Currier, B. C. Kaun, D. M. Rastler, S. B. Chen, A. L. Cotter, D. T. Bradshaw, W. D. Gauntlett A. A. Akhil, "DOE/EPRI Electricity Storage Handbook in Collaboration with NRECA," Albuquerque, New Mexico, 2015.

[129] J. Mandel, J. Morris G. Fitzgerald, "The economics of battery energy storage," 2015.

List of the figures